UNIVERSITY OF CALIFORNIA SAN DIEGO

Interactive Neurorobotics:
Brain and Body Coupling During Interactive Multi-Agent Scenarios

A dissertation submitted in partial satisfaction of the requirements for the degree

Doctor of Philosophy

in

Cognitive Science

by

Eric Jeffrey Leonardis

Committee in charge:

Professor Andrea Chiba, Chair
Professor Virginia de Sa
Professor Catherina Gere
Professor Douglas Nitz
Professor Lara Rangel

2022

The dissertation of Eric Jeffrey Leonardis is approved, and it is acceptable in quality and form for publication on microfilm and electronically.

University of California San Diego

2022

DEDICATION

In memory of Peter T. Cohn (1991-2015) and Josephine "Daisy" Leonardis (1917-2018).

I often wish I had put the books down for a moment and spent a few more hours with you.

TABLE OF CONTENTS

LIST OF FIGURES

LIST OF TABLES

LIST OF ABBREVIATIONS

MOB	Main Olfactory Bulb
CA1/CA2	Cornu Ammonis 1 / Cornu Ammonis 2 Hippocampus
CCM	Convergent Cross Mapping
CCS	Convergent Cross Sorting
MeA	Medial Amygdala
Amyg	Amygdala
PPO	Proximal Policy Optimization
RL	Reinforcement Learning
SLEAP	Social LEAP Estimates Animal Pose
OKS	Object Keypoint Similarity
AUC	Area Under The ROC Curve
AUC-PR	Area Under The Precision-Recall Curve
mAP	mean Average Precision
mAR	mean Average Recall
KL	Kullback-Leibler

ACKNOWLEDGEMENTS

Thank you to Andrea Chiba for taking in a wayward graduate student and being a great mentor. Her career is defined by a significant amount of foresight in her approach to science, leading to science that will remain insightful and inspiring for years to come. Thank you also to Laleh Quinn for her expert supervision and training as an electrophysiologist. Her openness to inquiry and bright spirit made working in the lab a true pleasure. Thank you to my dissertation committee, Doug Nitz, Ginny de Sa, Lara Rangel, and Cathy Gere, for supporting me along my academic journey, challenging me to do my best, and always asking the right questions.

Thank you to my partner Emily Yamate for sticking with me through thick and thin. Your kindness and sense of humor has made life worth living and I owe you enormous gratitude for putting up with my shenanigans. This would not have been possible without your love and support!

I owe significant thanks to Janet Wiles for her endless support and mentorship regarding robotics, dynamical systems and artificial neural networks. Thank you to the Australian robotics team: Scott Heath, Carlos Ramirez-Brinez, and Ola Olsson. Special thanks to Kristyn Hensby and Jt Taufatofua for making me feel truly welcome and part of the team, while making science fun!

Thank you to Ayse Pinar Saygin for always demonstrating excellent scientific rigor and giving a history major a chance to become a computational neuroscientist. I would like to acknowledge valuable conversations and mentorship from Burcu Aysen Urgen and Luke Miller.

I would like to acknowledge my collaborator and co-conspirator Leo Breston for lending his exceptional mathematical mind to this project, and for eating fish with me after climbing the Glasshouse mountains. Having a loyal cadre of research assistants has been the key to my success, a special thanks to Rhiannon Lucero-Moore, Leigh Sena, Raunit Kohli, Lacha “Chuck”

Gluzman, and Greyson Sims. I am very grateful for the support from my labmates in Chiba, Nitz and Rangel Lab: Luisa Schuster, PK Huang, Mary Mullane, Victor Minces, Marcelo Aguilar-Rivera, Emily Winokur, Nicole Butler, Estelita Leija, Akshay Nagarajan, Pam Riviere, Janet Tung, Mia Borzello, and Teryn Johnson. Thank you also to Andy Alexander and Jake Olsen for teaching me how to build neural implants. Warm thanks to Fernando Contreras and Hudson Cooper for making the lab feel like home and for sharing endless amounts of passion about cybernetics and complex systems.

Thank you to my cohort Carson Miller-Rigoli, Joey Relaford-Doyle, Rachel Bristol, Tom Donoghue, Richard Gao, Arturs Semenuks, Larry Muhlstein and Amanda Song. I wouldn't have made the transition from history to science without your unwavering support!

Thank you to Seana Coulson for allowing me to explore the philosophical basis of cognitive semiotics in animals, that was truly a lot of fun and I look forward to more collaborations in the future. Thank you to Marta Kutas for teaching me to have a good poker face and always pushing for rigorous scientific experimentation.

I am thankful for valuable collaborations and endlessly exciting conversations with Tessa Verhoef, Deborah Forster, Erfan Nozari, Beth Accomando, Miguel Rodriguez, Andrew Bollhagen, Noah Guzman, Andrew Wilson, Zed Sehr, John Peñate, David Rosenthal, Alex Kiefer, Michael Cohn, Michael Tolston, Gregory Funke, David Ferris, Alvin Li, Grant Leuning, Ryan Schwartz, Federico Rossano, Stefan Tanaka, Ikuma Adachi, and Mark Turner.

Thank you to my parents Jeffrey and Lois Leonardis and the rest of my family for always being there for me and being patient with me while I finished grad school.

Chapter 2, in full, is a reprint of the material as it has been submitted and is under review for publication in Frontiers in Psychology: Special Issue on Robots and Bionic Systems as Tools

to Study Cognition: Theories, Paradigms, and Methodological Issues, 2022, Leonardis, Eric J., Breston, Leo, Lucero-Moore, Rhiannon, Sena, Leigh, Kohli, Raunit, Schuster, Luisa, Barton-Gluzman, Lacha, Quinn, Laleh K., Wiles, Janet, & Chiba, Andrea A. The dissertation author was the primary researcher and first author of this paper.

Chapter 5, in full, is a reprint of the material as it appears in material from a paper that has been published in the journal Scientific Reports, 2021, Breston, Leo, Leonardis, Eric J., Quinn, Laleh K., Tolston, Michael, Wiles, Janet, & Chiba, Andrea. A. The dissertation author designed the experiment, collected the data used in this paper, and was co-author of this paper.

Chapter 6, in part, is a reprint of the material as it appears in IEEE/RSJ International Conference on Intelligent Robots and Systems (IROS), Madrid, Spain, 2018, Heath, Scott, Ramirez-Brinez, Carlos, Arnold, J., Olsson, Ola, Taufatofua, Jon, Pounds, Pauline, Wiles, Janet, Leonardis, Eric, Gygi, Emmanuel, Leija, Estelita, Quinn, Laleh, Chiba, Anderea. The dissertation author collected the data used in this paper and was co-author of this paper.

VITA

2022 Doctor of Philosophy in Cognitive Science
University of California, San Diego

2017 Master of Science in Cognitive Science
University of California

2014 Bachelor of Arts in History, Psychology and Chinese Studies
Hofstra University

AWARDS

2019-2017 "Discovering patterns in human-robot interaction: New tools for complex adaptive social systems" US-AU Air Force Office of Scientific Research / Defense Science and Technology Group Grant**.**
$300,000
Best paper award at the 1st Annual Review and Workshop AFOSR – DSTG Co-Sponsored Research Program on Trusted Autonomy

2017-2016 "A Neurobehavioral Foundation for Affective Computing: Rat-Robot Brain-Computer Interfaces for Dynamic Interaction"
Kavli Institute for the Brain and Mind (KIBM) Innovative Research Grant
$25,000

PUBLICATIONS

Leonardis, E.J., Breston, L., Lucero-Moore, R., Sena, L., Kohli, R., Schuster, L., Barton-Gluzman, L., Quinn, L.K., Wiles, J., & Chiba, A.A. (Under Review) Interactive Neurorobotics: Behavioral and Neural Dynamics of Agent Interactions. *Frontiers in Psychology Special Issue on Robots and Bionic Systems as Tools to Study Cognition: Theories, Paradigms, and Methodological Issues.*

Leonardis, E., Semenuks, A., & Coulson, S. (2021). What is indexical and iconic in animal blending? In Conceptual Blending in Animal Cognition: A Comparative Approach. *43rd Annual Cognitive Science Society Conference 2021*, Vienna, AUT

Leonardis, E. (Chair), Turner, M., Pelkey, J., Semenuks, A., Coulson, S., Adachi, I. & Forster, D. (2021). Conceptual Blending in Animal Cognition: A Comparative Approach. *Symposium at the 43rd Annual Cognitive Science Society Conference 2021,* Vienna, AUT

Breston, L., **Leonardis, E. J.,** Quinn, L. K., Tolston, M., Wiles, J., & Chiba, A. A. (2021). Convergent Cross Sorting for Estimating Dynamic Coupling. *Scientific Reports,* 11(1), 1-10.

Heath, S., Ramirez, C., Arnold, J., Olsson, O., Taufatofua, J., Pounds, P., Wiles, J., **Leonardis, E.,** Gygi, E., Leija, E., Quinn, L., Chiba, A. (2018) PiRat: An autonomous framework for studying social behavior in rats and robots. *2018 IEEE/RSJ International Conference on Intelligent Robots and Systems (IROS 2018), Madrid, Spain*.

Leonardis, E. (2017). Amygdala. & Hippocampus. *Encyclopedia of Animal Cognition and Behavior*. (Eds. Vonk, J. & Shackelford, T.K.) Springer.

Leonardis, E. & Saygin, A. (2015). Humanoid Robots and the Social Brain: Ethical Implications. *The Emergent Policy and Ethics of Human-Robot Interaction Workshop At Human-Robot Interaction (HRI) 2015 10th ACM/IEEE International Conference*.

TEACHING at UC San Diego

Instructor of Record, Dept. of Cognitive Science
COGS 8: Hands-On Computing, Spring 2022, Winter 2022, Winter 2021, Fall 2020, Spring 2020 Spring 2019
COGS 100: Cyborgs Now and In The Future, Winter 2019

Teaching Assistant, Dept. of Cognitive Science,
COGS 100: Cyborgs Now and In The Future, Fall 2021, Spring 2018, Fall 2018
COGS 170: Brain Waves Across Scales, Winter 2020
COGS 179: Electrophysiology of Cognition, Fall, 2019
COGS 8: Hands-On Computing, Fall 2016, Winter 2016
COGS 184: Modeling the Evolution of Cognition, Spring 2021, Winter 2015
COGS 17: Neurobiology of Cognition, Fall 2015
COGS 102C: Cognitive Design Studio, Spring 2015

Instructor, Dean's Extension, Academic Connections Program
AC Introduction to Cognitive Science, Summer 2015, 2016, 2017, 2018, 2019, 2020, 2021
AC Hands-On Computing, Summer 2020

ABSTRACT OF THE DISSERTATION

Interactive Neurorobotics:
Brain and Body Coupling During Interactive Multi-Agent Scenarios

by

Eric Jeffrey Leonardis

Doctor of Philosophy in Cognitive Science

University of California San Diego, 2022

Professor Andrea Chiba, Chair

This thesis is about the investigation of brain and body coupling with agents and objects at multiple scales in different contexts. We seek to characterize the reaction of behavioral and multi-region brain dynamics during interaction between rodents and other conspecifics, robots, and objects. Then we examine how these coupled agents and systems learn in the form of habituation during exploration of other agents. We highlight the importance of regulatory behaviors such as grooming, which may serve an important functional role in stabilizing the nervous systems using a phase alignment. The lessons learned from this empirical research are used to inform design

principles for an autonomous interactive robot. These regulatory observations will act as a foundation for the proposal of a new learning framework which emphasizes the functional role of regulatory behaviors for maximizing safety. Recent studies introduce interactive robots as a dynamic comparison case or control condition for object and social interactions for the purposes of neuroscience. This dissertation will examine how interactive robots, as dynamic objects or potentially social others, can act as tools for probing questions related to agency, animacy and autonomy in social cognition, self-regulation, and perceptual exploration. Descriptions of the current state of interactive neurorobotics as a field are set forth, while also establishing design principles based on empirically-grounded interaction design studies. Chapter 1 is an introductory chapter introducing brain and body coupling as the basis of social cognition, animat and systems research and neural coupling during agent assessment. Chapter 2 examines how agent-based interactions perturb behavioral and brain states by characterizing the dynamics of behavioral and brain states that emerge during interaction with rats, robots, and stationary objects. To quantify dynamic interactions, we demonstrate the use of convolutional neural networks for offline animal and robot tracking. Chapter 3 examines olfactory habituation with rats and robots. Chapter 4 compares phase-amplitude coupling across brain regions during exploratory sniffing and regulatory self-grooming behavior. Chapter 5 provides a dynamical systems interpretation of the behavioral and neural data using a novel method for measuring dynamic coupling between neural systems, known as Convergent Cross Sorting. This lexicon of neurobehavioral dynamics will be used to inform design principles for interactive neurorobotics platforms. The results suggest that allostasis and autonomic regulation are crucial for designing interactive robots. In Chapter 6, exploration and regulation-based principles learned from the empirical portion of the dissertation are applied to developing autonomous algorithms for interactive robots, suggesting an

ethologically grounded approach to learning. The Conclusion examines lessons learned overall and raises some ethical issues in the field of human-robot interaction.

CHAPTER 1: BRAIN AND BODY COUPLING IN SOCIAL COGNITION

Brain and Body Coupling in Social Cognition

Perception, action, and social cognition are inextricably entangled with the body, the environment, and with the other agents around us (De Jaegher & Froese, 2008). The 4E school of cognition asserts that cognition is embodied (body-based), embedded (environment-dependent), extended (includes other technologies, objects, and others) and enactive (exhibits sensorimotor autonomy) (Varela, Thompson, and Rosch, 1991; Wilson, 2002). These points of view compel us to look beyond the individual and challenge traditional notions of reductionism (Nunez and Freeman, 1999). While 4E approaches are often philosophically compelling, they lack sufficient mechanistic grounding in the biophysics of the brain and the body (Rojas-Libano & Parada, 2020; Bechtel and Abrahamsen, 2010). This dissertation will utilize an interdisciplinary approach merging insights from systems neuroscience, robotics, and nonlinear dynamical systems to lay the groundwork for a physiologically grounded theory of brain and body coupling in embodied social cognition.

Social cognition is said to result from an organism's history of coupling with the brain, body and world (Rojas-Libano & Parada, 2020). To develop a compelling embodied theory of social cognition, we must account for physiological processes such as sensorimotor exploration, autonomic self-regulation, and brain-body coupling within and between organisms. In service of investigating brain-body-world coupling in social appraisal, we have proposed and utilized a novel method for measuring nonlinear dynamic coupling. By examining non-linear coupling, we can shed light on how systems within the brain can form holistic bidirectional relationships that are not captured by previous methods. This method was applied to electrophysiological coupling between multiple brain regions in the rat brain during social and regulatory behaviors. These

methods will eventually be extended beyond the brain to examine coupling between agents and other social creatures.

Robots are physically present and embodied agents which can perform behaviors and actions that are more relevant to questions in social cognition research than traditional approaches have been. Neuroscientific studies of social cognition often compare the complexity of living organisms with static objects. The comparison with static objects leaves a lot to be desired, and as a result a new wave of studies have turned to the use of dynamic and interactive robots to serve as a better comparison case (Ishi et al, 2006; Wiles et al, 2012; Heath et al, 2018). This dissertation will utilize robots to examine the role of self-propelled motion, animation, and autonomy in social cognition and sensorimotor exploration. The lessons learned from these studies were used to develop autonomous robots and multi-agent systems better able to engage living rodents while accounting for their complex physiological reactions to physical presence.

Animats and Systems Theory

The synthetic approach to understanding behavior relies on our ability to design systems that serve similar functions to the behaviors they are meant to model. Animats are a type of simulated artificial animal that often act as hypotheses about target animal behaviors or functions. The animat approach seeks to capture the situated nature of interactions between sensors, effectors and the environment, taking inspiration from the situated cognition approach (Suchman, 1986; Kirsh, 2009). The animat approach uses methods from robotics, dynamical systems, adaptive learning algorithms, and minimalist design (Brand, Prokopowicz, & Elliot, 1995). Animat systems are types of 'ludic spaces,' an artificial space, lacking the sensory complexity and structure of real space, whose function is to support simplification and gamification of interaction (Adams, 2003). Despite the oversimplified nature of animat ludic

spaces, they serve as compelling arguments about how sensorimotor systems become embedded within a particular ecological niche (Brand, Prokopowicz, and Elliot, 1995). Animats can act as a way of examining and investigating questions in neuroethology by emphasizing sensorimotor contingencies. Despite the majority of animat research being restricted to virtual simulations of vehicles and creatures, a strength of this dissertation is that we will be examining the interaction between embodied animal robots and living creatures. Animats must not only learn about the environments they are in but also learn how to use their own bodies to complete goals (Barandiaran, 2008). In a framework like this, it is important to remain cautious and flexible about how directly the model relates to the target system, as the target system is often significantly more complex than the toy model (Godfrey-Smith, 2005).

The animat approach and field of artificial life (ALife) has a compelling set of principles, but like the themes of cyberpunk literature it is "high on tech, low on life." By creating a juxtaposition between biological and artificial agents, we hope it can highlight the relatively impoverished nature of artificial systems and where they can be improved by taking biology and behavior into account. This dissertation will rely on many frames and theories posited by animatists especially with relation to agency and autonomy. Autonomous agents lie on a continuum of computational entities. Objects are entities with declarative attributes and procedural capabilities. Agents are objects with goals, while autonomous agents are agents with motivations (Aube and Senteni, 1996). This established conceptual and simulation modeling paradigm involves a class of hypothetical systems that, through a resemblance relationship with a target system, should help us characterize and understand some of their essential features and functions. This means that the interrelated components and relations within these hypothetical animat systems gives rise to a set of characteristic features that are shared with the model system.

In his book *Vehicles: Experiments in Synthetic Psychology* (1984), Braitenberg presents to the reader a progression of thought experiments each in the form of a mobile robot controlled by a circuit which links sensors and motors forming elegant neuroethological theories of perception and action. A neurophysiologist who researched visual ganglia and cell assemblies in the fly, Braitenberg took his experience to developing a new toy world of vehicles, describing excitatory/inhibitory mechanisms with contralateral and ipsilateral connections relative to a light source as being in states of fear, aggression, and even love (**Figure 1.1**). When one of the vehicles is in a state of love, its light sensors have inhibitory connections to the actuators on the ipsilateral side. In Braitenberg's playful interpretation, this causes the vehicle to tend to its beloved light with doting admiration, coming just close enough to attend to its sweet lovely light. The synthetic approach championed by Braitenberg shows how connectivity between sensors and effects can result in interesting ecologically relevant behaviors.

We can trace the influences of the "animat way" and Braitenberg's *Vehicles* back to Jacques Loeb's "tropisms" in animals and man, which was heavily influential on the early learning theories of Watson (Greenspan & Baars, 2005; Loeb, 1918). A tropism is when an animal or plant is drawn to or orients towards an external stimulus . For instance, a heliotrope is the growth of a plant in the direction of the sun. Loeb was particularly interested in explaining bodily symmetry. Cited by Braitenberg as a key influence, Loeb proposed a mechanism that has excitatory and inhibitory heliotropic relations to external stimuli and presented diagrams of galvanotropic reactions of legs as they were related to stimulation (see **Figure 1.1**). Loeb was a champion for the "mechanistic conception of life" (the title of one of his books), specializing in mechanistic accounts of volitional and instinctive action in the nervous system. In *Forced Movements, Tropisms, and Animal Conduct,* Loeb introduces what he calls the "artificial

heliotropic machine," declaring that "the best proof of the correctness of our view would consist in the fact that machines could be built showing the same type of volition or instinct as an animal going to the light." Loeb goes on to describe an example of an artificial heliotropic machine by describing an orientation mechanism that was built into the "Hammond Dirigible Torpedo."

Tolman is a key figure in the cognitive psychology of the rodent, having posited cognitive theories during a time when such things were denounced as heresy. In light of the discovery of hippocampal place cells and the cell assemblies that support spatial navigation (O'Keefe and Dostrovsky, 1971), it became clear that one of Tolman's key ideas might really be the case, that is that animals actually have an allocentric cognitive map of their position in a maze. Tolman developed a theory of spatial orientation as an automaton (the "schematic sowbug"). Tolman was significantly influenced by the Gestalt psychologists, and rejected crude stimulus response reductionism in favor of cognitive behaviorism.

In addition to citing Loeb as an influence, Tolman cites the work of Gestalt psychologist Kurt Lewin, who is known as the father of both social and industrial/organizational psychology. Lewin was a general systems theorist who was particularly concerned with representing organism environment interactions using a series of diagrams that use vector fields to describe the behaviors and affordances of a particular situation. Lewin, the creator of Topological Psychology, was talented at representing and envisioning an organism's psychological environment in the form of mathematical formalisms and maps that could be visualized for the purposes of hypothesis generation and testing (**Figure 1.1**). Lewin's general systems approach paired with topological maps of the environment, conceptualized goal-oriented behavior in terms of vector forces that determined social behavior (**Figure 1.1**). A key lesson from Gestalt psychology is that animals may need to temporarily retreat from a goal in order to solve a task.

This was demonstrated in animal behavior through Lewin's colleague Wolfgang Kohler's ape experiments requiring retreating to a platform and moving it towards a suspended banana in order to acquire it. Lewin's topological diagrams allow for the modeling of such forces for the purpose of explaining goal oriented behavior. These insights are of key importance to the animat approach. Lewin had influential graduate students such as Fritz Heider, who would perform key experiments with Marianne Simmel in the classic 1944 social psychology experiment which demonstrated humans will automatically interpret animated shapes as having social, emotional, and intentional states.

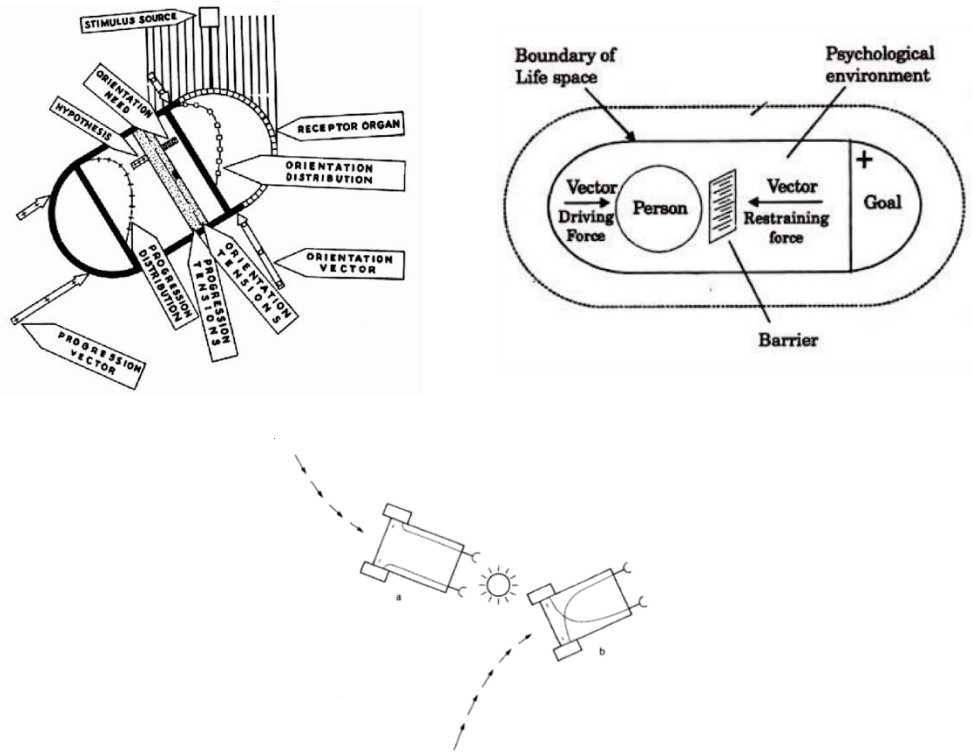

Figure 1.1: Tolman's Sowbug, Lewin's Life Space and Braitenberg's Vehicles

In addition to ethological approaches and situatedness the animat approach has an underlying theme of emphasizing neural architectures. Positing the neural underpinnings of mobile robots is nothing new. Neurophysiologist W. Grey Walter, a participant in the Macy

Conferences on Cybernetics in 1953, also contributed to this homeostatic robotic lineage with his self-charging robotic Tortoises. Walter's robots implemented specific tropisms and he studied their behavior maintaining a series of homeostatic feedback loops. The tradition set by Shannon, Walter, and Tolman paved the way for Braitenberg's Vehicles, and now as neuroscience matures provides an interesting framework to further investigate the role of situated body, brain and environment interactions underlying agency.

Neural Coupling During Agent Assessment

When assessing whether machines can think like humans, a popular method of agent assessment is the Turing Test (Turing, 1950). Turing posited a thought experiment where a human judge is physically separated from either a computer or a human on the other side. They can only interact with written language passed back and forth. For a computer to pass the test they must respond in such a way that the judge is convinced they are engaging in thinking. Saygin has advocated for an advanced version of the Turing Test with the dividers removed that she called the "Neural Turing Test," which posits that to truly pass the test the same brain areas recruited during social interaction with humans should also be recruited when interacting with humanoid robots acting as human replicants (Saygin, Cicekli, & Akman, 2000; Leonardis & Saygin, 2015). This points out the possibility that even if someone may consciously believe that the agent is human, some unconscious brain processes might have collected evidence to suggest the contrary. Saygin and Urgen have provided neuroimaging and electrophysiological results to suggest that brain areas that process the bodily form of a humanoid robot may respond to their human-likeness, however an android's unnatural motion characteristics can be a dead give away resulting in error signals propagated throughout the brain (Saygin et al, 2012; Urgen, Kutas, & Saygin, 2018). This dissertation is concerned with a similar set of questions as to what degree

mobile robots pass a version of the Neural Turing Test for animals. Robots may seem like an artificial or unnatural stimulus. However, urban ecology shows that rats are actually quite well suited to master human technologies, as evidenced by the proliferation of rats throughout human societies across the world (Sullivan, 2005). The use of animals allows for more invasive and fine grained measurements of the brain that are often not available for investigation in humans. This dissertation asks: are circuits of the brain that are usually recruited for social processing of a conspecific also recruited when assessing a mobile robot?

The mechanistic role of neural oscillations in cognition and behavior has been increasingly emphasized in systems neuroscience in recent years (Buszaki, 2006). Neural oscillations refer to the generated rhythmic patterns of electrical activity that groups of neurons naturally exhibit in vivo and have been widely studied (Buzsaki and Draguhn, 2004; Fries, 2006). While historically they were viewed as largely epiphenomena of single unit activity, recently it has been emphasized that neural oscillations are emergent properties in complex neural systems and may be causally efficacious components in cognitive mechanisms (Fries, 2006). Due to their mathematical similarity with the circadian rhythm mechanisms specified by Bechtel and Abrahamsen (2012), neural oscillations seem to be promising candidates for explanations of cognition and behavior.

Tinbergen suggested that observational ethology can generate hunches about the function of patterns of behavior, leading to the best way to solve that problem if the animal was designed by an engineer. Following behavioral ecology, the experimenter asking oneself about the concept of current utility relative to a particular behavior is a way to inquire about the function (Bateson & Laland, 2013). We recognize that this is not a traditional approach to cognitive neuroscience, because this methodology resists the temptation to impose psychological categories beforehand

and emphasizes the neural structure of naturalistic behavior. Whereas it may create experiments with a more observational bent in pursuit of ecological validity, it should be better equipped to tell us what the brain is trying to do for the system. We will utilize the methods of computational ethology to create a quantitative ethogram for the purpose of making these observations more concrete and testable using statistics (Datta et al, 2019). These methods will be used in service of the questions of neuroethology, which uses the tools of ethology to inquire about how brain functions support behavior.

In particular, in this study we will examine how the neural circuitry for assessing an individual's own state is co-opted to assess other agents (Fotopolou & Tsakiris, 2016). An individual's brain and body are intricately coupled in order to promote behavior that is adaptive to social demands and demands of the environment (Zhao, et al., 2022). In exploring new creatures, places and things, an individual inevitably uses their past perceptions, their ability to sense, and their decisive ability for action. We often consider the state of the brain in response to these processes, but it is also important to consider the way in which the body and brain coordinate through the autonomic nervous system and information coming from the body to the brain and vice versa (Livneh & Andermann, 2021). Rats have a keen capacity to recognize and act on olfactory information, not only based on past perceptions but even on stimulus predispositions and their evolutionary histories (Rosen et al, 2015). Thus, given limits on sampling from a variety of sensory areas, selecting olfactory sensing, and recording from the olfactory bulb, in rodents is intended to provide insight into sensing other agents and objects. Of added value, the olfactory bulb contains signal information about the autonomic system through signals indicative of respiration rate (Rojas-Libano et al, 2014). The vagus nerve carries visceral information from the autonomic system into the insular cortex and the amygdala, allowing

organisms access to the state of their bodily systems (for review see Chen et al, 2021). These two structures also receive direct projections from the olfactory system and are interconnected with each other. Additionally, the amygdala is densely interconnected with the hippocampus, a structure that inevitably codes spaces and places that can guide the state of an organism and their actions (McGaugh, Cahill, & Roozendaal, 1996). The hippocampus also receives heavy projections from the olfactory system, not surprisingly, as rodent olfaction can also guide spatial function (Jacobs, 2012). Taken together the circuit represents a dynamic system allowing an organism access to the state of their body and the outside world in space and at a particular point in time. Whereas each of the structures mentioned, the olfactory bulb, the amygdala, the insular cortex, and the hippocampus, can work in concert, the individual unit activity in the structures are demonstrated to have multiple roles in coding different aspects of the brain and body, in addition to expressing characteristic rhythms (Tort et al, 2018). To examine the dynamics, rhythmic signatures, and coupling capacity of the system, recording the oscillatory activity in each region was the best starting point to begin to understand the physiological space in which one might assess their own state and repurpose the same circuitry for incorporating the assessment of other organisms, objects, and agents in the environment.

Fries (2006) puts forward the ‘communication-through-coherence’ hypothesis which posits that the structure of neural communication between neural groups is ‘mechanistically implemented’ by coherence between neural oscillations. Coherence, in this view, refers to the phase-locking of oscillating neural groups as measured by fluctuations in spike-timing relative to the local field potential. The origin of the local field potential remains a mystery, but is likely some function of pre- and post- synaptic potentials, as well as subthreshold oscillations (Brea et al, 2009; Buzsaki, 2012). Fries suggests that these phase-locked oscillations open and close

rhythmic temporal windows where neurons can communicate effectively. Fries claims that for a "sending group to communicate a message effectively to a receiving group, the sending group's output has to be timed such that it arrives at the receiving group when that group is excitable" (2006, p. 476). When saying that these neural groups are "communicating a message" between a "sending group" and "receiving group," Fries appears to be appealing to a fairly traditional view of information processing in the brain. This concept is reminiscent of a set of coordinated telegraphs reminiscent of Shannon's formalization of information within a sender/receiver framework (Shannon, 1948). Given the lessons provided in traditional approaches to information theory by cybernetics and systems theory, such as the use of positive and negative feedback in these communication systems, Fries' explanation might lack sufficient complexity to provide an adequate explanation of component operations that underlie cognition and behavior. What Fries' paper does offer is an explanation for the operations of "neural groups" and lays a potential foundation for dynamic mechanistic explanations of large-scale neural communication, when considered in concert with some other proposed theories.

Fries' earlier collaborative work (Engel, Fries, & Singer, 2001) seems to suggest that neural groups are highly variable in terms of scale and organization depending on the explanandum of interest. These neural groups could either be composed of millions of neurons scattered throughout the cortex and measured by the local field potential, or of single units, each coordinating with a few thousand others in their local area. These neural groups seem to be highly dependent on the organization of the neural system in question. In order to clarify the meaning of Fries' "neural groups," we might be better served referring to them as 'cell assemblies.' Buszaki and Draguhn define 'cell assemblies' as "distributed networks of neuronal groups that are transiently synchronized by dynamic connections" (2004). They specify that the

mechanisms that produce these assemblies are not known, but one mechanism is the change of synaptic weighting of neural connections, the other being the cost effective use of oscillations in a similar fashion described by Fries (2006). This makes for an interesting problem, that "cell assemblies" are the components of the mechanism of interest and can only be defined in terms of their interaction. Buzsaki (2006) suggests that cell assemblies resemble clusters that form around network hubs in graph theoretic small world networks, mainly, clusters of highly interconnected nodes that are responsible for specific computational functions.

Neural oscillations are a prime candidate for dynamic mechanistic explanations of perceptual, cognitive and behavioral function, yet in its current state, defined components remain underspecified and the organization of systems often remains unclear (Bechtel and Abrahamsen, 2010). Fries' communication-through-coherence hypothesis offers one possible component operation performed by neural assemblies, but it is not clear how these simple operations coordinate between components to explain perceptual and cognitive mechanisms of interest. Rather than "communication-through-coherence" this dissertation argues for "communication-through-coupling" as a better model of neurophysiological communication. We fully address this by developing methods for examining coupling dynamics in Chapter 5. In the forthcoming chapter, we first establish a study examining the introduction and assessment of different rats, agents, and robots, in addition to the space of exploration. Subsequent chapters delve into the efficacy of individual behaviors evident within this framework, culminating in the development of multi-agent autonomous robotic systems with coupled artificial neural networks that operate within the developed ethological framework.

CHAPTER 2:
INTERACTIVE NEUROROBOTICS:
BEHAVIORAL AND NEURAL DYNAMICS OF AGENT INTERACTIONS

The content within this section, titled “Chapter 2: Interactive Neurorobotics: Behavioral and Neural Dynamics of Agent Interactions” reflects material from a paper that is in review at Frontiers in Psychology Special Issue on Robots and Bionic Systems as Tools to Study Cognition: Theories, Paradigms, and Methodological Issues. The full citation is as follows:

Leonardis, E.J., Breston, L., Lucero-Moore, R., Sena, L., Kohli, R., Schuster, L., Barton-Gluzman, L., Quinn, L.K., Wiles, J., & Chiba, A.A. (Under Review) Interactive Neurorobotics: Behavioral and Neural Dynamics of Agent Interactions. *Frontiers in Psychology Special Issue on Robots and Bionic Systems as Tools to Study Cognition: Theories, Paradigms, and Methodological Issues.*

Abstract

Interactive neurorobotics is a subfield which characterizes brain responses evoked during interaction with a robot, and their relationship with the behavioral responses. Gathering rich neural and behavioral data from humans or animals responding to agents can act as a scaffold for the design process of future social robots. The goals of this research can be broadly broken down into two categories. The first, seeks to directly study how organisms respond to artificial agents in contrast to biological or inanimate ones. The second, uses the novel affordances of the robotic platforms to investigate complex phenomena, such as responses to multisensory stimuli during minimally structured interactions, that would be difficult to capture with classical experimental setups. Here we argue that to realize the full potential of the approach, both goals must be integrated through methodological design that is informed by a deep understanding of the model system, as well as engineering and analytical considerations. We then propose a general framework for such experiments that emphasizes naturalistic interactions combined with multimodal observations and complementary analysis pipelines that are necessary to render a holistic picture of the data for the purpose of informing robotic design principles. Finally, we demonstrate this approach with an exemplar rat-robot social interaction task which included simultaneous multi-agent tracking and neural recording

Introduction

Figure 2.1: A. An artist's depiction of rat-robot and rat-object interactions inspired by Quinn et al., 2018 (Illustration by Rosana Margarida Couceiro). B. A picture of live rat-robot interaction.

As technology and automation increasingly permeate every aspect of modern life, our relationship with these systems have begun to blur the lines between tool use and social interaction. Humans are routinely being asked to engage with artificial agents in the form of chat bots, recommender systems, and social robots which all exhibit facets of agency more familiarly associated with living beings (Saygin et al., 2012; Saygin & Cicekli, 2002; Gazzola et al., 2007). Such a promethean transition has raised an urgent need to study how biological organisms adapt and extend their social mechanisms to new digital simulacra (Baudrillard, 1981). The proliferation of technology has made sophisticated robotics accessible to many more scientists,

empowering them to create a wide array of new applications, such as the use of robots to investigate animal models by physically interacting with those animals.

The goals of this research can be broadly broken down into two categories. The first, seeks to directly study how organisms respond to artificial agents in contrast to biological or inanimate ones. The second, uses the novel affordances of the robotic platforms to investigate coordination dynamics complex interaction phenomena between agents, such as coordinated dynamics during minimally structured interactions that either peak the organism's curiosity or evoke avoidance and fear responses resulting in a rejection. Here we propose that to realize the full potential of the approach, both goals must be integrated as they provide complementary information necessary to contextualize one anothers results. For example, if one were to use a robot to study acceptance, without characterizing the organism's differential response to robots and conspecifics, then it would be difficult to know whether the results reflected a generalizable reaction, or was an artifact of the animal's particular response to the robot. Despite these epistemological liabilities, the degree to which animals' responses differ between agent types, as well as the character of those differences, remains an open question.

At the nexus of our broadly construed categories is the nascent field, interactive biorobotics, that uses robots to experimentally probe questions in behavioral ethology, neuroscience, and psychology, using a variety of human and animal assays (Ishii et al., 2006; 2013; Gergely et al., 2016; Lakatos et al., 2014; Narins et al., 2003; Narins et al., 2005). Robot frogs that can emit auditory calls have been set up in environmental habitats and elicit fighting and even mating responses from wild frogs (Narins et al., 2003; Narins et al., 2005). Robot fish that interact with living schools of fish and vibrating robots that attract bees have shown effects on collective behavior in laboratory and naturalistic environments (Schmickl et al., 2021). Robot

rats, like the Waseda Rat and the iRat, interact with living rats and affect their behavior in laboratory settings (Ishii et al., 2006; Wiles et al, 2012).

In this paper we provide multimodal recordings from rats engaged in a social experiment with rats, robots, and objects. We show that interactions with agents of varying animacy and motion characteristics evoke different behavioral responses. In addition, we show measurable variations in the activity of multiple brain regions across different interactive contexts.

Background

Real organisms do not exist within a sterile world, acting against a quiescent backdrop. The world they adapted to is dynamic, inhabited by other agents, each behaving and interacting according to their own imperatives. Therefore, if science is to actually understand how the brain synthesizes stimuli and produces effective behavior it must tackle these complex, weakly constrained settings. It is technically complex to administer experimental manipulations in a minimally constrained environment, and the availability of new technology created an opportunity for experimentalists to partner with roboticists and computationalists to create data capture and analysis tools necessary to extract robust effects from the results of their use.

Interactive biorobotics presents a promising new approach to facilitate experimental manipulation while retaining the complexities of inter-agent dynamics. As Datteri suggests, interactive biorobotics is a methodologically novel field that is distinct from classical biorobotics (Datteri, 2020). In classical biorobotics experiments, the robot is meant to “simulate” or replicate a function of a living system without direct interaction with the organism itself. In interactive biorobotics, the robot is meant to stimulate interaction with living systems and is instead bestowed with certain capacities to engage and stimulate a living system. The target of the explanation is the behavior of the living system in response to the robotic agent. A key aspect of

interactive biorobotics is the integration and habituation of living systems to interactive robot counterparts (Quinn et al. 2018, Datteri, 2020). A popular example of an interactive biorobotics paradigm with animals was the Waseda Rat, a rat-like robot that continuously chases a living rat to induce anxiety-like behavior (Ishii et al, 2006; Shi et al, 2013).

Many experiments have demonstrated the viability of this technique for investigating neuroscientific questions. These results are the purview of interactive neurorobotics, a subfield which characterizes brain responses evoked during interaction with a robot, and their relationship with the behavioral responses. An early example of a pioneering interactive neurorobotics study is Saygin et al. (2012), which used neuroimaging to present human subjects with robots and androids for the purposes of studying the neural basis of the "uncanny valley." This is an effect which shows that as a robot's appearance increases in human-likeness, the more eerie or creepy it may seem to a human during interaction (Mori, 1970; Saygin et al, 2012). Behavioral evidence has been presented suggesting that macaque monkeys also have a similar response when presented with virtual avatars (Steckenfinger & Ghazanfar, 2009). However, it is unknown to what extent the uncanny valley effect is present in other animals, like rodents. While this is a fascinating question, this paper seeks to examine neural and behavioral responses to non-rodent-like robots with hopes of sidestepping any potential uncanny valleys leading to easier acceptance.

An example of an interactive neurorobotics experiment, where the brain is measured along with animal behavior, was conducted with the predator-like robot known as "Robogator." This robot alligator that can walk and bite, interacted with rats in a dynamic foraging task (Choi & Kim, 2010). In their task, as a rat approaches a food reward, the Robogator suddenly snaps its jaws towards the rodent, resulting in an approach-avoidance conflict paradigm. In this

experiment, Choi and Kim (2010) drastically inhibited amygdala function by locally infusing muscimol (a GABA agonist) and inducing electrolytic lesions. They found that without amygdala function, animals showed diminished fear responses towards the robot. They also demonstrated that local infusions of muscimol globally suppressed amygdala activity, leading to increased exploration of the robot. Similar approach and avoidance dynamics are present in a variety of behavioral paradigms related to predation, social interaction, reward learning, and threat detection (Jacinto et al., 2016; Mobbs & Kim, 2015). The increase in exploration under conditions in which the amygdala is suppressed underscores the importance of the state of the animal in approaching potentially threatening, frightening, or unknown stimuli.

When potential danger or even conditions of high uncertainty are present, there is a cost to exploration due to rats' natural propensity for neophobia (Mitchell, 1976; Modlinska et al., 2015). Inherent in introducing robot counterparts to rats is not only the uncertainty of novelty but also risk assessment regarding the fear of harm. Thus, in order to explore robots, rats must engage in regulatory behaviors allowing the neural system to enter states that allow exploratory behaviors. Inevitably, this necessitates a balance between the sympathetic nervous system and the parasympathetic nervous system, invoking allostatic processing in which systemic stability is achieved through continuous change. Robots have been more often used in fear and stress inducing paradigms with novel robots that exert extreme regulatory demands on the rat (Ishi et al, 2006; Choi and Kim, 2010). During the management of uncertainty, self-regulatory behaviors actively modulate internal demands to meet external demands (Nancy & Hoy, 1996).

In addition to examining behaviors related to novelty and fear, studies have also been performed examining the similarity between rodent social behaviors and behaviors toward a robot. Rats have been shown to behave similarly towards mobile robots as they do to rats,

exhibiting behaviors such as: approaching, avoiding, sniffing, and following (del Angel Ortiz et al, 2016; Wiles et al, 2012; Heath et al, 2018). The analysis showed that the rats demonstrated similar relative orientation formations when interacting with another rat or moving robot. Analysis of relative spatial position in rat-rat dyads in comparison with rat-robot dyads show similarities, raising the question of whether these dynamic interactions might have social elements (del Angel Ortiz et al, 2016). Endowing robots with coordination dynamics that mitigate concerns of dominance still leave uncertainty regarding potential animacy of the agent.

A robot's ability to engage in self-propelled motion is crucial for its potential to elicit social and attentive behaviors. Studies of social recognition and novel object recognition traditionally disregard dynamic objects that exhibit self-propelled movement despite early demonstrations that even two-dimensional objects that exhibit self-propelled movement are often associated with sociality, agency, and animacy detection (Heider & Simmel, 1944). Self-propelled motion can take various forms. Biological motion is associated with maximizing smoothness and can be recognized as animate even with minimal representation (Flash & Hogan, 1985; Todorov & Jordan, 1998; Saygin et al., 2004). Mechanical and materials constraints on interactive robots make the use of biological motion rare and difficult to achieve. However, interactive robots provide an opportunity to experimentally manipulate agency by utilizing elements of animation through movement trajectories and temporal coordination (Hoffman & Ju, 2014).

A robotic platform that displayed emergent semi-naturalistic movement patterns is the iRat neurorobotics platform (Ball et al., 2010, Wiles et al, 2012). The iRat was originally developed with a neurally feasible model that simulated the function of the hippocampus, entorhinal cortex and parietal cortex for the purpose of learning spatial environments (Ball et al.,

2010). By virtue of entering an environment and exhibiting appropriate spatial navigation and object avoidance, iRat garnered observational attention from on-looking rats (Wiles et al.,2012). This brought about the question of whether iRat could be driven to behave in a socially interactive manner that would result in rats engaging in prosocial behavior with the iRat as they do with conspecifics (Rutte & Taborsky, 2008; Bartal et al., 2011). Quinn et al. (2018) used the iRat to interact with rats for the purpose of eliciting social responses and examining prosocial behavior towards robots (For Artists Depiction and Picture of Live Interaction See Figure 2.1). Rats will not only engage in prosocial behaviors with each other, such as freeing other rats from an enclosed restrainer, but have also been shown to reciprocate with robots (Quinn, et al. 2018, Wiles et al., 2012).

In this paper we further prior work by investigating the effect of agent type on both behavioral and neural outcomes. For our experimental model we considered rats engaging in a socio-robotic experiment developed according to principles of rodent-centered design (See Figure 2.1). In this study, rats interacted in a circular arena with other rats, robots, or objects. They engaged in naturalistic behaviors during this time and the resultant observational data was used to characterize the dynamics of rats' behavioral repertoires in the presence of different agents or objects. While the rats were freely behaving, we used multi-site electrophysiological recordings to examine brain states during different behavioral states. We examine how the agent-based interactions influence neural oscillations within local field potentials in the olfactory bulb, amygdala and hippocampus (see Brain Areas of Interest) during grooming, immobility, and rearing behaviors (see Behaviors of Interest). To investigate dynamic interactions, we demonstrate the use of deep learning video tracking for offline multi-animal and robot tracking.

Brain Areas of Interest

The neural circuit examined in this paper was chosen because it spans specific functional aspects critical for social behavior. Together, the olfactory bulb, amygdala, and hippocampus form a tightly connected network (for review see Brodal, 1947) that provide information about autonomic, sensory, spatio-temporal, and affective context (Moberly et al, 2018, Jacobs, 2022) (See Figure 2.2). They are, thus, well situated to provide valuable information regarding the benefits and liabilities of the external environment during social interaction, exploration, and sampling of the sensory information. Further, they have well characterized anatomical connectivity and diverse observed forms of frequency dynamics which makes them an excellent subject for studying the holistic closed loop processing of social information.

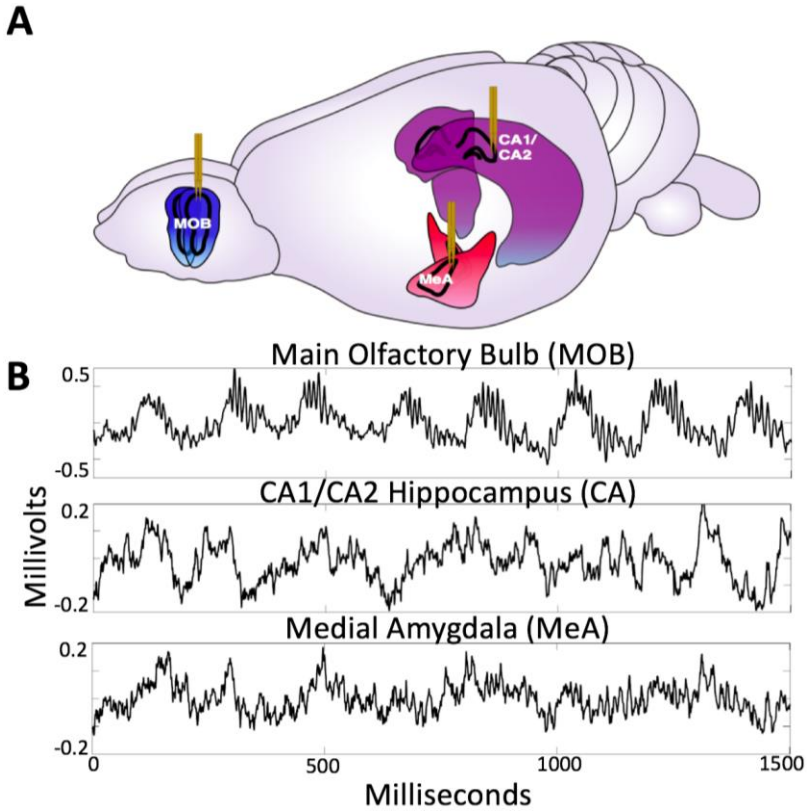

Figure 2.2: A, Diagram of electrode placement in the Main Olfactory Bulb (MOB), Medial Amygdala (meA), Hippocampus (CA1/CA2). Figure adapted from scidraw.io under Creative Commons 4.0 license (Tang, 2019). B, Raw traces from the MOB, Ca1/Ca2 and meA.

The olfactory bulb is a dominant primary sensory organ for rodents, playing a central role in odor discrimination and social cognition for rats (Dantzer et al., 1990). The main olfactory bulb (MOB) local field potential exhibits neural oscillations associated with sensory processing (Kay et al., 2009). Kay et al. (2014) have shown that the frequency of the theta oscillation in the olfactory bulb LFP reliably follows respiration rate (2-12Hz). Respiration-entrained oscillations provide information about the state of the autonomic nervous system, and are distinct from theta oscillations (Tort et al., 2018). It is important to note that respiratory rhythms are not restricted to the olfactory bulb, and are also found throughout the brain (Heck et al., 2017; Rojas-Libano et al., 2014). The following study seeks to highlight the important contribution of olfaction and respiratory-related brain rhythms to brain dynamics (Jacobs, 2012; Lebedev et al., 2018), in order to simultaneously examine sensory and autonomic dynamics as they relate to agent and object interactions. Olfactory and hippocampal theta oscillations also show coherence during olfactory discrimination tasks (Kay, 2014). Recent work also suggests coupling of the beta rhythm from olfactory bulb to hippocampus, which suggests a directionality of functional connectivity going from OB to hippocampus (Gourévitch et al., 2010). The olfactory bulb also exhibits two distinct gamma oscillations associated with contextual odor recognition processing, low gamma (50-60Hz) during states of grooming and immobility and high gamma (70-100Hz) associated with odor sensory processing (Kay, 2005). The low gamma range was selected based on Kay et al (2009). Future work will highlight the role of these rhythms, whereas the current work focuses on dynamics within the theta, respiratory, and beta frequencies. (For raw traces of the MOB LFP see Figure 2.2).

The amygdala is a complex of historically grouped nuclei located in the medial temporal lobe, commonly associated with affective processing, saliency, associative learning, and aspects

of value (Gallagher and Chiba, 1996). Oscillations in the amygdala and their coherence with other brain structures have been linked to learning and memory performance (Paré et al., 2002). The function of the medial amygdala (MeA) is associated with the accessory olfactory system, which receives inputs from the vomeronasal organ, playing a role in social recognition memory, predatory recognition, and sexual behavior (Bergan et al., 2014). The MeA receives input from accessory olfactory areas and has projections to hypothalamic nuclei that regulate defensive and reproductive behavior (Swanson & Petrovich, 1998). The basomedial nucleus has been linked to the regulation and control of fear and anxiety-related behaviors (Adhikari et al, 2015). Amir et al (2015) investigated how principal cells in the basolateral amygdala respond to the Robogator robot during a foraging task. A group of cells reduced their firing rate during the initiation of foraging while another group increased firing rate. It was found that this depended on whether the rat initiated movement, with the authors' suggesting that the amygdala is not only coding threats and rewards, but also is closely related to the behavioral output. (For raw traces of the MeA LFP see Figure 2.2).

The CA1/CA2 subregion of the hippocampus is functionally associated with spatial navigation, contextual information, and episodic memory formation. The CA1 region of the hippocampus is commonly associated with spatial navigation dorsally and social/affective memory ventrally (van Strein et al., 2009). The hippocampal theta rhythm is a 4-10Hz oscillation generated from the septo-hippocampal interactions, which temporally organize the activity of CA1 place cells according to the theta phase. The CA2 region of the hippocampus plays an important role in modulating the hippocampal theta rhythm and also is an essential part in social memory (Mercer et al., 2007; Hitti & Siegelbaum, 2014, Smith et al 2016). CA2 receives projections from the basal nucleus of the amygdala, which plays an important role for contextual

fear conditioning (Pitkanen et al., 2000; Goosens & Maren, 2001). Ahuja et al. (2020) demonstrated that CA1 pyramidal cells were responsive to a robot that indicates a shock zone. Robots have also been developed for the purpose of improving behavioral reproducibility when examining aspects of rodent spatial cognition in neuroscience. When rats navigate through a maze, there can often be a variety of factors that an experimenter might want more control over. In this case a robot with an onboard pellet dispenser was used to regulate the rat's direction and speed as they moved through the maze (Gianelli et al.,2018). (For raw traces of the CA1/CA2 LFP see Figure 2.2B).

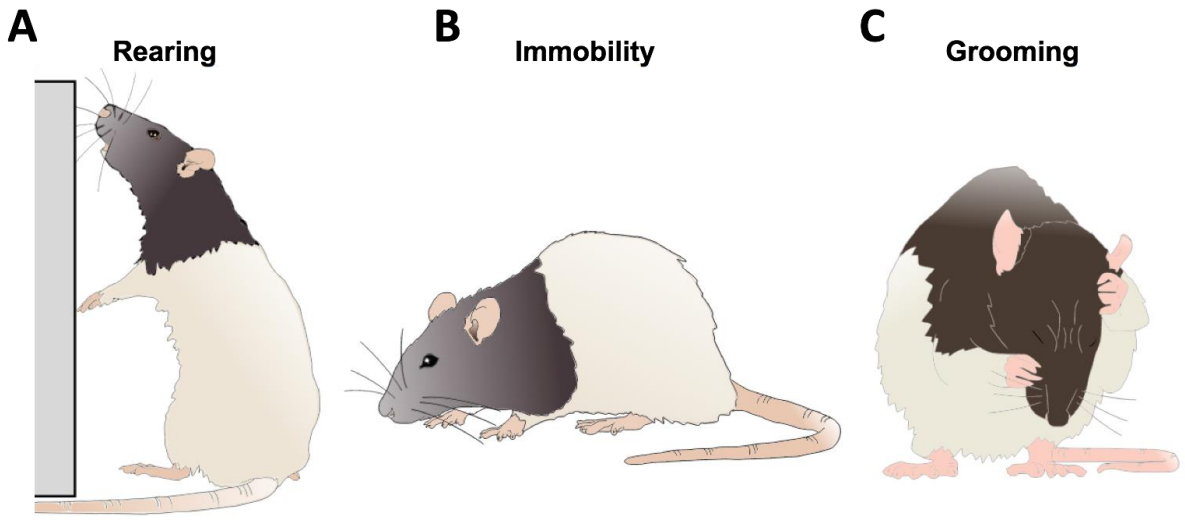

Figure 2.3: A depiction of a rat engaging in rearing, immobility and grooming behaviors. Figure adapted from scidraw.io under Creative Commons 4.0 license.

Behaviors of Interest

The types of behavioral epochs used for the comparative neural analysis were chosen due to their ready identifiability and representation of distinct types of exploratory and self regulatory behavior. The behaviors are generally demonstrated when the rat temporarily stopped running or walking and was not physically exploring the other agent on the open field. The behaviors we prioritized include immobility, self-grooming, and rearing (See Figure 2.3). Given that the state

of the rat differed widely across behaviors, it was particularly important to examine how the presence of different agents (rat, robot, or object) perturbed their state within a particular behavior.

Immobility is a complex behavior distinguished by the motionlessness exhibited by the subject. This behavior is made distinct and significant as an intermediary behavior between the regulatory and exploratory states rats can alternate between. During immobility, the rat is likely in a heightened state of arousal, with an intensity of alertness. With current comprehension, engaging in immobility is a behavior indicative of risk assessment, occurring preemptively to a threat or as a result of one (Kay, 2005). Immobility allows the rat time to acquire and interpret environmental stimuli, triangulate any potential discomfort or stressors, and act accordingly.

Self-grooming, hereafter referred to as grooming, is a behavior inherent to rodents that is communicative of not only hygienic regulation, but also self-regulation of stress relief (Fernandez-Teruel & Estanislau, 2016). Grooming is a regulatory process, which often serves the function of de-arousal (Kalueff et al., 2016). Grooming includes sequences of rapid elliptical strokes, unilateral strokes, and licking of the body or anogenital area. Due to the behavioral complexity of grooming, frequency and duration of grooming bouts is dependent on context (Song, Berridge, & Kalueff, 2016).

Rearing is an exploratory action, exhibited as a means of increasing the rat's access to stimuli in the environment. In both instances, the rat straightens and lengthens their spine and maneuvers their forelegs to increase their height. When rearing, rats increase their sensory exploration of the surrounding environment (Lever, Burton, & O'Keefe, 2006). This fluid behavior varies greatly in its duration and frequency. For the purposes of this paper, rearing was specifically defined with relation to the wall of the environment.

Materials and Methods

Animals and Housing

All experiments and maintenance procedures were performed in an American Association for Accreditation of Laboratory Animal Care (AAALAC) accredited facility in accordance with NIH and Institutional Animal Care and Use Committee (IACUC) ethical guidelines and preapproved by the IACUC committee. 6 Sprague-Dawley rats (n = 6) (Harlan Laboratories) performed in the behavioral experiments. 3 rats (n = 3) were surgically implanted with electrodes for electrophysiological recordings. They were acquired at 6 weeks old and housed in pairs. Cagemates were put together in an enriched environment for 30 minutes a day and were maintained on a 12 hour day/night cycle. After receiving surgery, the implanted rat was single-housed for the whole of the experiment. To offset the lack of social enrichment from being single-housed, they were taken out to play in the enriched environment with the former cagemate on the same schedule.

Experimental Conditions and Trial Information

Trials were collected from a rat and a robot freely roaming in an arena (n = 40). Comparison conditions included object trials (n = 21), social interaction trials with other rats (n = 20), and solo open field exploration (n = 84) (See SI for Animals and Housing). Trial lengths were approximately 3 minutes long. Trials were counterbalanced for order effects. The robots and the animals' were recorded using an overhead camera. The videos were used to hand-label behaviors and estimate position of the interacting agents for each video frame (See SI Behavioral Coding). Rats were surgically implanted with electrodes in the main olfactory bulb, hippocampus and amygdala simultaneously to record local field potentials during freely moving behavior (See SI for Surgical Procedure and Neural Implants and Recordings).

Surgical Procedure

Rats (n = 3) underwent surgery for electrode implantation in order to record local field potentials from multiple brain areas simultaneously. Surgeries were performed in accordance with IACUC ethical guidelines. The rats were treated with isoflurane anesthesia (4-5% induction, 1-2% maintenance) and were placed in a stereotaxic apparatus to allow for placement localization (Kopf Instruments). Three holes were made through the skull, and the underlying dura was removed. LFP signals were referenced to a skull screw above the cerebellum. Anchor screws were inserted around the skull to support the neural implant which was cemented using dental cement. For the stereotrodes, pairs of 25 μm tungsten wire were twisted together and threaded through polyamide insulation. For the tetrodes, four sets of 12 μm wire were twisted together, and threaded through polyimide insulation (California Fine Wire). Electrodes were cut to the same length and wires were gold-plated in solution (Sifco) until impedances were reduced to approximately 100–300 kΩ measured at 1 kHz (Impedance tester IMP-1; Bak Electronics, Germantown, MD, USA). The stereotrodes were implanted using the stereotactic apparatus into the main olfactory bulb (8.5AP, 1.5ML, -3.5 DV), basomedial amygdala (-2.12AP, ±4.0ML, -9.2DV) and CA2/CA1 region of the hippocampus (-3.8AP, 3.8ML, 3.2DV) laterally.

Neural Implants and Recordings

The stereotrodes and tetrodes were connected using gold pins to create contact between the wire and a Neuralynx E/I board cemented to the skull and anchor screws that send the electrical signal to an amplifier for signal processing. In the first rat, activity from 5 stereotrodes encased in polyamide tubing were connected to a 16-channel Neuralynx electrode interface board (EIB-16) that was cemented to the skull. The signals acquired from the E/I board were amplified using the Cheetah-32 system and Lynx-8 amplifiers (Neuralynx Technologies,

Bozemon, MT). Amplifiers were integrated with the Cheetah data acquisition software provided by Neuralynx Technologies. The sampling rate for the recorded local field potentials was 1010.10Hz. Video was recorded from a camera above the field at 29.97FPS at 720x480 pixel resolution. Video was captured through the Cheetah data acquisition software, allowing for alignment between the timestamps of the neural data and video frames.

Signal Processing

Local field potential recordings from amygdala, hippocampus, and main olfactory bulb were indexed according to hand-coded behavioral epochs. To control for amplitude differences between subjects, LFP traces were normalized by overall standard deviation of the LFP per brain region for each rat. An infinite impulse response (IIR) bandstop filter was applied between 59-61Hz in order to filter out 60Hz line noise. Events with artifacts were detected using a .4 millivolt threshold on the CA1/CA2 and amygdala channels, and a .6 millivolt threshold on the MOB channels. An FIR bandpass filter was used to isolate the respiratory rhythm (2-6Hz), theta (6-10Hz), and beta (15Hz-35Hz). Although the respiratory rhythm commonly varies between 2 Hz and 12 Hz, the respiratory frequency overlaps with the theta so the range was restricted (Rojas-Libano et al, 2014). Shifts from respiratory to theta ranges often correspond to slower and faster sniffing rates (Tort et al, 2018). Power spectral densities and spectrograms were estimated using the Julia Fourier Analysis library, which is a windowed average across the log of the absolute value of the fast fourier transform (FFT) of the signal. The FFT decomposes the signal into frequency and amplitude features which can be used to identify the presence of oscillations or aperiodic rhythms in the signal.

Robot

The iRat (n = 2) is a robotics and modeling platform created by the Complex and Intelligent Systems Laboratory (Ball et al, 2010). iRat is a two wheeled mobile robot that is 180mm x 100 mm x 70 mm. The iRat is capable of both WoZ interaction and performing pre-programmed behaviors. Robots were distinguished visually by color (red and white iRat / green and white iRat) and using distinguishing olfactory odors. The Red iRat was tagged with frankincense essential oil, the green iRat was tagged with myrrh essential oil. These odors were chosen in order to match preference profiles and are within the same category of woody scents. Our lab has previously shown that rats do not demonstrate a preference for either scent (Quinn et al, 2018). For information about the experimenter's control of the robot's movement dynamics see SI Wizard of Oz (WoZ). For the experiment, locomotion of both robots was limited and reduced to below 0.5m/s. In addition to the iRats, multiple Arduino-based mobile robots were also used.

Wizard of Oz

While ultimately the goal of interactive neurorobotics as a field will be to examine the interactions between rats and autonomous robots. This experiment is concerned primarily with how the form and motion of the robots compares with the animal data using Wizard of Oz methods and semi-autonomous robots to modulate the robots dynamics. The current experiment uses more traditional HRI methods, like WoZ and semi-autonomous methods. This experiment was performed using the iRat and DIY OpenSource Board of Education Shield robots. Robots and rats freely roamed the open field while the robot was controlled using Wizard of Oz mode (Riek, 2012). Experimenters controlling the robot were instructed to avoid dominance displays, cautiously approach, and modulate the position and movement dynamics to engage exploration

and attentive behavior from the rat. The goal of the driver was to get the rat to follow, chase, or engage in tag-like play with the robot.

Objects

6 Objects (n = 6) were assembled by gloved hands with LEGO pieces. A small drop of diluted essential oils was placed on the back end of the object with a cotton swab so that they could more easily distinguish between the objects. Scents included frankincense, myrrh, tea tree, cedarwood, pine and rosemary. The objects had a length by width by height of 15x10x8cm. Much like the affordances of robots, the objects could support rearing and even climbing or mounting by the rat. Object position was varied from trial to trial to avoid place preferences.

Board of Education Shield Arduino Robot (DIY Option)

Another set of robots (n = 4) were created using an Arduino UNO, an OpenSource prototyping microcontroller that executes code written in Arduino programming language, and the Board Of Education (BOE) Robot Shield Kit by Parallax Inc. These robots were used because they are readily available OpenSource robots that are easily accessible. The BOE kit includes the necessary parts for constructing a three wheeled robot with two continuous servo motors in the back of the robot, and one wheel on the front to allow for stability. Plastic Memorex CD cake boxes were melted and shaped to cover the electrical components of the device to ensure safety. This kit allows for remote-controlled driving by the experimenter (Wizard of Oz (WoZ) mode) or the execution of pre-programmed movements.

Behavioral Video Coding

Video was coded for behavioral epochs using ChronoViz (Fouse, Weibel, Hutchins, Hollan, 2011), as well as ELAN 6.0. The following epochs were extracted during the experiments/trials, with each event having variable length. Rearing was coded when the rat

lengthened their spine and extended their nose in order to better investigate the environment with their paws either braced against an object or wall, or held against the rat's chest when free-standing. Immobility was the final coded behavior, in which a rat remained motionless and alert, while interpreting incoming environmental stimuli. Self-grooming was identified as the animal going through the behavioral sequence of paw licking, unilateral strokes, bilateral strokes, body and anogenital licking. There were three agent subcategories present within the condition, labeled as robot, object, and rat, indicating who or what the subject interacted with during each trial. 1,212 behavioral events were identified in the video data. During trials with the robot agent, there were 75 counts of immobility, and 71 counts of rearing. During the trials with the rat agent, there were 15 counts of immobility, and 39 counts of rearing. The trials with the object, had 128 counts of immobility, and 62 counts of rearing. For the open field trial, there were 119 counts of immobility, and 575 counts of rearing. 128 baseline epochs were pulled from the open field data from epochs where the animal is neither rearing or immobile. When asked to label 100 randomly drawn clips of the behavioral epochs, agreement between two independent raters for these behaviors was high (Cohen's Kappa = .9).

Neural Network Offline Tracking, Training, and Validation Results

Position tracking for the rat and the robot was performed with U-Net convolutional neural network trained using the Social LEAP Estimates Animal Pose (SLEAP) tracking system (Pereira et al., 2020). Videos were recorded at 29.97 FPS with a frame size of 720x480 pixels. SLEAP has been shown to be robust to multi-animal tracking issues with intersecting parts, close interaction, and swaps. The bottom-up approach was utilized to compute probability maps known as partial affinity fields for each frame of the video. Skeletal landmarks were estimated by computing a part confidence map and fitting gaussians for each part. Each body part

estimation is the peak of the fit gaussian. The rats' skeletal tracking points were defined according to the specification of Sturman et al. (2020), including the nose, head center, left ear, right ear, neck, left side, body center, right side, left hip, right hip, and tail base. A Kalman filter was used to address the temporal association problem of shifts between frames to maintain identity of the skeletons.

The iRat tracker performed the most accurately based on 477 labels. The BOE robot tracker was trained on 1573 labels. 1/5th of the labels were set aside as the test set, while the remaining labels were included in the training set. The multi-animal rat tracker was trained on 6,700 labeled instances of rats from 3380 video frames from single and multi-rat trials. For accuracy results on the multi-rat tracker and robot trackers see Figure 2.4. For training and validation loss results see Figure 2.4.

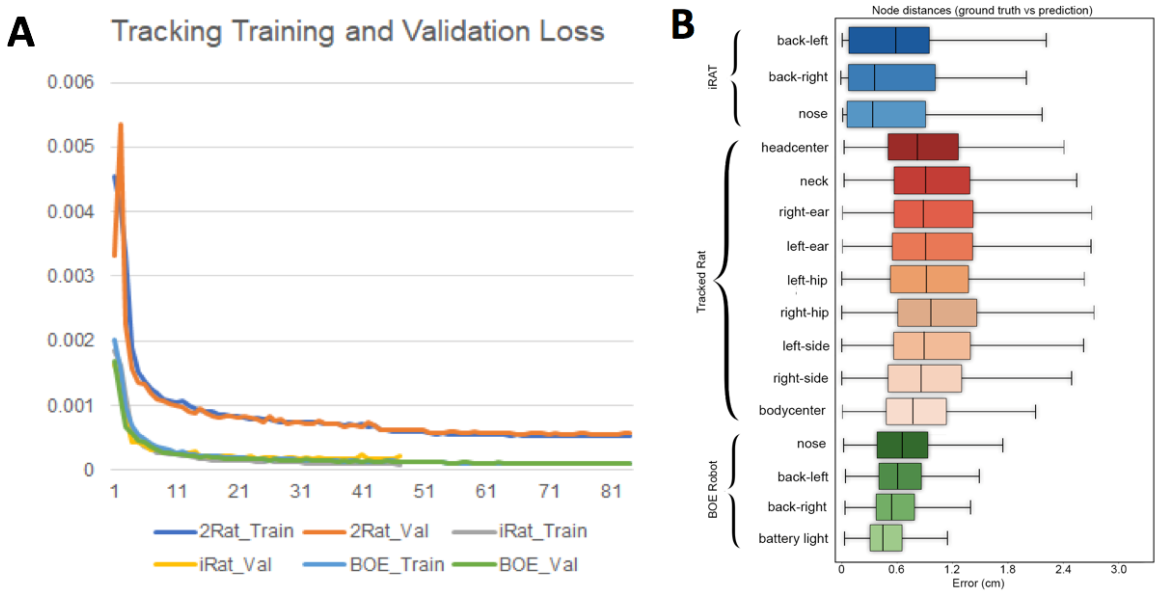

Figure 2.4: A, Training and validation results from neural network tracking of multi-rat, iRats and BOE robots. B, Accuracy results for the neural network tracker for multi-rat, iRat and BOE robots.

Automated Tracking-Based Behavior Segmentation

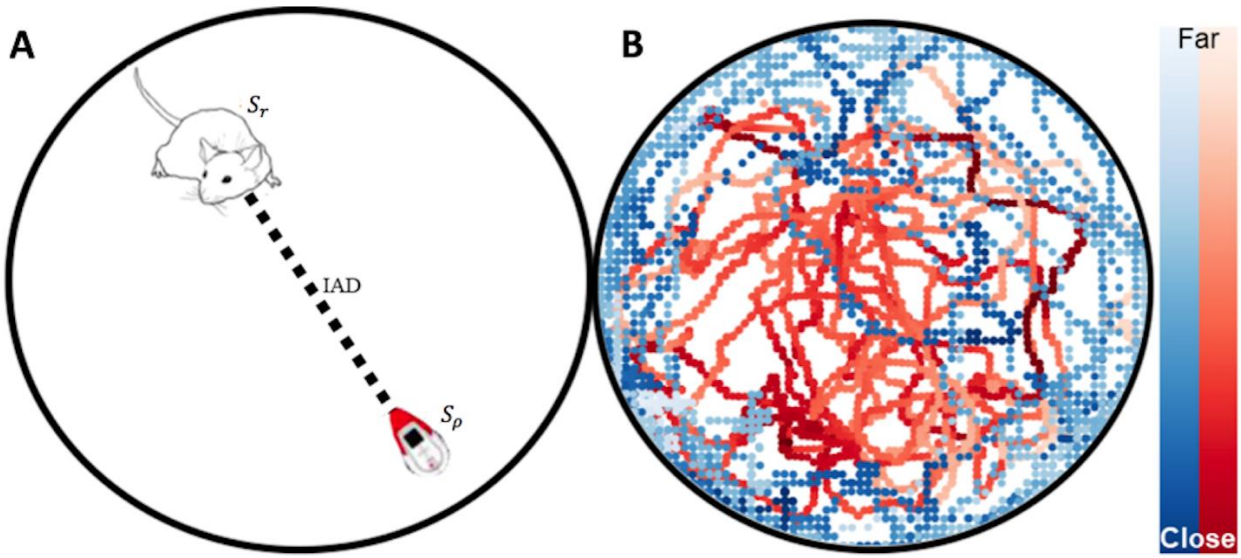

Figure 2.5: A, Animal and Robot Position Tracking With SLEAP. Automated tracking-based behavior segmentation with state vectors S_r and S_ρ , and the inter-agent distance (IAD). B, Tracking data from a robot freeroam trial is plotted.

Let S refer to the agent's state which is the position in Cartesian x,y coordinates over time and θ orientation in radians over time t by video frames (See Figure 2.5). The position and orientation for the rat is denoted by $S_r = \{x_{rat}, y_{rat}, \theta_{rat}\}$ and the robot $S_\rho = \{x_{robot}, y_{robot}, \theta_{robot}\}$. Inter-agent distance (IAD) was calculated by taking the euclidean distance between S_r and S_ρ position vectors.

Behavioral and Tracking Statistics

For the tracking data, inter-agent distances were calculated using the euclidean distance between agents for the rat-rat, rat-robot, and rat-object interaction conditions. The distributions of inter-agent distances, mean event counts per trial, and mean event duration per condition were compared using one way Welch's t-tests, and effect sizes were calculated using Cohen's d. For the behavioral events, the event frequency was calculated per trial and the mean duration for each behavioral event type was calculated per condition. The events and durations were also compared using one way Welch's t-tests, and effect sizes were calculated using Cohen's d.

Mixed Effects Model

A general linear mixed-effect model was constructed to perform an ordinary least squares regression of a response variable as a function of mixture of fixed and random effects. Fixed effects include the behavior and agent type, while random effects include the influence of the variance of each individual rat on the response variable within the region. Null distributions were created by taking the aggregate average of all behavioral events. This allows for the comparison of changes in average power within rats, while controlling for any uneven sample sizes and individual differences in overall power within brain regions. The effect size was estimated by subtracting the means in question and dividing by the standard deviation of the residual. The mean coefficients, standard errors, z scores, p values, and effect size estimates are reported. The intercept of the baseline group is reported as Int., standard error of the mean as SEM, and the mean coefficients of the comparisons are reported as M. Z scores and p values are also reported.

Results

Tracking Results

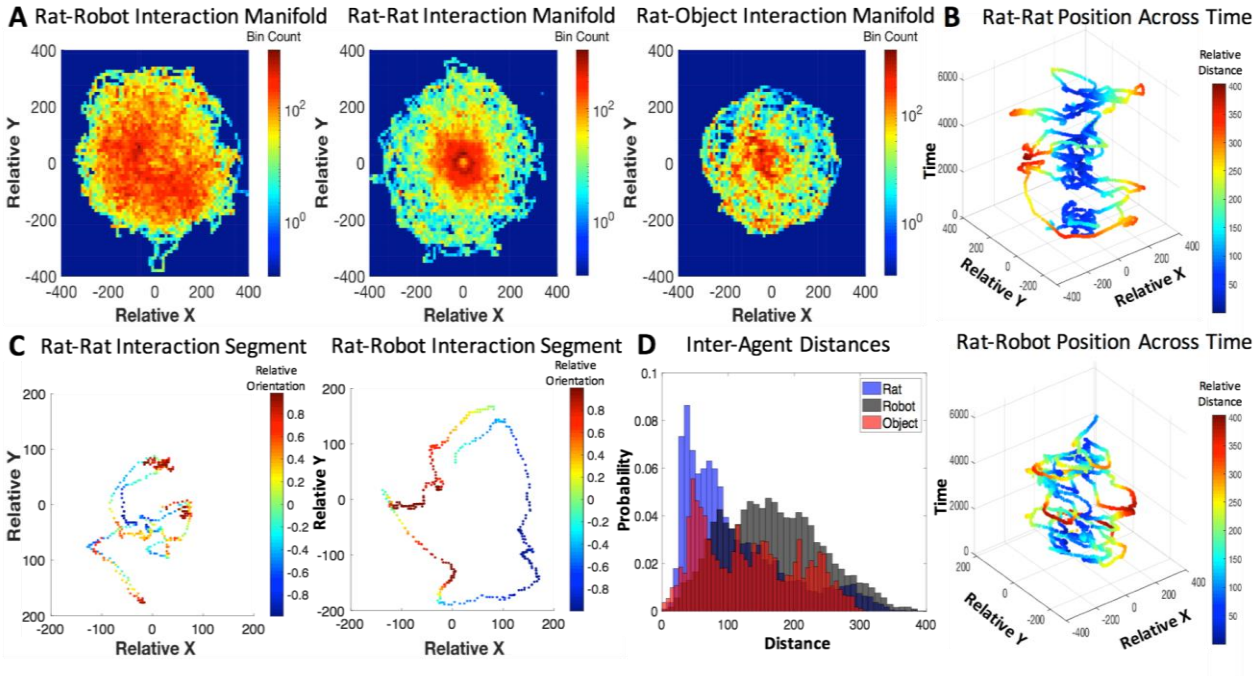

Figure 2.6: A, Agent-based interaction manifolds represented by 2D histogram bins along the relative x and y position axes. B, Relative position over time for the rat-rat and rat-robot interactions with a colormap revealing inter-distance between agents C, shorter segments of relative position of rat-rat and rat-robot interactions with a colormap revealing relative orientation. D, a histogram of inter-agent distance per rat, robot and object conditions.

The inter-agent distances maintained during interaction were minimal between rats, slightly longer for rats and objects, and the longest for rats and robots (See Figure 2.6). The inter-agent distances for rat-robot interactions indicate that the rat and robot maintain a significantly longer distance on average (M = 167.09 pixels, SEM =.14) than interactions with conspecifics (M =110.20 pixels, SEM = 0.21, t = 227.86 pixels, p < e-10, d = .75). The rat-robot inter-agent distance distribution had a significantly higher mean than the rat-object distance distribution (m=131.44, sem=.22, t=135.56, p < e-10, Cohen's d = .48) The rat-object inter-agent distance distribution showed a significantly higher mean than rat-rat distances (t = 69.93, p < e-10, d = .28).

Behavioral Hypothesis Tests

For a summary of the hand-coded behavioral event identification please see SI Behavioral Video Coding.

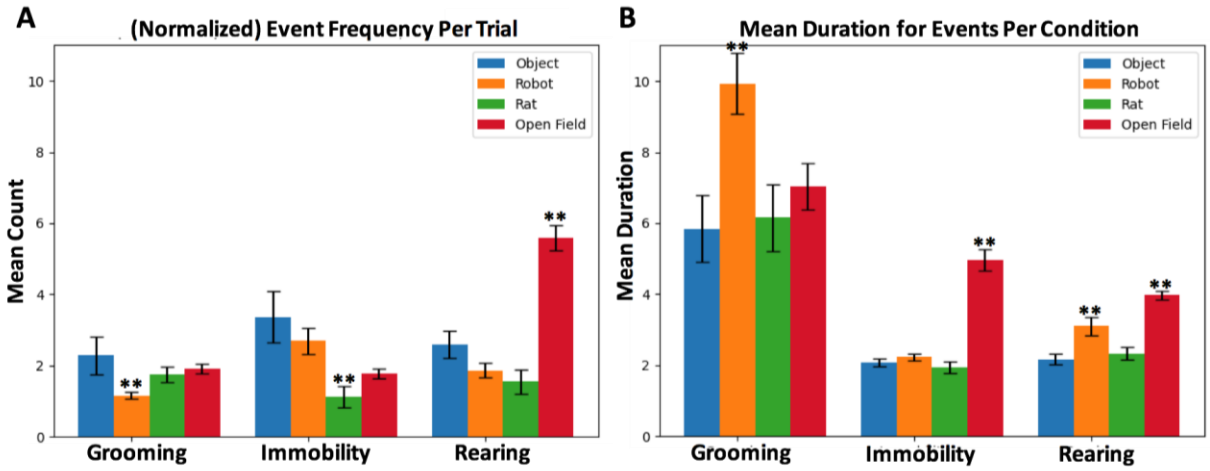

Figure 2.7: Mean counts per trial and mean duration per condition for grooming, rearing and immobility events. Error bars indicate the standard error of the mean.

Immobility

It was predicted that interaction with the robot leads to increased risk assessment behaviors, signified by increased immobility behavior (See Figure 2.7). The mean frequency of immobility events during rat-robot interactions (M = 2.70, SEM = .37) per trial was significantly larger than those from rat-rat interactions (M = 1.31, SEM = .31, t = 3.29, p = .001, d = .75). The mean duration of immobility during open field interactions (M = 4.95, SEM = .30) was significantly longer than robot (t = 2.73, p < e-4, d =1.44), rat (t = 8.77, p < e-4, d = 1.15) and object (t = 9.06, p < e-4, d = 1.40) interactions.

Grooming

Another hypothesis was that the robot would perturb grooming behavior due to distress related to a possible threat and stimulus uncertainty (See Figure 6). During interaction with the robot, although grooming events were significantly less frequent (which was counter to our prediction) on average per trial (M = 1.16, SEM = .11) than the rat (M = 1.74, SEM = .22, t =

2.38, p = .012, d = .82) and object interactions (M = 2.29, SEM = .11, t = 2.07, p < .04, d = 1.00). Despite being less frequent, grooming events during interaction with the robot (M = 9.93, SEM = .85) show a marginally longer duration than interaction with rats (M = 6.15, SEM = .94, t = 1.78, p < .04, Cohen's d = .36) and objects (M = 5.8, SEM = .93, t = 1.93, p < .03, d = .39), indicating an alteration in duration of distress related grooming in the presence of robots.

Rearing

It was predicted that the robot and open field will result in increased rearing as escape-related exploratory response (See Figure 2.7). Rearing events during interaction with the robot (M = 3.09, SEM = .26) show a significantly longer duration than rat (M = 2.32, SEM = .18, t = 2.36, p = < .01, Cohen's d = .30) and object (M = 2.17, SEM = .16, t = 2.94, p < .002, d = .38), confirming the hypothesis that the presence of a robot might elicit exploration. The mean duration of rearing events during open field interactions (M = 3.9, SEM = .12) was significantly longer than the robot (t = 2.99, p < .002, d = .34), object (t = 8.99, p < e-4, d = .76), and rat (t = 7.62, p < e-4, d = .69) conditions. Empty open fields typically elicits exploratory vigilance, thus it appears that the open field induces an increase in hypervigilance relative to the robot.

Neurophysiological Results

Neurophysiological signals were recorded in rats during their behavioral displays (grooming, immobility, and rearing) occurring throughout interaction sessions with different agents (rat, robot, object). The behavioral epochs were extracted from continuous data and occur naturally throughout the interaction sessions. This means that the display of behaviors varies both with respect to inter-agent position and order of occurrence. The event durations of these naturalistic behavioral epochs differ, so as not to impose artificial cut-offs on natural display of behaviors.

Spectrograms

To demonstrate an example of inter-agent variation within one behavior type, spectrograms below (see Figure 2.8) show multi-region brain dynamics from periods in which implanted rats exhibited immobility behaviors during rat, robot or object interactions. The pre- and post- event windows are 1 second in length providing a sense of scale for the viewer. In Panel A the period of immobility to a rat is approximately one second and in Panel B the period of immobility to robot is approximately 3 seconds.

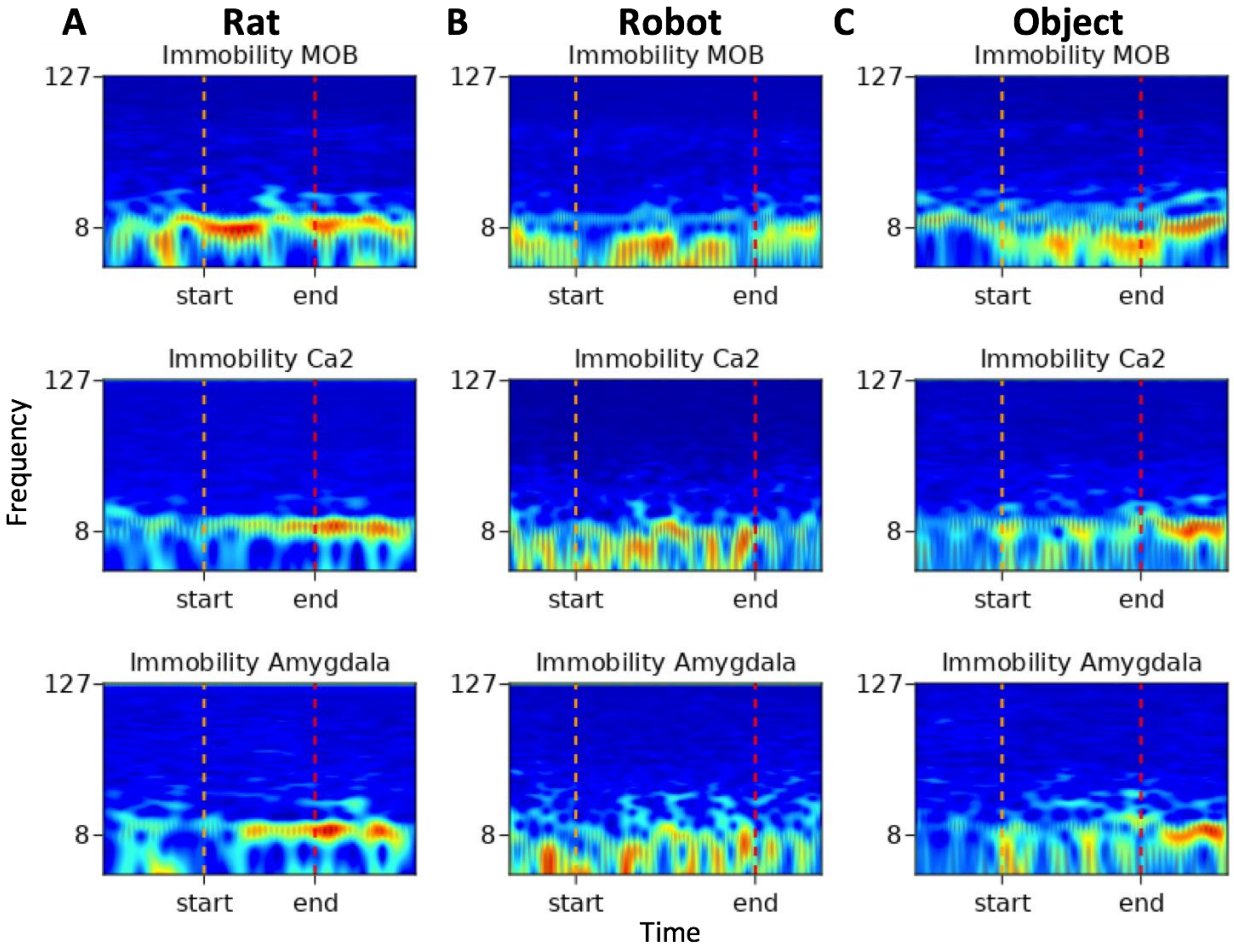

Figure 2.8: Spectrograms of immobility events from rat, robot and object conditions. Frequency (Hz) is represented along the y-axis with markers for 8Hz and 127 Hz, time is represented along the x-axis, the colormap represents high amplitude in red and low amplitude in blue. The start and end indicators denote the onset and offset of the variable duration behavioral events.

The immobility event which occurred during rat-rat social interactions in Figure 2.8 Panel A shows increased amplitude within the theta range in all brain regions with some transient beta oscillations in MOB and amygdala towards the end of the event. The immobility events that occurred during robot and object interactions in Figure 2.8 Panels B and C show high amplitude in respiratory oscillations in all regions with more pronounced beta oscillations in the amygdala during the event.

Power Spectral Densities

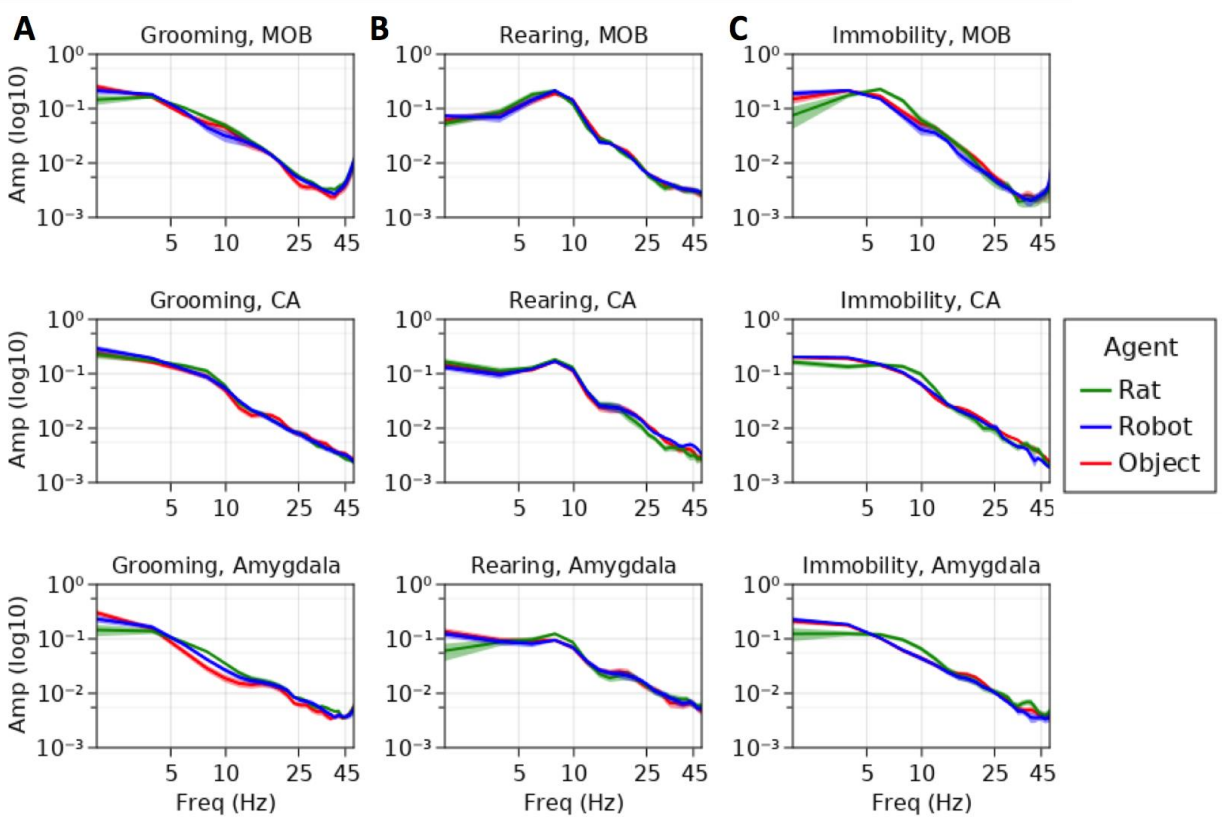

Figure 2.9: Average power spectral densities for MOB, CA1/CA2, and Amygdala for A, grooming, B, rearing, and C, immobility events. Amplitude is represented on the y-axis, frequency is represented along the x-axis. Average amplitudes during interaction with rats is represented in green, robots in blue and objects in red.

Neural Hypothesis Testing

The results of the mixed effects model showed a variety of effects in the respiratory, theta, and beta frequency ranges (See Figure 2.9 for average power spectral density plots). There are also marginal effects in the gamma range that will require a larger data set for validation and will not be addressed in this study.

Theta Oscillations: Olfactory Exploration and Salience

Other conspecifics were expected to elicit heightened sensorimotor exploration relative to robots and objects (See Figure 2.9). Rats are inherently more complex olfactory stimuli, and this is indicated by theta oscillations. Immobility events showed significantly higher theta amplitude in MOB during the rat-rat interaction trials (Int = .026, SEM = .0055) compared to the events from the robot (M = -.0057, SEM = .0020, $z = -2.83$, $p < .005$, $d = -.96$) and marginally larger than object trials (M = -.0043, SEM = .0018, $z = -2.36$, $p < .02$, $d = -.7$). In the MOB, the rat-robot interactions showed significantly lower theta amplitude during grooming events (Int = .010, SEM = .002) than rat-rat interactions (M = .0028, SEM = .0009, $z = 2.75$, $p < .003$, $d = .82$) but no difference from objects (M = .0008, SEM = .0013, $z = .65$, $d = .24$). Rearing events during rat-rat interactions (Int. = .0015, SEM = .0001) exhibited significantly larger amygdalar theta oscillations than rearing events during rat-robot interactions (M = -.0002, SEM = .0001, $z = -2.76$, $p < .006$, $d = -.59$) but showed no difference from rat-object interactions (M = -7.2e-5, SEM = .0001, $z = -.62$, $d = -.29$).

Respiratory Rhythms: Autonomic State and Distress Regulation

As an indicator of autonomic state and distress regulation, we predicted higher amplitude respiratory oscillations for the object and robot interactions during grooming (See Figure 2.9). Immobility events showed a significantly higher respiratory amplitude in the amygdala during

the rat-robot interactions (Int. = .0032, SEM = .0001) than rat-rat interactions (M = -.001, SEM = .0003, z = -3.06, p < .0022, d = -1), but showed only a trend towards a significant difference between rat-object interactions (M = -.0004, SEM = .0002, z = -2.07, p < .04, d = -.4). Respiratory rhythm amplitudes in the amygdala during grooming events from rat-robot interactions (Int. = .0039, SEM = .0004) were significantly larger than events from rat-rat interactions (M = -.00016, SEM = .0006, z = -2.75, p = .006, d = -.8), but showed no significant difference from rat-object interactions (M = e-5, SEM = .0007, z = -.04, p = .96, d = -1.47e-2). Taken together these findings indicate that both robots and novel objects elicited an increase in arousal relative to conspecifics. Consistent with this interpretation, rearing also showed a significantly larger amygdalar respiratory amplitude for rat-robot conditions (Int. = .0022, SEM = .0002) when compared with rat-rat (M = -.0007, SEM = .0003, z = -2.55, p < .01, d = -.7), but not significantly different from rearing events from rat-object interactions (M = -.0001, SEM = .0003, z = .43, p = .67, d =-.1).

Theta and High Beta Oscillations: Sensorimotor Exploration and Recognition

Although we did not have explicit prior hypotheses regarding the hippocampus and amygdala theta oscillations during grooming, we did expect that there may be differences revealing whether the rat was recognizing the robot more as an object or more as a conspecific (See Figure 2.9). Hippocampal theta amplitude during grooming events from rat-rat interactions were significantly different from the object conditions (M = -.0015, SEM = .0005, z = -3.05, p < .002, d = -1.5), but showed no difference when compared with robot (M = -.0009, SEM = .0001, z = -1.42, p = .16, d = -.9). The amplitude of theta oscillations in the amygdala during grooming events from rat-rat interactions (Int = .0013, SEM = .0001) were significantly larger than object conditions (M = -.0002, SEM = .0001, z = -2.58, p < .01, d = -1) but not significantly different

from robot conditions (M = -.0001, SEM = .0001, z=1.28, p = .2, d = -.5). One implication of this is that movement dynamics of another rat may elicit larger theta than the moving robot or stationary objects. Although this may be obligatory movement coding in the hippocampus, this dynamic might also serve to monotonically index rat, robot, and object based on this parameter.

As observed in previous work, it was expected that the object would result in a robust burst at beta frequency (15Hz-30Hz) in the hippocampus due to learning of the object stimulus (Rangel et al, 2015) Instead, the presence of increases in high amplitude beta in this work were moreso within the high beta/low gamma range (35Hz-45Hz) observed in the hippocampus during object place associations (Trimper et al, 2017). The amplitude of beta during rearing events from rat-object interactions (Int. = .0005, SEM = e-5) were significantly higher than events from rat-rat (M = -.0002, SEM = 1e-5, z = -4.9, p < 1e-6, d = -2) and rat-robot interactions (M = -.0001, SEM = 1e-5, z -4.17, p < 1e-4, d = -1). This too indicates that the rat is likely associating the object with its place and differentiates the object from the robot and rat, both of which are moving.

Discussion

Animals are inextricably embedded within an environment and situated within a rich social world, bound to active exploration in recursive loops of perception and action (Kirsh & Maglio, 1995; De Jaegher & Froese, 2008). Brain dynamics rapidly and transiently switch from exploring the external world to evaluating the internal effect of the world on the organism (Marshall et al, 2017). Artificial systems often lack the complexity, adaptivity and responsiveness of animate systems, but can mimic kinematic and dynamic properties that inanimate objects often lack. It is an open question in the literature as to whether the rat perceives the robot as an animate or inanimate object and to what degree their coordinated

movement resembles social interaction or object exploration. This study presents data to suggest that brain regions preferentially dissociate between rat, robot, and object based on sensorimotor exploration, salience, and autonomic distress regulation, indicating that the robot bears similarity to both a rat and an object. Primarily, this study outlines a general approach for such experiments that emphasize naturalistic interactions and complementary analysis pipelines that are necessary to render a holistic picture of the behavioral and brain dynamics evoked during interactive neurorobotics experiments.

Dynamic behavioral data regarding inter-agent distance suggest that the rat may be initially engaging in risk assessment behaviors when interacting with the robot, whereas they more readily approach another conspecific or stationary object. This may indicate that the rat feels safer approaching conspecifics and stationary objects than a robot. The distance between agents was also affected by the robot more often occupying the middle of the field and the rat showing a preference for the wall, a thigmotactic strategy generally attributed to safety seeking (Lipkind et al, 2004). While that may have influenced the distance, the trajectories over time show a spiraling between rat and robot which suggests that the rat was actively avoiding the robot. The trajectories also suggest that as time passes the rat may become habituated to the robot and allow for decreased inter-agent distance at the end of a trial (see Figure 2.6). This differs from two prior robot-rat studies, the Waseda rat and the Robogator, where rats' engagement with the robot is primarily enemy avoidance (Choi and Kim, 2010; Shi et al, 2013). Instead the rats in our study begin to engage in closer interactions across time rather than keeping their distance. This is more consistent with a behavioral study of the robot e-Puck and rats in which the robot elicits social behaviors from the rats (del Angel Ortiz et al, 2016).

In the present study, however, rats do show distress responses to the robot that exceed those to a conspecific or a novel object. However, they demonstrate maximal anxiety on the empty open field (used to test anxiety, Prut & Belzung, 2003); this indicates that the robot on the open field might provide comfort or that it presents a degree of behavioral competition between curiosity and anxiety. Specifically, interactions with a robot elicited or perturbed immobility, grooming, and rearing behaviors. The authors note that the rat-rat interactions resulted in few instances of immobility due to their active engagement, and reduced self-grooming likely due to the availability of social grooming by the other conspecific and the absence of distress with the conspecific. Rat conspecifics interacted, heavily engaging in coordinated exploration, following, interactive play, and anogenital exploration (also see Figure 2.6). This is consistent with findings detailed in a prior study (del Angel Ortiz et al, 2016).

Thus, this initial data from our exemplar rodent-centered design study suggest that agent-based comparisons within behavior are a promising direction moving forward in the field of interactive neurorobotics. A limitation of this study is that the robots' motion dynamics were animated by human drivers, this introduces potential issues with anthropomorphism of interaction which can be dealt with better using automatic and autonomous robots. However, WoZ is a necessary step in the development of autonomous systems allowing for a diverse collection of movement dynamics that autonomous robots currently lack the complexity and sensitivity to exhibit. Follow up studies will be performed using autonomous robotic systems, such as PiRat (Heath et al, 2018). Autonomous robots allow for the manipulation of dynamics or functions that can be systematically manipulated according to model-based reasoning.

From a design perspective, roboticists look for cues regarding whether the rat perceives the robot as more of an object or as an animal. Neuroimaging studies of human subjects viewing

social androids and their movements addressed this question, discovering that the brain dissociates between androids and humans according to form and motion interactions (Saygin et al, 2012). Neural data in the present study demonstrate both robust and subtle differences to the rat, the robot, and the object. Specifically, hippocampal theta during grooming differentiates the rat from the object, however the robot (falling in between the two) is not significantly different from either. Here it is possible that the rat is coded according to spatiotemporal dynamics that are missing from the object, and that the moving robot carries features of each.

In contrast, theta dynamics in the MOB are similar for robot and object while differentiating the rat. This was expected based on the complexity of the inherent biological odors of the rat. The increased amplitude in respiratory rhythms during alert immobility in the amygdala to robot and object suggest autonomic regulation related to increased distress related arousal when compared with a rat. This suggests that interacting with a rat may be more engaging and less distressing. This finding is consistent with the behavioral interaction data. Thus, the brain appears to differentiate between a rat and our robots, but also distinguishes between the robot and objects. These findings provide support for the context-based modulation of brain signals (Kalueff et al, 2016). They also imply that through iterative design of robots, one could eventually produce a robot for which many regions of the brain do not readily distinguish the robot from a rat.

Comparing the neurobehavioral states evoked by conspecifics, robots and objects may clue us into some of the minimal requirements for an animal to perceive artificial agents as social others. A key insight from Datteri (2020) about the philosophical foundations of the field is that interactive biorobotics experiments by themselves do not necessarily tell us about how organisms interact with conspecifics or predators, and suggests we should examine these interactions in

their own terms before drawing unwarranted conclusions from the observations. This does not preclude a comparative approach, it just requires that we first take the robot case on its own terms and then compare it with data from social, object, and predator interactions.

Future directions will also involve collecting a larger data set for the purpose of examining transient gamma activity, especially during investigation of the other agent or object. Rhythms like high gamma indicate active processing of the external sensory world, while low gamma is likely related to regulating an animal's internal interoceptive milieu (Kay et al, 2009). It is recommended to use techniques such as burst detection to capture the more transient agent-based brain responses within behavior. Future approaches should also examine inter-regional communication, such as coherence and dynamic coupling (Fries, 2015; Breston et al, 2021). Additionally, future studies should also incorporate a richer repertoire of stimuli and robots.

Interactive robots have visual, auditory, olfactory, tactile and even gustatory aspects that should be actively taken into account during the design process. For instance, audition plays a key role. It is critical that interactive robots exhibit audio frequencies outside of the range of rodent distress calls, which induce panic, irritation, or stress responses. When designing interactive robots for animals it is also critical to take the animals preferred sensory systems into account, which for rats brings olfaction to the foreground and is why the robots in this study were tagged with olfactory stimuli. Contestabile et al (2021) used a dynamic moving object as a control for complex social stimuli and found that mice prefer complex social stimuli where more multisensory information such as tactile, visual, olfactory and auditory cues are available. They demonstrate that the object imbued with social odor does not recapitulate the complexities of social interaction, but instead the authors emphasize the importance of multisensory integration.

Future approaches for designing interactions should emphasize the multisensory nature of the design problem.

Robotics has significant potential to offer animal research because its use enables experimenters to control complex experimental parameters and to test embodied computational models that interact with the real world (Webb, 2000). The dynamics of sociality are non-trivial and require convergent data regarding the model system. The holistic framework of capturing naturalistic behaviors in multiple contexts with fine-grained analyses, sets forth rich neural and behavioral data to scaffold the design process of future social robots (See SI Proposed Framework). The field of interactive neurorobotics allows for the examination of how robots evoke emergent behavior and brain dynamics in living creatures during a variety of agent-based interactions. This approach can be generalized to other animals and to humans. Social robotic interactions with humans also have affective dimensions that are indexed by autonomic signals and design principles can be improved by taking detailed behavioral interactions and neural signaling into account. It is essential that we also look beyond these narrow experimental contexts and generalize these lessons to our own technologically enmeshed world. With the increasing integration of human life with autonomous systems, we have the opportunity to use the methods and insights gained from interactive neurorobotics to mold them into cooperative companions.

Studying interactions between animals and robots might clue us into some of the minimal requirements for an animal to treat an artificial agent as being social. Robotics has a significant amount to offer animal research by allowing for experimenters to control complex experimental parameters and to test embodied computational models that interact with the real world (Webb, 2000). When studying social interaction, robots give us the opportunity to carefully manipulate

parameters of interaction in order to measure differences in the reciprocal behavior of the conspecific. This approach is primarily concerned with the neurophysiological and autonomic signals that underlie social behavior, and will also attempt to explore a much larger question: What are the minimum interactive capabilities required of an artificial agent to elicit social behaviors.

Acknowledgements

Chapter 2, in full, is a reprint of the material as it has been submitted and is under review for publication in Frontiers in Psychology: Special Issue on Robots and Bionic Systems as Tools to Study Cognition: Theories, Paradigms, and Methodological Issues, 2022, Leonardis, Eric J., Breston, Leo, Lucero-Moore, Rhiannon, Sena, Leigh, Kohli, Raunit, Schuster, Luisa, Barton-Gluzman, Lacha, Quinn, Laleh K., Wiles, Janet, & Chiba, Andrea A. The dissertation author was the primary researcher and first author of this paper.

CHAPTER 3: HABITUATION TO RATS AND ROBOTS

Introduction

Social and interactive cognition is fundamentally linked to how coupled agents learn about each other. This requires a constitutive type of coupling where a creature's body adapts to other agents with concurrent changes in neural coupling between brain regions. This chapter is concerned with characterizing learning about other social and robotic agents. One of the most fundamental types of learning is habituation, and is indicated by increased exploration of novel stimuli and a decrease in responsivity to familiar stimuli (Sokolov, 1963; Gheusi et al, 1994; Thompson, 2009). However, if an animal is under sufficient stress, it will choose to engage the familiar conspecific more often (Sachser, Dürschlag, Hirzel, 1998). This chapter is concerned with how multiple brain regions involved in olfaction, salience detection, memory formation and autonomic regulation habituate to social and robotic stimuli.

Evidence suggests that neural oscillations emerge during learning dynamics and are indicative of aspects of habituation. Olfactory learning paradigms have shed significant light on the dynamical properties of the brain supporting learning and behavior. Olfaction has been shown to play a significant role in these recognition processes, as bulbectomized animals show relative indifference between novel and familiar conditions (Dantzer, Tazi, & Bluthé, 1990). Following habituation learning, upon repeated presentation of an odor stimulus rather than showing a stable discrete representation, the olfactory bulb shows decremented response to learned stimuli (Freeman, 1987). Breathing is a fundamental rhythm of brain function and is a critical channel for coordinating activity in many brain regions (Heck et al, 2017). Nasal respiration has been shown to entrain neural populations globally across the rodent brain (Tort, Brankack, & Draguhn, 2018). Without taking sniffing and respiration into account respiratory

effects are often mistaken as delta at slow respiration rates and theta at large respiration rates (Rojas-Libano et al, 2014). The olfactory bulb local field potential has been shown to reliably follow diaphragmatic EMG.

When encountering novel stimuli, animals exhibit complex and structured exploratory behavior. Rodents attempt to maximize novelty for maximizing new information for the purposes of learning. After being exposed to highly novel states, rats often have a novelty triggered retreat behavior (Gordon, Fonio, and Ahissar, 2014). In addition to the olfactory bulb, the exploration of a novel environment shows differential modulation of hippocampal interneurons (Nitz and McNaughton, 2004). The amygdala has also been shown to respond to repeating visual stimuli that are familiar to a subject (Wilson & Rolls, 2004; Farovik, Place, Miller, Eichencaum, 2011).

In service of the recognition of conspecifics and predators, animals have evolved complex and intricate mechanisms for assessing other agents in the world in terms of affect, identity, and interaction history. Animals learn to easily sense affective states such as aggression, fear, or distress in their conspecifics, as well as in their prey and predators (Bartal, Decety, & Mason, 2011). Using social memory systems to process olfactory cues, animals can associate the identity of a conspecific with information such as kin recognition, mate selection, social hierarchy, and prosociality (Gheusi, Bluthe, Goodall, & Dantzer, 1994; Kogan, Frankland, & Silva, 2000; Thor & Holloway, 1982; van der Kooij & Sandi, 2012). Distinctions have been made between the operational definitions for “social” and “individual recognition”. “Social recognition” is the classification of conspecifics based on their general properties, such as male/female, subordinate/dominant, and kin/non-kin. “Individual recognition”

is specifying the identity of an individual based on that individual's idiosyncratic traits (Gheusi, Goodall, Dantzer, 1997).

In this study, we will examine whether these same recognition processes extend from conspecifics to mobile robotic agents. A rat's primary sensory modality is olfactory in nature, so in order to study habituation we will be looking at exploratory sniffing behavior during agent assessment. The recognition and interpretation of the multitude of signals supporting social cognition requires the interplay between many neural populations. This study examines the habituation of socially relevant neural populations during agent assessment with rat and robot in the main olfactory bulb, medial amygdala, CA1/CA2 hippocampus, and the insular cortex.

Additional Behaviors of Interest

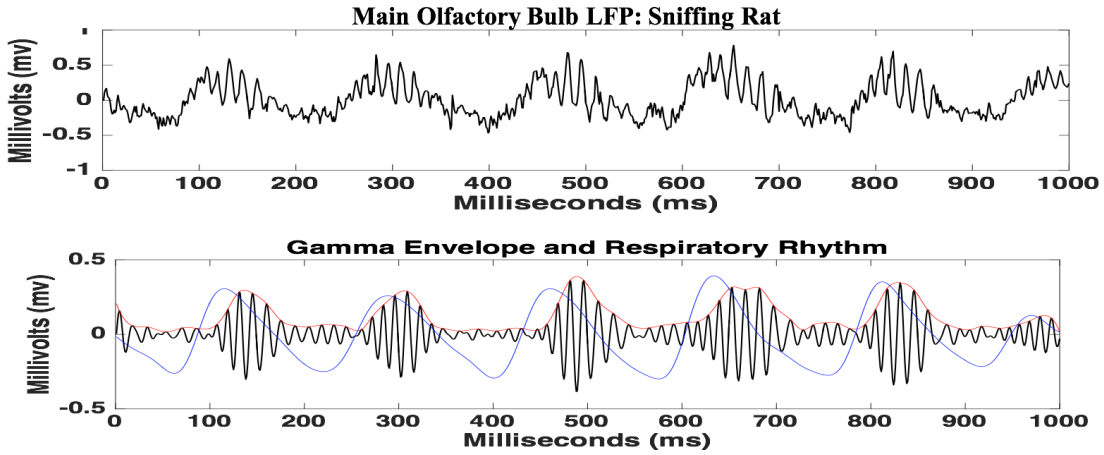

Figure 3.1: MOB raw trace during a social sniffing event when sampling another rat. The raw trace was filtered for the respiratory and high gamma rhythm to illustrate the relationship between the amplitude gamma envelope and respiratory phase.

Sniffing

This study will examine exploratory sniffing behavior of other conspecifics, robotic agents and objects. Sniffs are defined as the behavioral events where the implanted animal nose pokes through a hole of the enclosure and samples the olfactory information of the agent. Sniffs serve as a key perceptual structure for the rodent (Kepecs, Uchida, & Mainen, 2006). Sniffing

has a periodic structure of phases of inhalation and exhalation, which exhibit changes in frequency in response to internal and external demands and coordinate neural oscillations across the brain (Heck et al, 2017; Tort, Brankack, & Draguhn, 2018). Phase-amplitude coupling is an encoding mechanism which commonly relates the phase of a low frequency oscillation with the amplitude of faster oscillations, and is believed to coordinate communication between neural populations. This chapter will examine variations in phase-amplitude coupling between respiratory rhythms, low gamma and high gamma oscillations in the olfactory bulb, amygdala, hippocampus and insular cortex during olfactory exploration of novel and familiar agents.

Brain Areas of Interest

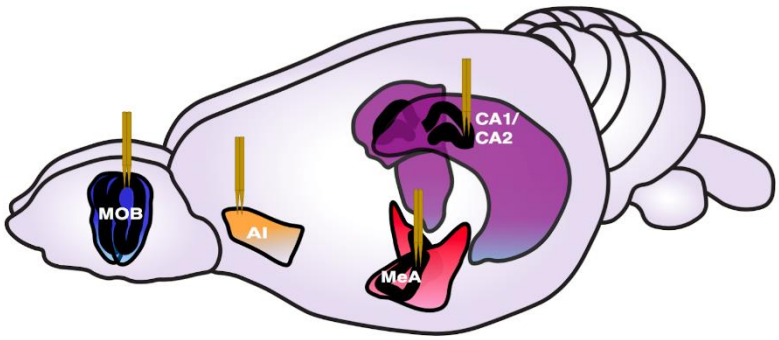

Figure 3.2: A diagram of electrode placement in the main olfactory bulb (MOB), medial amygdala (MeA), CA1/CA2 hippocampus, anterior insular cortex (AI).

Anterior Insular Cortex

From humans to rodents, the insular cortex is considered to be an anatomical hub, receiving signals from visceral organs (Saper, 2002) that are essential for an organism's ability to engage in interoception or perceiving their own internal state (Craig, 2003; Livneh & Andermann, 2021). The ability to perceive internal state is thought to be used to monitor health, energy, the impact of the present context on self, "state of being", and has even been extended

to assessing the state of other creatures (Decety, 2015). The anterior insula shares bidirectional projections from the nucleus tractus solitarius in the dorsal medulla and thalamic relays (Saper 2002, Gogolla, 2017). The insula monitors bodily states related to blood pressure, oxygenation, motility of the digestive system, heart beats, hunger, itch, nausea, tickle, pain, and many more bodily sensations (Craig, 2003, Gogolla, 2017). The insula also exerts strong control over autonomic functions like heartbeat regulation, blood pressure, and gastric motility through the connections to the nucleus tractus solitarius and areas like the lateral hypothalamus (Ruggiero et al, 1987, Cechetto, 2014, Gogolla, 2017). The behavioral manifestation of this connectivity results in the anterior insular cortices' involvement in interoceptive and allostatic processing, such as sensory perception of gastrointestinal malaise (Aguilar-Rivera et al, 2020). The insular cortex also receives inputs from primary sensory areas, thalamic nuclei, and many other subcortical structures. The insular cortex has reciprocal connectivity with the basolateral amygdala, nucleus accumbens, and ventral pallidum (Chikama et al, 1997). Through the integration of sensory cues and interoceptive cues, the insular cortex has been shown to mediate behaviors that are integral to successful social interactions in rats, including appropriate approach and retreat behavior from conspecifics (Rogers-Carter, et al 2018). Notably, these behaviors may heavily rely on an assessment of the conspecific.

Medial Amygdala, Hippocampus, and Main Olfactory Bulb

Please see Chapter 2 Brain Areas of Interest for more information.

Methods

After characterizing a rat's reaction to a rat, robot, and object with unrestricted exploration in previous chapters, we wanted to use a learning framework to examine a more restricted type of agent and object exploration. Rats, robots and objects were placed into an

enclosure which restricts their motion, and the implanted rats were allowed to explore the enclosures. The enclosures had small circular openings on the side which would allow for the rats to nosepoke and sample olfactory information in a more controlled way. This more constrained behavior allows for the characterization of habituation in terms of behavioral and brain responses to novel and familiar agents. This chapter is concerned with how rats learn about social, robotic and object stimuli. The agents and objects used in the study vary in terms of complexity. The rat was the most complex definitively social stimulus. The robot and object were tagged with the same scents but different in terms of dynamic motion or lack thereof.

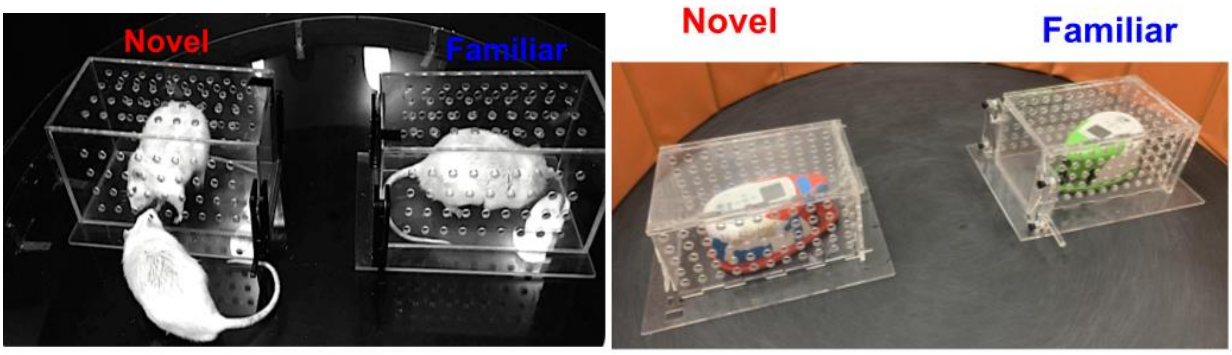

Figure 3.3: Live pictures of interaction trials with the rat and robot.

Habituation

Rats were habituated to the robots by being presented inside of enclosures and performed pre-programmed automated behaviors (See Figure 3.3). After the initial free roaming exposures describe in Chapter 2, one robot (20 trials), rat (76 trials), or object (17 trials) was presented at a time inside of the enclosures for the rat to freely investigate. When inside the enclosures, the iRat performed simple forward and backward movements for a small number of trials and the BOE robots were placed in semi-autonomous mode which performed those movements in a more controlled but non-periodic fashion for a majority of trials.

Table 3.1: Robot's Automated Movements For Habituation and Interaction

Behavior Sequence	Action 1	Action 2	Action 3
1) Forward/Back	Forward: 300ms	Stop: 500ms	Back: 300ms
2) Stop		Stop: 2000ms	
3) Side-To-Side	Turn Left: 200ms	Stop: 500ms	Turn Right:200ms
4) Stop		Stop: 2000ms	
5) Forward/Back	Forward: 100ms	Stop: 500ms	Back: 100ms
6) Stop		Stop: 2000ms	
7) Side-To-Side	Turn Left: 200ms	Stop: 500ms	Turn Right: 200ms
8) Stop		Stop: 1500ms	
9) Forward/Back	Forward: 200ms	Stop: 400ms	Back: 200ms
10) Stop		Stop: 3500ms	

Interaction Task

Novel and familiar rats (25 trials), robots (22 trials) and objects (5 trials) were placed in a plexiglas enclosure while another rat, on the outside of the enclosure and free to roam the field, sniffed through holes in the side of an enclosure. Due to a small number of object trials, objects were left out of the subsequent analysis. The implanted rat on the outside was presented with two enclosures in the field. Depending on the trial, the rat will either see one rat in each enclosure or one empty. Rats were removed from the field after 3 minutes after the onset of a trial. Sixteen rats (n = 16) were presented inside of the enclosures in various combinations, counterbalancing for novelty by switching the novel and familiar enclosures between trials. The robots performed the same movements as described in the habituation condition.

Surgical Procedure

Rats (n = 4) underwent surgery for electrode implantation in order to record local field potentials from multiple brain areas simultaneously. Surgeries were performed in accordance with animal care guidelines. The rats were treated with isoflurane anesthesia (4-5% induction, 1-2% maintenance) and were placed in a stereotaxic apparatus to allow for placement localization (Kopf Instruments). Three holes were made through the skull, and the dura under the skull was removed. LFP signals were referenced to a skull screw above the cerebellum. Anchor screws were inserted around the skull to support the neural implant which was cemented using dental cement. For the stereotrodes, pairs of 25 μm tungsten wire were twisted together and threaded through polyamide insulation. For the tetrodes, four sets of 12 μm wire twisted together, and threaded through polyimide insulation (California Fine Wire).

Electrodes were cut to the same length and wires were gold-plated in solution (Sifco) until impedances were reduced to approximately 100–300 kΩ measured at 1 kHz (Impedance tester IMP-1; Bak Electronics, Germantown, MD, USA). The stereotrodes were implanted using the stereotactic apparatus into the main olfactory bulb (8.5AP, 1.5ML, -3.5 DV), basomedial amygdala (-2.12AP, ±4.0ML, -9.2DV), and anterior insular cortex (2.7AP, 4.4ML, 4.0DV), and CA2/CA1 region of the hippocampus (-3.8AP, 3.8ML, 3.2DV) laterally. For the three rats, tetrodes were implanted above the CA2/CA1 region of the hippocampus (-3.8AP, 3.8ML, 3.2DV).

Robots

The robots used for the habituation experiment were either the iRat or BOE arduino robot. The iRat was controlled via the WoZ method, while the BOE robot automatically produced forward/backward, still, and side-to-side motions in an irregular rhythm. Designing and Constructing Robots: The robots were created using an Arduino UNO, an OpenSource

prototyping microcontroller that executes code written in C programming language, and the Board Of Education (BOE) Robot Shield Kit by Parallax Inc. The BOE kit includes the necessary parts for constructing a three wheeled robot with two continuous servo motors in the back of the robot, and one wheel on the front to allow for stability. Electrical tape was put over the holes in the wheels in order to protect the rat's tails from becoming caught. Tape was also used to cover any wires that were protruding from the bottom of the robot. Plastic Memorex CD cake boxes were melted and shaped to cover the electrical components of the device to ensure safety. This kit allows for remote controlled driving by the experimenter (Wizard of Oz (WoZ) mode) or the execution of pre-programmed movements. To allow for wireless remote controlled driving, an HC-06 bluetooth slave was attached to the serial communication pins of the arduino allowing for pairing with a Dell Precision M2800 laptop which executed a program that used the Arduino serial port to control the robot's velocity and direction. X-Keys XK-24 USB Programmable Keypad was used to execute macros which sent the necessary commands to the serial port allowing for more fluid control of the system (rather than typing keyboard commands). For the Novel/Familiar Robot Test, the robot executed a series of automated forward/backward, still, and side-to-side motions. Time intervals were chosen for each movement behavior as to not exhibit rhythmic patterning, although the same pattern was repeated in a loop during the experiment.

Stimulus Properties

Table 3.2: Stimulus properties of rat, robot and object, stimuli with respect to pheromone, olfactory, auditory, visual, tactile and movement.

Stimulus	Rat	Robot	Object
Pheromone	☑	✕	✕
Olfactory	☑	☑	☑
Auditory	☑	☑	✕
Visual	☑	☑	☑
Tactile	☑	✕	✕
Movement	☑	☑	✕

Table 3.2 denotes that agents have different stimulus properties relative to different senses and capabilities. Rats have the most complex olfactory stimulus including complex pheromone signaling. Robot and Object were tagged with olfactory odors for the purpose of discrimination. The see-through enclosure and holes allowed rats to see what was inside. Rats emit complex auditory signals as well in the form of alarm calls and other vocalizations. The robots motors emit an auditory signal as well, however the objects do not. Both the rat and the robot have self-propelled motion but the objects do not. The rats often engaged in controlled tactile stimulus, by licking each other through the hole and touching nose-to-nose allowing some whisker interaction. The robot and object did not come as close to the hole so were not available for tactile interaction.

Neural Implants and Recordings

The electrodes were connected using gold pins to create contact between the wire and a Neuralynx E/I board cemented to the skull and anchor screws that send the electrical signal to an amplifier for signal processing. In the first rat, activity from 5 stereotrodes encased in

polyamide tubing were connected to a 16-channel Neuralynx electrode interface board (EIB-16) or EIB-36 Narrow that was cemented to the skull. The signals acquired from the E/I board were amplified using the Cheetah-32 system and Lynx-8 amplifiers (Neuralynx Technologies, Bozemon, MT). Amplifiers were integrated with the Cheetah data acquisition software provided by Neuralynx Technologies. The sampling rate for the recorded local field potentials was 1010.10Hz. Video was recorded from a camera above the field at 30Hz at 720x480 pixel resolution. Video was captured into the Cheetah data acquisition software allowing for alignment between the timestamps of the neural data and video frames.

Signal Processing

Local field potential recordings from amygdala, hippocampus, main olfactory bulb, and insular cortex were indexed according to hand-coded behavioral epochs. To control for amplitude differences between subjects, LFP traces were normalized by overall standard deviation of the LFP per brain region for each rat. An infinite impulse response (IIR) bandstop filter was applied between 59-61Hz in order to filter out 60Hz line noise. Events with artifacts were detected using a .4 millivolt threshold on the hippocampal, insular, and amygdala channels, and a .6 millivolt threshold on the MOB channels. An FIR bandpass filter was used to isolate the respiratory rhythm (2-6Hz), theta (6-10Hz), beta (15Hz-35Hz), low gamma (50Hz-59Hz) and high gamma (70Hz-100Hz). Although the respiratory rhythm commonly varies between 2 Hz and 12 Hz, the respiratory frequency overlaps with the theta so the range was restricted (Rojas-Libano et al, 2014). Shifts from respiratory to theta ranges in the MOB often correspond to slower and faster sniffing rates (Tort et al, 2018). Power spectral densities and coherence was estimated using the Julia Fourier Analysis library, which is a windowed average across the log of the absolute value of the fast fourier transform (FFT) of the signals. For the phase-amplitude

coupling analysis FIR bandpass filter was used to isolate the MOB respiratory rhythm (2-12Hz), and low gamma (50Hz-59Hz) and high gamma (70Hz-100Hz) in all regions. A Hilbert transform was used to extract instantaneous phase information from the respiratory range oscillations and instantaneous amplitude from low and high gamma oscillations. The mean phase amplitude coupling metrics were normalized into a z-score and rose plots were generated for all phase bins. A circular mean was used to calculate the mean to account for the wrap-around at 0 and 2π. Phase values were randomly shuffled to create null distributions for testing the significance of phase amplitude coupling values.

Mixed Effects Model

A general linear mixed-effect model was constructed to perform an ordinary least squares regression of a response variable as a function of mixture of fixed and random effects. Fixed effects include the behavior and agent type, while random effects include the influence of the variance of each individual rat on the response variable within the region. Null distributions were created by taking the aggregate average of novel and familiar sniffing events This allows for the comparison of changes in average coherence within rats, while controlling for any uneven sample sizes and individual differences in overall coherence within brain regions. The effect size was estimated by subtracting the means in question and dividing by the standard deviation of the residual. The mean coefficients, standard errors, z scores, p values, and effect size estimates are reported. The intercept of the baseline group is reported as Int., standard error of the mean as SEM, and the mean coefficients of the comparisons are reported as M. Z scores and p values are also reported.

Convolutional Neural Network Tracking Evaluation

Position tracking for the rat and the robot was performed with U-Net convolutional neural network trained using the Social LEAP Estimates Animal Pose (SLEAP) tracking system (Pereira et al., 2020). Videos were recorded at 29.97 FPS with a frame size of 720x480 pixels. 80% of data was included in the training set. 20% of data was held out in the validation set. Models were evaluated with the sleap.nn.evals.evaluate function operating on ground truth labels from the validation set and predictions on the validation set. Localization error was calculated by the Euclidean distance between the ground truth labels and predictions for each body part (See Chapter 2: Neural Network Offline Tracking Training and Validation Results for more details about the body parts). Mean average precision is the calculation of the area under the curve of the average precision of the predictions. Mean average recall is the calculation of the area under the curve of the average recall of the predictions relative to the ground truth validation set. The object keypoint similarity (OKS) was calculated with a standard deviation of .125 to account for variability in the ground truth labels and is scaled by the area of the instance. The area under the precision-recall curve (AUC-PR) was calculated for 5 OKS thresholds (.5, .6, .7, .8 and .9). The iRat tracker performed the most accurately based on 477 labels. 1/5th of the labels were set aside as the test set, while the remaining labels were included in the training set. The multi-animal rat tracker was trained on ~6600 labeled instances of rats from 2083 video frames from multi-rat trials. A Kalman filter was used to address the temporal association problem of shifts between frames to maintain identity of the skeletons.

Tracking-Based Behavioral Analysis

An interaction zone was identified in a 100 pixel diameter around the enclosure for novel and familiar rats. The tracking data from the freely roaming rat outside of the enclosure was used to determine the amount of timesteps spent within the novel and familiar interaction zones. For

each trial, the ratio of time spent with the novel rat and robot was calculated by taking the total time spent in the novel interaction zone divided by the amount of timesteps in the trial. A ratio of time spent with familiarity was calculated using the same method. These ratios were calculated for both the rat and robot conditions for the interaction test. Welch's t-tests were performed to compare whether rats spent more time near the novel or familiar stimulus within the rat and robot conditions. Cohen's d was also calculated to estimate effect size.

Results

Tracking Results

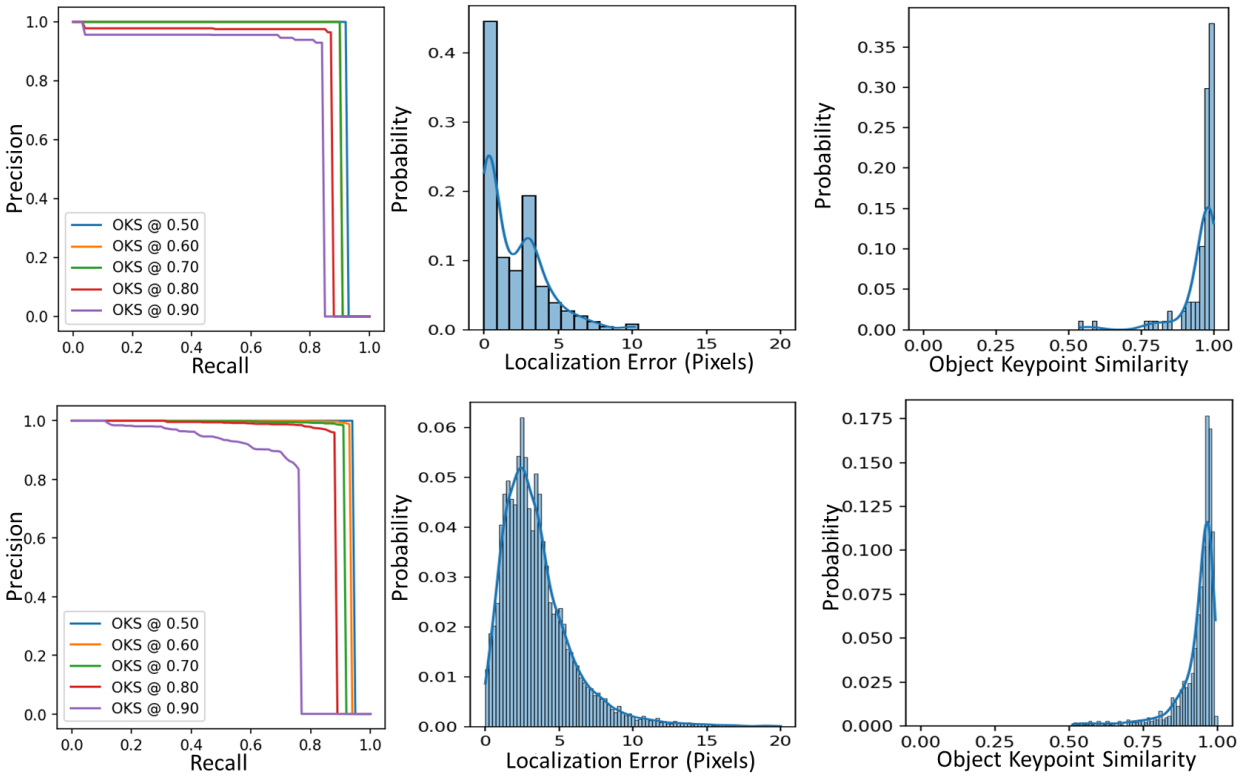

Figure 3.4: Precision-Recall Curve, Object Keypoint Similarity, and Localization Error for multi-rat tracking (top) and multi-robot tracking (bottom).

Figure 3.4 shows the precision recall curves for the rat and iRat neural network tracker. The robot tracker shows a mean average recall of .87 and mean average precision of .85. The

multi-rat tracker shows a mean average recall of .86 and a mean average precision of .84. See Table 3.3 for the results from the area under the precision-recall curve (AUC-PR) calculation.

Table 3.3: The area under the precision-recall curve (AUC-PR) at 5 object keypoint similarity thresholds

	AUC-PR	
OKS Threshold	Multi-Robot Tracker	Multi-Rat Tracker
.5	.93	.95
.6	.91	.93
.7	.91	.91
.8	.86	.88
.9	.81	.73

Behavioral Results

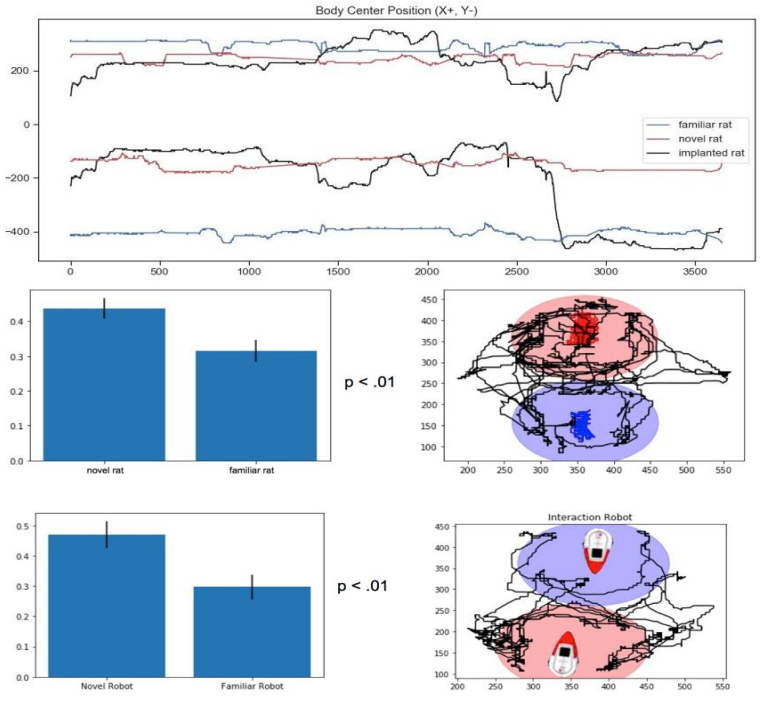

Figure 3.5: Tracking results for rat and robot interaction trials, samples of the multi-rat x,y trajectories are shown in a time series. The 2D plot depicts the implanted rats position in the rat and robot trials. Red and blue circles illustrate the interaction zone for the novel and familiar agents, respectively.

Trajectories show that the freely roaming rat had preferential exposure for the novel agent and spent less time exploring the familiar agent for both rat and robot conditions (See Figure 3.5). The tracking results show that the ratio of time spent in the novel rat's interaction zone (M = .44, SEM = .028) was significantly larger than the familiar rat (M = .31, SEM = .03, t = 3.05, $p < .01$, d = 1). The ratio of time spent with the novel robot's interaction zone (M = .47, SEM = .045) was also significantly larger than time spent with the familiar robot (M = .30, SEM = .04, t = 2.84, $p < .01$, d = .97). The rat was more likely to climb on top of the enclosures if there was a rat inside as demonstrated by the example trace.

Power Spectral Densities

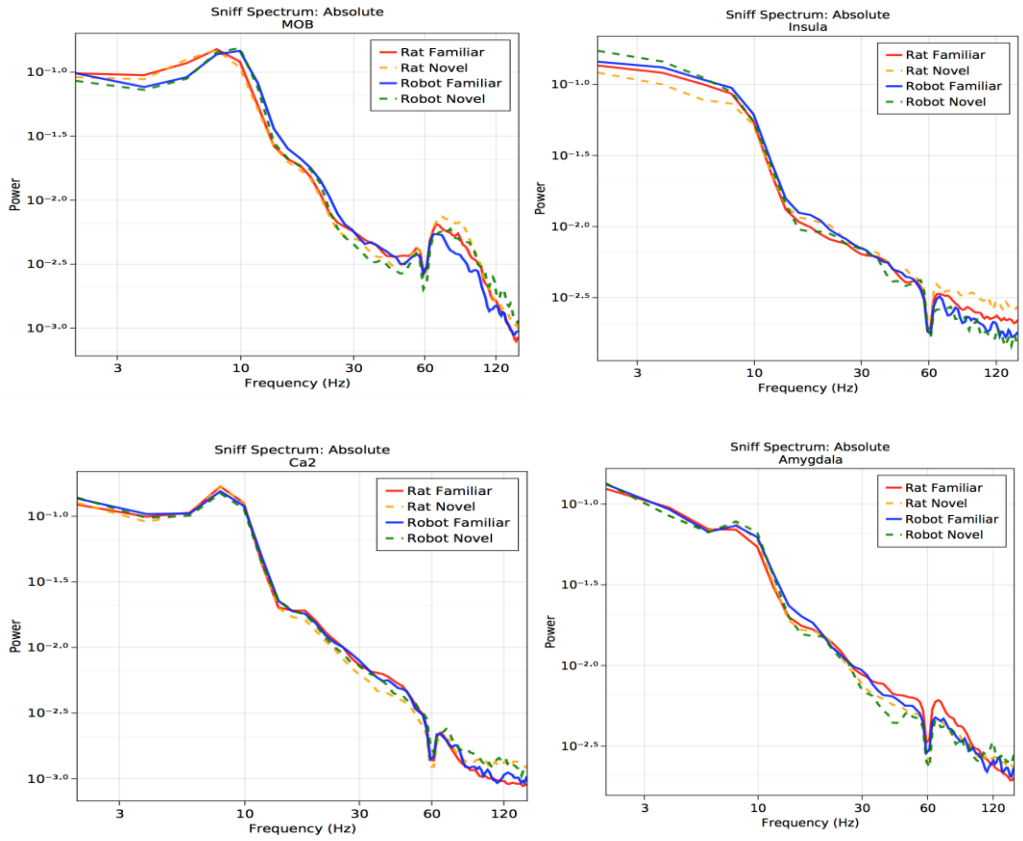

Figure 3.6: Power spectral densities for novel and familiar sniffing events for rat and robot.

Power spectral densities in the MOB indicate larger high gamma amplitudes to novel rats (Int = .006, SEM = 5.5e-4) when compared with familiar rats (M = -6.3e-4, SEM = 3.3e-4, z = -1.95, p = .05, d = .3). The same effect holds for the novel robots (Int = .0047, SEM = .0004) when compared with familiar robots (M = -.0011, SEM = .0004, z = -3.13, p = .0018, d = .55). Power spectral densities in the MOB indicate an increase in amplitude in the slower respiratory rhythm (2-6Hz) when sniffing the rat (Int. = .098, SEM = .008) when compared with the robot (M = -0.015, SEM = .005, z = -3.2, p = .0014, d = .37). The MOB shows an increase in respiration rate in the theta (6-12Hz) range when sniffing the robot (Int = .115, SEM = .006) when compared to the rat (M = -0.011, SEM = .0039, z = -2.79, p = .005, d = .3). This indicates a frequency shift of faster sniffing during olfactory sampling of the robot. The insula shows an increase in amplitude of high gamma oscillations to the novel rat (Int = .0041, SEM = .0008) in comparison with the familiar rat (M = -.0003, SEM = .0001, z = -2.43, p = .015, d = .3). Insula showed no difference between the novel and familiar robot (Int. = .0025, SEM = .0003; M = 1.4e-5, SEM = .0002, z = .08, p > .05, d = .02). The insula shows lower amplitude theta (Int = .057, SEM = .005) and respiratory rhythm for the rat (Int = .106, SEM = .016) when compared with the robot theta (M = -.005, SEM = .002, z = -2.23, p = .025, d = .25) and respiratory rhythms (M = M = -.011, SEM = .005, z = -2.39, p = .016, d = .27).

The hippocampus shows an increase in amplitude of high gamma oscillations for the novel rat (Int = .0015, SEM = .0001) when compared with the familiar rat (M = -.0001, SEM = 4.8e-5, z = -2.85, p = .004, d = .2). There was no significant difference in hippocampus between novel robots (Int = .0015, SEM = .0002) when compared with familiar robots (M = -7.9e-5, SEM = .0001, p > . 05, d = .1). The hippocampus shows a larger theta amplitude for rats (Int = .116, SEM = .004) when compared with robots (M = -.007, SEM = .003, z = -2.43, p = .015, d = .23).

Beta oscillations show higher amplitude when sniffing robots (Int = .0102, SEM = .001) when compared with rats (M = -.001, SEM = .0003, z = -3.30, p = .001, d = .3).

The amygdala shows no significant difference in high gamma amplitude for the novel rat (Int = .004, SEM = .0006) when compared with familiar (M = -.0002, SEM = .0001, z = -1.49, p = .13, d = .14). When compared with sniffing rats (Int = .01, SEM = .003), the amygdala shows a higher beta amplitude for robots (M = 8.8e-4, SEM = 3.1e-4, z = 2.82, p = .0047 , d = .26). This agent-based effect is also apparent in the amygdala theta rhythm to robot when compared with rat (Int = .0004, SEM = .021; M = .0037, SEM = .0018, z = 2.04, p = .04, d = .2), as well.

Discussion

Rodents use a wide variety of olfactory signals to process complex social information in their environments (Gheusi, Goodall, & Dantzer, 1997; Johnston, 2003; van der Kooij, & Sandi, 2012). In most social interaction studies, experiments with rodents have used static objects as a comparison case to understand the significance of the behavioral and neural changes observed (Tendler & Wagner, 2015). This study has presented a novel method for using robots as an intermediary control for complex social stimuli for learning experiments. The brain and behavioral data indicates that there is differential responsivity to novelty and familiarity corresponding to rat and robot. The behavioral data exhibit the expected novel/familiar effect in the rat and robot conditions as seen in previous habituation/dishabituation paradigms with rodents and objects.

The neural data showed expected changes in the olfactory bulb, hippocampus, and insula for the novel/familiar rat and robot conditions. The data indicated a forward frequency shift when sniffing the robot compared to the rat indicating a higher arousal state possibly related to panic. Another explanation is a possible dominance display, because dominant rats have been

shown to increase their sniff frequency relative to subordinate rats. It was also shown that if the subordinate did not slow their respiratory frequency that would lead to an escalation of aggressive behavior by the dominant rat (Wesson, 2013). Beta effects to the robot may relate to signaling uncertainty with respect to the safety of the stimulus (Quinn, Nitz & Chiba, 2010). These findings could be explained by increased motor function, for future directions a properly velocity controlled study is required to tease out these movement related effects.

Learning is crucial for agent assessment which involves not only olfactory habituation but nuanced risk assessment involving unusual stimuli. The decrement of olfactory high gamma oscillations in the MOB to the familiar rat and robot indicate successful olfactory learning and habituation. High gamma oscillations in the insula distinguish between novel and familiar rats but not the robot, which indicates that the rat is inducing coupling between the physiological state of the biological conspecific. Future experiments could be performed to try to induce an insular response by imbuing the robot with signals which resemble biological rhythms like breathing and heart rate.

CHAPTER 4: EXPLORATION, REGULATION, AND COUPLING

Introduction

Exploration, Regulation and Coupling

Active exploration of the environment requires balance. To maximize the effectiveness of exploratory learning an animal must feel safe and remain calm. Rodent exploratory patterns involve establishing a home base, a place the animal deems safe that they commonly return to engage in regulatory behaviors like grooming (Eilam & Golani, 1989). When a rat grooms does it ease the learning and memory process? In other words, does the exploration process include self-regulation in the service of learning? Embodiment implies that cognition is extended, including actions performed by the body (Varela, Thompson, & Rosch, 1991). In translating this to rodent behavior, self-grooming is an embodied act which can facilitate learning. Regulatory subsystems involve an animal dynamically decoupling from the environment and coupling with its own body in the service of motivations (Barandarian and Moreno, 2008). Self-grooming is a behavior inherent to most animals that involves not only hygienic regulation, but also self-regulation of stress relief (Fernandez-Teruel & Estanislau, 2016). Self-grooming involves the regulation of a variety of physiological processes like maintenance of hygiene, thermoregulation, de-arousal and social communication (Kalueff et al., 2015). Due to these functional roles, grooming is a behavior which is highly related to interoception. Self-grooming is a particular form of body-brain coupling where the organism turns inwards and actively regulates their bodily and brain states. Grooming involves slower breathing patterns and these respiratory patterns appear across the brain (Heck et al, 2017; Karalis & Sirota, 2022). It is possible that grooming plays a functional role in the alignment of brain signals for the purpose of stabilizing neural systems to promote readiness for exploration.

Exploratory behavior is central to active perception and is important for the purposes of learning about other agents and the environment. Regulatory behaviors provide an important link between autonomy, motivation and resource management (Aube and Senteni, 95; 96). Grooming has a characteristic effect on frequency and amplitude encoding in the brain. It has been shown to elicit a frequency shift in areas like the main olfactory bulb, which suggest that the animal is slowing their breathing or sniffing rate (Kay, 2009). Grooming leads to increased amplitude of low gamma oscillations in the olfactory bulb (Kay, 2009). High gamma is commonly present during behaviors like sniffing and rearing which involve processing external sensory stimuli. High gamma is aligned with the rising phase of the respiratory rhythm, and low gamma is aligned with the exhalation phase of the respiratory rhythm and may relate to memory consolidation and the processing of the internal milieu (Karalis & Sirota, 2022).

Fotopolou & Tsakiris (2016) have proposed that the process of interacting with other social beings is scaffolded by the same processes that monitor an organism's own homeostatic regulation. Due to the behavioral complexity of grooming, frequency and duration of grooming bouts is dependent on context (Song, Berridge, & Kalueff, 2016). Grooming is a highly contextual behavior which can occur in anticipation or after being exposed to a stressful stimulus. It has been suggested that the "fight or flight" response be revised in rodents to be the "freeze, fight, flight, and groom" response. It is important to note that grooming bouts evoked by stressful high arousal situations might differ greatly from those evoked in states of low-arousal comfort and medium arousal novelty-seeking (Song, Berridge, & Kalueff, 2016). Though linked to external demands, grooming behavior is better characterized as a type of turning inward or turning toward the body rather than the environment.

Stability in the brain may arise from the alignment of brain regions elicited by bouts of grooming. Integration of neuronal populations is thought to be achieved by coupling the phase and amplitude of oscillatory activity across brain regions (Munia & Aviyente, 2019). Phase-amplitude coupling is an encoding mechanism which often relates the phase of a low frequency oscillation with the amplitude of faster oscillations resulting in a nested relationship. Phase is a circular statistic that characterizes the fraction of a cycle in a repeating function (commonly measured in degrees and radians). Phase relations denote a temporal relationship between two oscillatory signals, which capture to what degree repeating waveforms are shifted relative to each other. This encoding method may support communication between both local and distant neural populations. It has been proposed that effective communication between neural populations is likely to some degree dependent on their phase relations (Maris, Fries, & van Ede, 2015). To support the functional relevance of phase, it is important to show that phase relationships can be modulated by sensorimotor events (Maris, Fries, & van Ede, 2015). Little is known about how regulatory behaviors lead to the coordination of multi-region phase-amplitude coupling at the level of the local field potential.

This chapter will examine variations in phase-amplitude coupling between respiratory rhythms, low gamma and high gamma oscillations in the olfactory bulb, amygdala, hippocampus and insular cortex during exploration and regulation.

Methods

Signal Processing

Signals were filtered with a 60Hz notch filter to filter out line noise. An FIR bandpass filter was used to isolate the MOB respiratory rhythm (2-12Hz), and low gamma (50Hz-59Hz) and high gamma (70Hz-100Hz) in all regions. A Hilbert transform was used to extract

instantaneous phase information from the respiratory range oscillations and instantaneous amplitude from low and high gamma oscillations. Mean high and low gamma amplitudes for olfactory bulb, amygdala, hippocampus and insular cortex were extracted and calculated in relation to the phase of the olfactory respiratory rhythm and hippocampal theta rhythm. For all statistical tests, vector strength based on mean amplitude per phase bin was used. A moving mean with periodic boundary conditions was used to calculate the average to account for 0 and 2π being adjacent values. Phase values were shuffled using random permutations to generate null distributions with a mean of zero for the purposes of testing for the significant presence of non-zero PAC. Welch's t-tests were performed to compare the differences in magnitude of phase preference and phase difference for all regions during sniffing and grooming. For the purposes of visualization, the mean phase amplitude coupling metrics were normalized into a z-score and rose plots were generated for all phase bins. In this transformed distribution, negative z-values correspond to the anti-phase component of the coupling. The anti-phase components when represented visually cause the relationship to be cluttered on the polar plot, so only the positive components were included.

Grooming and Sniffing Behavioral Analysis

Video was coded for behavioral epochs using ChronoViz (Fouse, Weibel, Hutchins, Hollan, 2011), as well as ELAN 6.0. The following epochs were extracted during the experiments/trials, with each event having variable length. There were three agent subcategories present within the condition, labeled as robot, object, and rat, indicating who or what the subject interacted with during each trial. See Chapter 3 for information about video coding for sniffing behavior and Chapter 2 for self-grooming behavior.

Results

Phase-Amplitude Coupling Results

Table 4.1: Statistical Tests for The Presence of Non-Zero PAC

Amplitude		Phase					
Main Olfactory Bulb		Respiratory Rhythm			Hippocampal θ		
Behavior	Frequency	t	p	d	t	p	d
Sniff	High γ	33.01	e-99	1.6	22.46	e-67	1.27
	Low γ	15.38	e-40	.79	16.14	e-42	.9
Groom	High γ	36.59	e-99	2	25.19	e-76	1.46
	Low γ	20.49	e-60	1.09	15.86	e-41	.89
Hippocampus		Respiratory Rhythm			Hippocampal θ		
Behavior	Frequency	t	p	d	t	p	d
Sniff	High γ	15.16	e-39	.79	22.53	e-84	.83
	Low γ	17.06	e-46	.93	28.37	e-99	1.1
Groom	High γ	16.85	e-45	.94	22.30	e-77	1
	Low γ	18.97	e-53	1	20.49	e-60	1.1
Amygdala		Respiratory Rhythm			Hippocampal θ		
Behavior	Frequency	t	p	d	t	p	d
Sniff	High γ	23.14	e-73	1.21	20.41	e-60	1.08
	Low γ	17.47	e-49	.9	30.88	e-99	1.18
Groom	High γ	21.46	e-64	1.12	22.07	e-76	.94
	Low γ	20.41	e-60	1.08	24.18	e-87	1.09
Insula		Respiratory Rhythm			Hippocampal θ		
Behavior	Frequency	t	p	d	t	p	d
Sniff	High γ	16.12	e-39	1	28.47	e-99	1.15
	Low γ	15.42	e-37	.98	25.01	e-92	1.05
Groom	High γ	16.89	e-42	1.14	25.19	e-76	1.4
	Low γ	16.75	e-41	1.08	15.86	e-41	.89

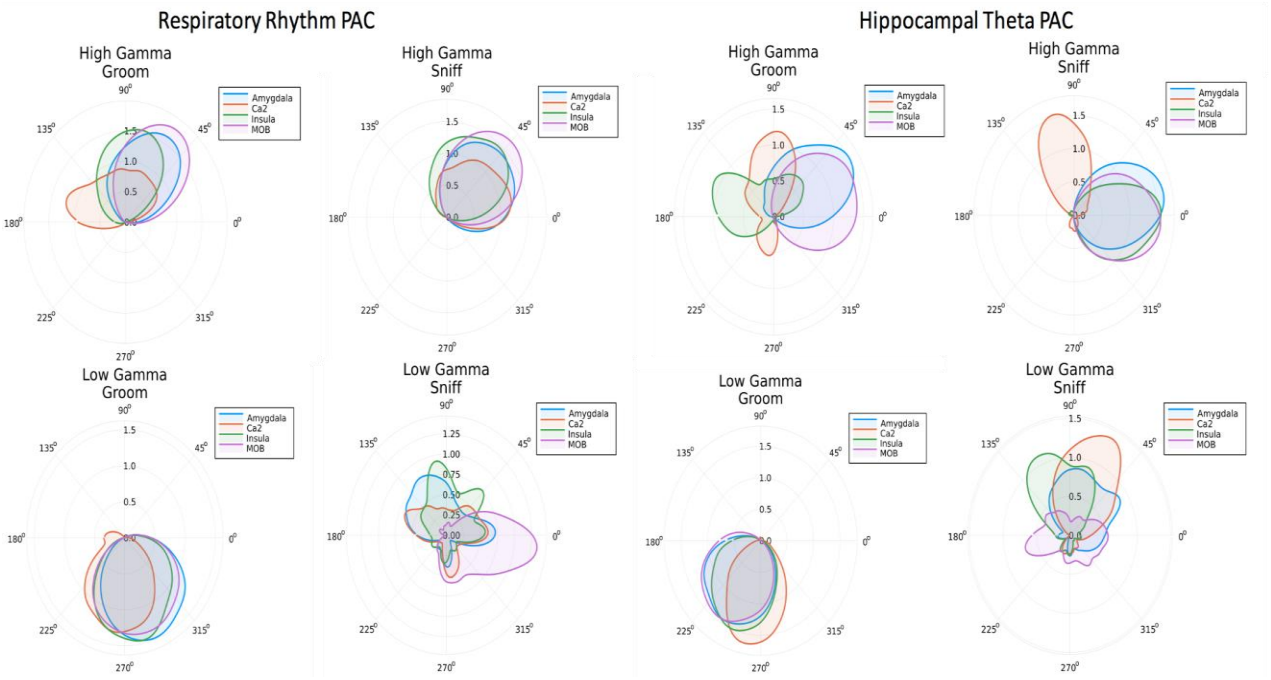

Figure 4.1: Mean high and low gamma amplitude per olfactory respiratory phase bin during grooming, immobility, rearing and sniffing behaviors.

Results generally show precise selectivity of gamma amplitude to the phase of respiratory rhythm and hippocampal theta (See Table 4.1 and Figure 4.1). All regions show a significant phase difference between high and low gamma oscillations relative to the respiratory rhythm during grooming across all regions ($t = 23.98$, $p < e\text{-}99$, $d = .66$). However, during sniffing there is a more modest phase difference relative to the respiratory rhythm between high and low gamma oscillations across all regions ($t = 6.9$, $p < e\text{-}11$, $d = .19$). For sniffing, there is no significant difference in phase preference to hippocampal theta between high and low gamma oscillations across all regions ($t = .9$, $p = .35$, $d = .02$). For grooming, there is a significant difference in phase preference to hippocampal theta between high and low gamma oscillations across all regions ($t = 13.16$, $p < -37$, $d = .35$).

For exploratory behaviors like sniffing there is increased magnitude in phase preference to the hippocampal theta oscillations in the high gamma range when compared with grooming for the hippocampus ($t = 3.1$, $p = .0017$, $d = .12$), amygdala ($t = 4.9$, $p < e\text{-}5$, $d = .2$), insula ($t = 3.4$, $p < .001$, $d = .14$), and olfactory bulb ($t = 3.99$, $p < e\text{-}4$, $d = .18$). There is increased magnitude in phase preference for sniffs between respiratory oscillation and high gamma range when compared with grooming for the hippocampus ($t = 2.9$, $p = .003$, $d = .16$), amygdala ($t = 2.3$, $p = .02$, $d = .12$), insula ($t = 2.7$, $p = .007$, $d = .18$), and olfactory bulb ($t = 4.3$, $p < e\text{-}4$, $d = .23$). There is increased magnitude in phase preference for grooming between the respiratory oscillation and low gamma range when compared with sniffing for the hippocampus ($t = 3.5$, $p < .001$, $d = .2$), amygdala ($t = 6.16$, $p < e\text{-}8$, $d = .32$), insula ($t = 3.45$, $p < .001$, $d = .16$), and olfactory bulb ($t = 12.05$, $p < e\text{-}28$, $d = .64$). There is no increase in magnitude in phase preference for grooming between the hippocampal theta oscillation and low gamma range when compared with sniffing for the hippocampus ($t = 1.7$, $p = .08$, $d = .06$). There is no increased magnitude in phase preference for grooming between the hippocampal theta oscillation and low gamma range when compared with sniffing for the amygdala ($t = 7.13$, $p < e\text{-}11$, $d = .26$), insula ($t = 5.9$, $p <-8$, $d = .22$), and olfactory bulb ($t = 7.74$, $p < e\text{-}13$, $d = .42$).

Discussion

Evidence presented in this paper suggests that sniffing and grooming behaviors lead to strong phase preferences of the amplitude of gamma oscillations in the amygdala, insular cortex, and hippocampus with the olfactory bulb respiratory rhythm and hippocampal theta. Large effect sizes indicate the presence of respiratory and hippocampal theta coupled PAC. Precise alignment between brain regions may induce stability in neural systems, possibly priming the

communication of distant brain regions for the purpose of promoting a state ready for assessing and learning about the external and internal environment.

Sniffing is a primary way that rodents explore the world. Behaviors like self-grooming play an important role in regulating internal states in the form of de-arousal. Rhythms like high gamma indicate active processing of the external sensory world, while low gamma is likely related to regulating an animal's internal interoceptive milieu (Kay et al, 2009). During grooming, high and low gamma usually occupy opposite phases for behaviors relative to the respiratory rhythm and hippocampal theta. However, during sniffing there is an upwards shift in the phase preference of the low gamma oscillation for all regions. High gamma oscillations and having a phase preference at the peak of lower frequency oscillations may be a channel by which the olfactory bulb, amygdala, insular cortex, and hippocampus organize to process external sensory stimuli. Exploratory states seem to promote phase diversity (Maris, Fries, and van Ede, 2016).

Grooming is characterized by a downward shift in respiration denoted by increased low frequency respiratory rhythm amplitude in the olfactory bulb. Grooming behavior also shows an increase in low gamma activity. In comparison with the sniff results from Chapter 3 which more directly involve the processing of external stimuli, the grooming events lead to a decrease in variability in low gamma oscillations. The strong increase in the magnitude of phase preferences in multiple regions to the respiratory rhythm in the olfactory bulb is indicative of the integration of their own olfactory information and potentially a de-arousal signal for the purpose of stabilizing brain dynamics. Low gamma oscillations may be a channel by which areas like the olfactory bulb, amygdala, insular cortex, and hippocampus organize with slower rhythms such as theta and respiratory rhythms to signal the internal state of the organism. Grooming leads to

increased low gamma coupling at precise phase delays between regions in comparison with exploratory brain states. One possibility is that the effect of increased coupling could be explained by the animal being more familiar with their own odor than other odors, given that olfactory bulb phase relationships have been shown to fall into attractors upon presentation of a well-learned stimulus, but a larger dataset would be required to make this judgment.

While measures like PAC are interesting metrics for analyzing inter regional communication, more work is required to understand the nonlinear nature of coupling between regions. We propose using nonlinear coupling methods, such as convergent cross mapping, to examine the bidirectional nature of inter-regional communication. This will allow us to investigate the hypothesis of whether grooming not only serves as a de-arousal function but also stabilizes bidirectional coupling between brain regions to promote readiness for learning and memory consolidation.

CHAPTER 5:
CONVERGENT CROSS SORTING FOR ESTIMATING DYNAMIC COUPLING

The content within this section, titled “Chapter 5: Convergent Cross Sorting for Estimating Dynamic Coupling” reflects material from a paper that has been published in the journal Scientific Reports. The full citation is as follows:

Breston, L., Leonardis, E. J., Quinn, L. K., Tolston, M., Wiles, J., & Chiba, A. A. (2021). Convergent cross sorting for estimating dynamic coupling. *Scientific Reports*, *11*(1), 1-10.

Abstract

Natural systems exhibit diverse behavior generated by complex interactions between their constituent parts. To characterize these interactions, we introduce Convergent Cross Sorting (CCS), a novel algorithm based on convergent cross mapping (CCM) for estimating dynamic coupling from time series data. CCS extends CCM by using the relative ranking of distances within state-space reconstructions to improve the prior methods' performance at identifying the existence, relative strength, and directionality of coupling across a wide range of signal and noise characteristics. In particular, relative to CCM, CCS has a large performance advantage when analyzing very short time series data and data from continuous dynamical systems with synchronous behavior. This advantage allows CCS to better uncover the temporal and directional relationships within systems that undergo frequent and short-lived switches in dynamics, such as neural systems. In this paper, we validate CCS on simulated data and demonstrate its applicability to electrophysiological recordings from interacting brain regions.

Introduction

Previous chapters have utilized methods that assume there are linearly separable oscillatory frequency bands that can be neatly isolated by filtering. Methods like power spectral density and coherence estimated by Fourier methods assume a linear separation of sine waves of different frequencies. Rather than advocating for the "communication-through-coherence" hypothesis, this dissertation advocates for the "communication-through-coupling" hypothesis. This chapter will be concerned with using a novel nonlinear coupling method to examine the bidirectional interaction between brain regions during grooming and social sniffing behaviors.

While linear methods may be easier to use, that does not necessarily mean that they capture the right aspects of coupling relevant to the highly nonlinear and dynamic brain. While traditionally information flow in the brain is usually measured with algorithms with stochastic linear assumptions like Granger Causality, cross-mapping tools provide promising tools for estimating and quantifying nonlinear and deterministic coupling patterns. These methods are meant to uncover correspondences between the trajectories of dynamical systems, which can lead to subsequent predictions about coupling and hypotheses which can be tested in an interventionist paradigm. Sugihara's convergent-cross mapping algorithm was originally designed to map weather systems and biological populations, and has also been applied to neural and behavioral systems. Convergent cross-mapping is a method for estimating correspondences between attractors that have generated the time series observations. Using Takens' delay embedding theorem for phase-space reconstruction, methods like Convergent Cross Mapping can be used to estimate nonlinear coupling between measured observations. One critical aspect of Takens' embedding theory is that when variables are coupled, they are inseparable, that is to say that each variable contains information about other variables within itself. New methods

which expand on the CCM algorithm are sensitive to weak-to-strong coupling and are informative beyond frequency decomposition methods like coherence. The proposed method Convergent Cross Sorting expands CCM to a larger range of applicable systems.

Convergent Cross Sorting for Estimating Dynamic Coupling

Determining the "causal" relationships between the components of a system is a ubiquitous challenge across the sciences. To this end, many methods have been developed to estimate these interactions from their observed time series. Each method's domain of applicability is determined by its definition of causality, and its assumptions about the underlying system. Convergent Cross Mapping (CCM) is an approach, based on state space reconstruction (SSR) (also referred to as phase space reconstruction), which is best suited for complex, nonlinear systems, such as those found in neuroscience, ecology, and the social sciences (Sugihara et al, 2012; Ma, Aihara & Chen, 2015; Quyen et al, 1999; Hlaváčková-Schindler et al, 2007; Chicharro & Andrzejak, 2009; Arnhold et al, 1999; Schiff et al, 1996; Ye et al, 2015; Cummins, Gedeon, & Spendlove, 2015). These systems' myriad feedback loops and deterministic components cause the information about their variables to become inseparably mixed (1). This presents a challenge to methods based on stochastic processes, such as Granger Causality (GC), because they define causation as the ability of one process to provide additional predictive information about another (Granger, 1969). These assumptions may not be as suitable for deterministic systems because every coupled variable carries information about the others, meaning that variables cannot be fully removed from the system for analysis, which violates the assumptions of GC (Sugihara et al, 2012).

In contrast, CCM tests for causal coupling by measuring the correspondence between the SSRs produced from time series of two different variables. If there is a smooth mapping

between them, then both variables are likely part of the same dynamical system and thus deterministically coupled. CCM has been successfully applied to a diverse range of systems, including fisheries, online social networks, and fMRI (Sugihara et al, 2012, Luo, Zheng, & Zeng, 2014; Wismüller et al, 2014).

Despite its success, CCM has several practical problems that have been noted in the literature: It requires a large number of samples to converge, it struggles in cases containing strongly coupled variables or synchrony, and its performance degrades with noise (Chicharro & Andrzejak, 2009; Schiff et al, 1996; Ye et al, 2015; Cummins, Gedeon, & Spendlove, 2015). Subsequent work has tried to address some of these problems. For instance, Ye, et al. introduced lagged CCM estimates to improve performance on strongly coupled variables, while Ma, et al. introduced Cross Map Smoothness to reduce the required time series length (Ma, Aihara, & Chen, 2015;Ye et al, 2015). Though these approaches were successful, they only address individual failure modes.

To improve CCM's performance on issues related to coupling strength, noise and sample size, we propose a new implementation known as Convergent Cross Sorting (CCS). CCS measures the correspondence between reconstructed manifolds by comparing the relative ranking of the pairwise distances between samples. This approach affords multiple advantages including selectively sampling the most informative distances and normalizing for geometric transformations that distort absolute distance but preserve relative order.

In this paper we validate CCS's ability to identify the existence, directionality, and relative strength of coupling relationships for a wide range of simulated signal and noise characteristics. We also highlight the importance of using CCS on well-characterized systems with known structural connectivity informed by the functional dynamics reported in prior

literature. As an exemplar, we demonstrated the multiple uses of CCS as applied to neural recordings from known anatomical circuits to examine dynamic network states during complex behaviors.

Results

Theoretical Model Validation

Simulated Data

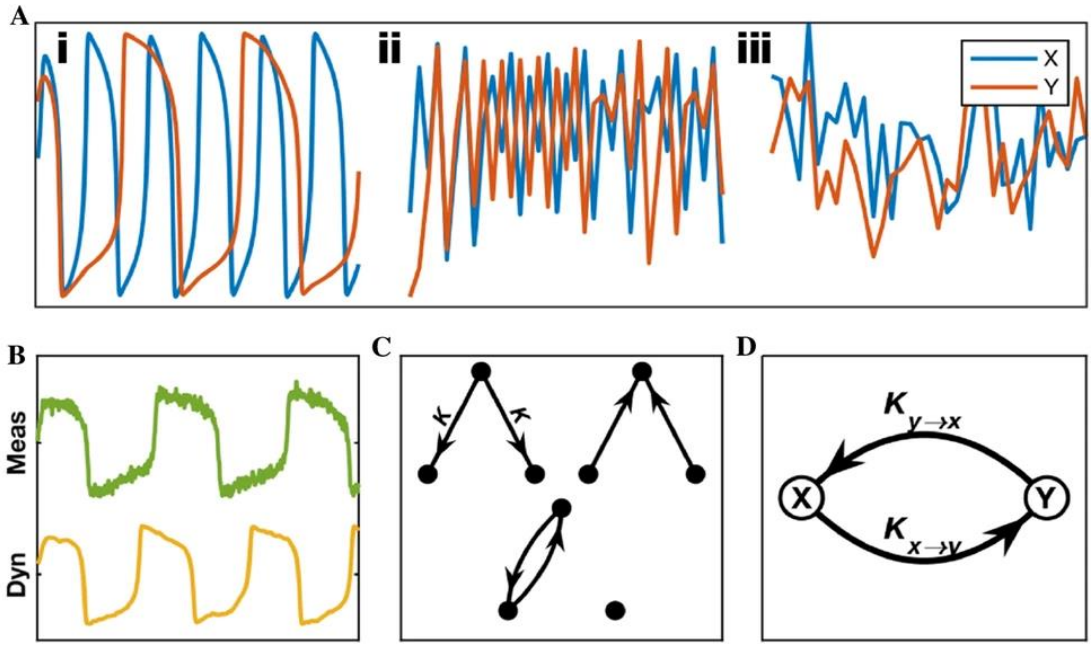

Figure 5.1: Simulated Data. (**A)** Time series from the three classes of model used for validation: **(i)** Van der Pol Oscillators, **(ii)** Logistic Maps, **(iii)** Autoregressive Models. **(B)** Trace of a VDP with measurement noise(**top)** and **(Bottom)** dynamic noise. **(C)** Types of causal networks used to generate trials for assessing detection accuracy. Three variable networks afford the ability to test a method's performance in the presence of third party confounds such as the common driver of two uncoupled variables in **(Top Left)**. All other three variable topologies had to be omitted because they contain transitive causal relationships which leads to ambiguous pairwise results. In each network the coupling strength, K, of both edges is the same. **(D)** Two variable network used to test the response to coupling parameters. $K_{x\to y}$ and $K_{y\to x}$ can vary independently.

To validate CCS, we compared its performance to CCM on simulated data sets for which the true coupling parameters were known. To cover a wide range of potential signal properties,

we considered three types of model systems: Van der Pol oscillators (VDP), Logistic Maps (LM) and Autoregressive Models (AR). **(Fig 1A, SI Simulated Data)** VDPs are deterministic, continuous, and approximately periodic; LMs are deterministic, discrete, and chaotic, while ARs are linear and stochastic. ARs were included to test the SSR methods' performance when applied to processes which violate their underlying assumption of nonlinearity and have a high degree of dynamic stochasticity.

Additionally, to test the methods' robustness to noise, we corrupted the signals with both measurement noise, ε, and dynamical noise, ϵ. (**Fig 1B, SI Simulated Data)** Measurement noise was simulated by adding gaussian noise to the final output time series, while dynamical noise was injected into the system's ongoing dynamics. To normalize the units for measurement noise we used the Signal to Noise ratio (SNR) of the magnitude of the uncorrupted time series to the magnitude of the added noise.

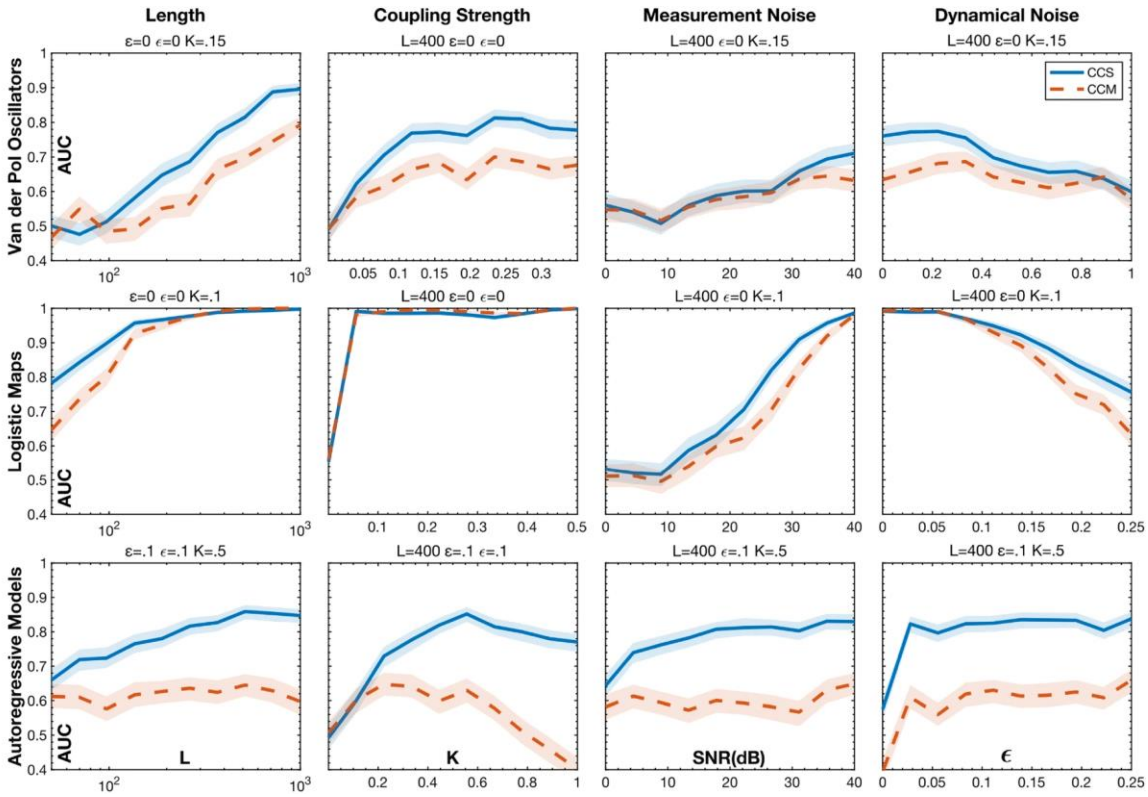

Figure 5.2: The ROC AUC of CCS and CCM for detecting causal coupling in networks of three variables as a function of signal type, time series length, coupling strength, measurement noise, and dynamical noise. For each condition, the area under the curve (AUC) was calculated using 200 trials of three variable networks. The shaded boundaries represent the 95% confidence intervals of the AUCs.

Detection Accuracy

Fig 2 compares the accuracy of CCS and CCM at identifying the causal relationships in networks of three variables **(Fig 1C)** for varying time series length, L, coupling strength, K, SNR, and ϵ. Each method's accuracy was quantified using the Area Under the Curve (AUC) of the Receiver Operator Characteristic (ROC). This is a measure of how well an ideal classifier could separate the coupled vs non-coupled time series and corresponds to the probability that a method will score a randomly chosen coupled relationship higher than a non-coupled one.

CCS broadly outperformed CCM on the deterministic systems (VDPs and LMs). It had the largest advantage on VDPs, maintaining an approximately .1 higher AUC than CCM for

trials with $L > 100$ and $K > .04$. CCS also had better accuracy for $\epsilon < .78$, at which point the system became too noisy for either method to perform much above chance. While both methods, were degraded by measurement noise, CCS had slightly better accuracy for $SNR > 30\ dB$.

For LMs, CCS and CCM both had excellent accuracy under noise free conditions, however, CCS had much higher accuracy on short trials with $L < 100$. At $L = 50$, CCS had an AUC of .78 compared to CCM's .64. CCS also had better accuracy in the case of high dynamical noise with an AUC of .75 at the highest ϵ value.

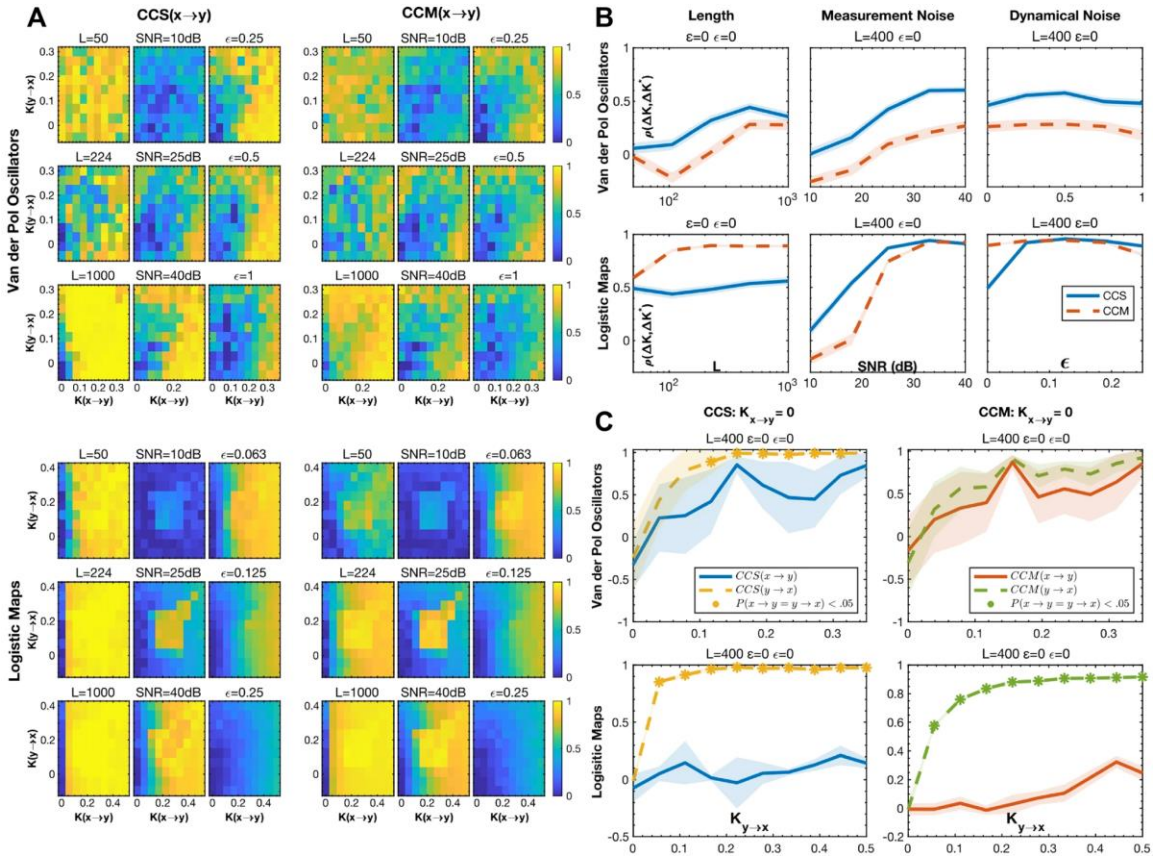

Figure 5.3: A comparison of CCS and CCM's ability to determine the relative strength and directionality of coupling. **(A)** CCS and CCM scores for the drive from $x \to y$ as a function of the $K_{x \to y}$ and $K_{y \to x}$, signal type, L, SNR, and ϵ. $L = 400$, SNR=∞, and $\epsilon = 0$, unless otherwise specified. **(B)** The Spearman correlation between the true difference in coupling strength, $(K_{x \to y} - K_{y \to x})$ and the estimated one, $score(x \to y) - score(y \to x)$. **(C)** CCS and CCM $score(x \to y)$ and $score(y \to x)$ as a function of $K_{y \to x}$ where $K_{x \to y} = 0$ (i.e., unidirectional coupling). The asterisks show the points at which the means of the two distributions of scores was significantly different. The shaded regions in **B** and **C** represent 95% confidence intervals.

Relative Bidirectional Coupling Strength

Beyond identifying the existence of causal coupling, it is also desirable to know the relative magnitude of the interactions between bidirectionally coupled variables, such as those shown in **Fig 1D**. This case is widely applicable to many complex natural systems that have ubiquitous feedback loops. **Fig 3A** shows the CCS and CCM scores for the coupling from $x \rightarrow y$ as a function of the generating parameters, $K_{x\rightarrow y}$ and $K_{y\rightarrow x}$. Ideal performance would look like a graded increase from left to right and no variation from top to bottom. This would represent a monotonic response to coupling strength without any dependence on the drive in the opposite direction.

To quantify how well these scores reflect the true, relative coupling strength, we found the Spearman correlation between the difference in estimated strength and the difference in generating coefficients, $\rho = corr\big(\ score(x \rightarrow y) - score(y \rightarrow x), K_{x\rightarrow y} - K_{y\rightarrow x}\ \big)$. Since the differences are signed, ρ captures each method's accuracy in estimating both the magnitude and direction of the difference in coupling parameters. Furthermore, since the Spearman correlation is a rank statistic, it is strictly testing for the monotonicity of the relationship.

Fig 3B shows the ρ of CCS and CCM as function of system type, L, SNR, and ϵ. CCS has much better accuracy for every condition other than very low noise LMs. CCM actually has a negative correlation for VDPs with $L < 200$ and $SNR < 20\ dB$ and LMs with $SNR < 20\ dB$, which means that its score systematically misidentified the direction of the coupling. This incorrect bias can be seen clearly in the top right quadrant of **3A** where higher $K_{y\rightarrow x}$ decreases $score(x \rightarrow y)$ for constant $K_{x\rightarrow y}$ above moderate values.

The first column in the bottom left quadrant of **3A** shows that CCM outperforms CCS on low noise LMs because CCS saturates at weak coupling strengths. The second two columns

demonstrate how small amounts of noise significantly improve the CCS correlation by preventing this saturation.

Unidirectional Coupling

Fig 3C shows how well the methods differentiated between bidirectional and strong unidirectional coupling. The graphs contain the CCS and CCM scores for $x \to y$ and $y \to x$ as a function of $K_{y \to x}$ while holding $K_{x \to y} = 0$. Both methods performed very well on LMs. They accurately identified the direction of coupling, and their scores for $x \to y$ remained close to zero at even high values of $K_{y \to x}$. Each method had small tradeoffs: The CCM estimate for $x \to y$ had a slightly larger dependency on $K_{y \to x}$, increasing from ≈ 0 to $\approx .2$, and the CCS estimate had a higher variance. The VDPs presented a more difficult challenge because they are much more susceptible to synchrony. Both methods' scores for $x \to y$ had a strong dependency on $K_{y \to x}$. However, only the CCS scores were statistically distinguishable. The mean of its score for $y \to x$ was significantly greater than that of $x \to y$ for trials with $K_{y \to x} > .1$.

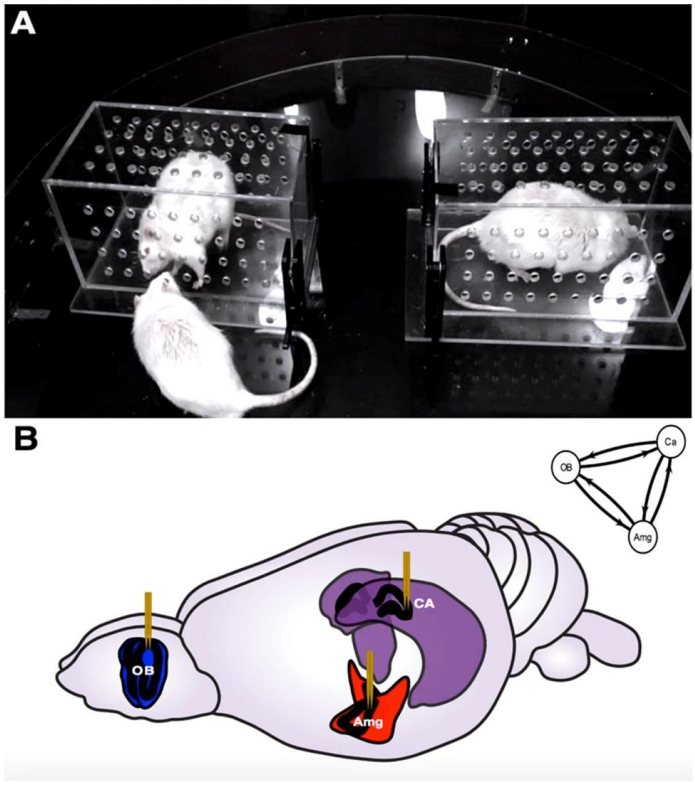

Figure 5.4: Neural experimental setup. **(A)** Two rats were placed in separate Plexiglas enclosures, while an implanted rat on the outside was free to roam the field and sniff through the holes in those enclosures. The implanted rats were presented with both a novel and a familiar rat. The implanted rat freely roams the field and investigates either the novel or familiar rat. Rats were removed from the field 2 minutes and 30 seconds after the onset of a trial. Trials were counterbalanced to control for place preferences, so novel and familiar rats were presented on alternating sides of the field with each trial (See SI for more info on Social Interaction Task and Animals and Housing). **(B)** Rats were surgically implanted with electrodes for electrophysiological recordings in the main olfactory bulb (MOB), hippocampus (CA region) and medial amygdala (MeA) (See SI for more details on Surgery and Neural Recordings). Figure adapted from scidraw.io under Creative Commons 4.0 license (16).

Applications

Neural Recordings

To demonstrate the effectiveness of CCS at revealing directional relationships in noisy real-world data, it was applied to estimate dynamic coupling in time series data collected from the olfactory bulb (OB), hippocampus (Ca), and amygdala (Amg) during social interaction and self-grooming behavior of laboratory rats. The social behavior of interest is the olfactory

investigation of another conspecific. **(Fig 4A)** Self-grooming behavior promotes hygiene maintenance and involves tactile self-soothing, as well as olfactory self-investigation (See Behavioral Video Coding in SI). Oscillatory activity was measured by examining local field potentials (LFPs) **(Fig 4B)** occurring at different anatomical points in a neural circuit proposed to be important for social memory processing (Bielsky & Young, 2004) (See Surgical Procedure and Neural Recordings in SI). This network has previously been shown to elicit increased coupling during social behavior (Tendler & Wagner, 2015). The application of CCS to this simultaneous multi-region LFP data allows for the examination of the coupling strength and direction of coupling between these reciprocally connected brain structures during complex behavioral changes. These relationships are determined by the system's anatomical and functional connectivity.

Structural Connectivity

The amygdala shares reciprocal connectivity with the main olfactory bulb (Pitkänen, 2000). The amygdala and hippocampus share strong bidirectional connectivity (18). Amygdalar activity can also play a key role in influencing hippocampal activity through amygdalo-entorhinal networks (Pare, Dong, & Gaudreau, 1995). The hippocampus and the olfactory bulb also share connectivity in both directions (Martin, Beshel, & Kay, 1995).

Functional Connectivity

The olfactory bulb LFP contains rich information not only about smell but also the autonomic nervous system, by generating respiratory rhythms that follow inhalation and exhalation cycles (Rojas-Líbano et al, 2014; Kay et al, 2009). Hippocampal theta, one of the most well characterized oscillations in the brain, is associated with spatial mapping and memory (Buzsaki, 2002). Respiration-coupled activity has also been found in hippocampus (Sirota et al,

2003; Lockmann et al, 2016; Heck et al, 2017). The OB and hippocampal LFP exhibit coupling during odor discrimination (Martin, Beshel, & Kay, 2007). The amygdala LFP has been associated with the formation of emotional memories, and exhibits coupling with hippocampus (Paré, Collins, & Pelletier, 2002).

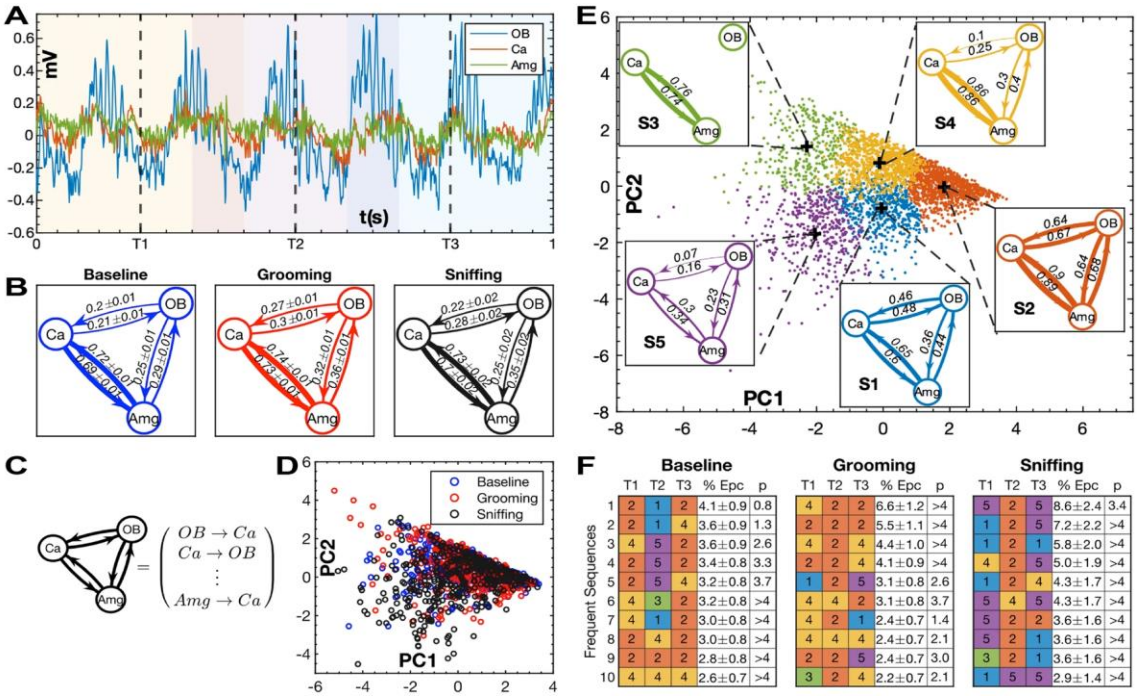

Figure 5.5: Application of CCS to multi-region neural recordings in rats. **(A)** Example LFP trace from a 1 second epoch. The blue, red, and green lines represent the signals from the Main Olfactory Bulb (OB), Hippocampus (Ca) and Amygdala (Amg), respectively. The time points, T1, T2, and T3 are the centers of 400 millisecond windows shown by the shaded regions of the plot. **(B)** Average 1 second CCS scores between the three regions during baseline, grooming, and sniffing behavioral epochs. The error values represent the SEM of each score. All of the scores have a significance $< 10^{-5}$. **(C)** Illustration of how the CCS scores can be represented by a 6-dimensional vector. **(D)** The distribution of 400ms CCS scores colored by type of behavior and plotted using the first two principal components. **(E)** The distribution of 400ms CCS scores colored according to k-means cluster using five means. The inserted graphs show the network diagram corresponding to the centroid of the cluster indicated in the bottom left corner. The values in these diagrams have been corrected for the normalization and whitening transformations used for the PCA. Edges with negative values have been omitted. **(F)** Tables with rows showing the most frequent temporal sequences of CCS states during epochs from each of the behavioral conditions. The first three columns are the moving CCS estimates labeled and colored according to their cluster from **E**. The 4th column is the percentage of epochs with that sequence. The error value is the standard error of the percentage. The 5th column is the negative log of the p-value that nth most frequent pattern would have a frequency as extreme as the one observed.

Average Network State

Fig 5B Shows the average CCS scores for each behavior. The coupling was strongest between CA and Amg for every condition, which is consistent with the regions' degree of anatomical connectivity. Grooming exhibited the highest overall coupling, containing the maximum score for every edge in the network. Sniffing saw the largest asymmetry in the reciprocal coupling between regions. During sniffing the drive from CA to OB and Amg to OB was 27% and 40% higher, respectively, than the coupling in the reverse direction. In the other two behaviors, the reciprocal coupling differs by no more than 16%.

In general, the results (in **Fig 5B**) follow previously established patterns of connectivity. For example, as expected, CCS demonstrated that the hippocampus and amygdala share more connectivity in general than with the distant olfactory bulb (Pitkänen, 2000, Pitkänen et al, 2000). These results suggest that the amygdala and olfactory bulb share increased coupling during social investigation relative to baseline, and that the amygdala and hippocampus both show a larger influence over the MOB than in the feedforward direction. During the grooming behavior, all regions showed increased coupling relative to baseline, with more balanced bidirectional coupling between regions than the social sniffing behavior.

Temporal Dynamics of Network States

For higher temporal resolution, we computed 6-dimensional CCS scores using a moving window on each 1s epoch. **(Fig 5A, 5C) Fig 5D** shows a scatterplot of the first two principal components of these scores, colored according to behavioral type. The plot doesn't show obvious clustering according to behavior, meaning that at that time scale the different behaviors are composed of varying distributions of similar network states.

To understand the temporal dynamics of the network, we analyzed each epoch's trajectory through the 6-dimensional coupling space. To make comparisons more tractable, we quantized the space using five k-means clusters which assigned every CCS score to one of five network states **(Fig 5E)** (Coates & Ng, 2012).

Fig 5F shows the most common sequences of network states during the epochs from each type of behavior. Since the epochs were extracted from larger events, and from video with a lower sampling rate than the neural data, the order of the sequences is not informative and cyclic permutations should be considered the same. The three behaviors differed in both the specific highly represented patterns, and the general distribution of sequences. Baseline tended to oscillate from high to moderate coupling, grooming remained in a consistent highly coupled state, and sniffing oscillated between low and high coupling. Baseline also had the flattest distribution of sequences. The top ten most frequent sequences in that condition comprised between 4.1% to 2.6% of the epochs, while the most frequent sequence in grooming and sniffing comprised between 6.6% to 2.2% and 8.6% to 2.9%, respectively. This result makes sense since baseline is the least restrictive of the behavioral conditions which means it should have the most diverse temporal patterns. Taken together, the results in **Fig 5D** and **Fig 5F** show that the dynamics of the network during the three behaviors are composed of similar bases of states but differ in their distribution of sequences.

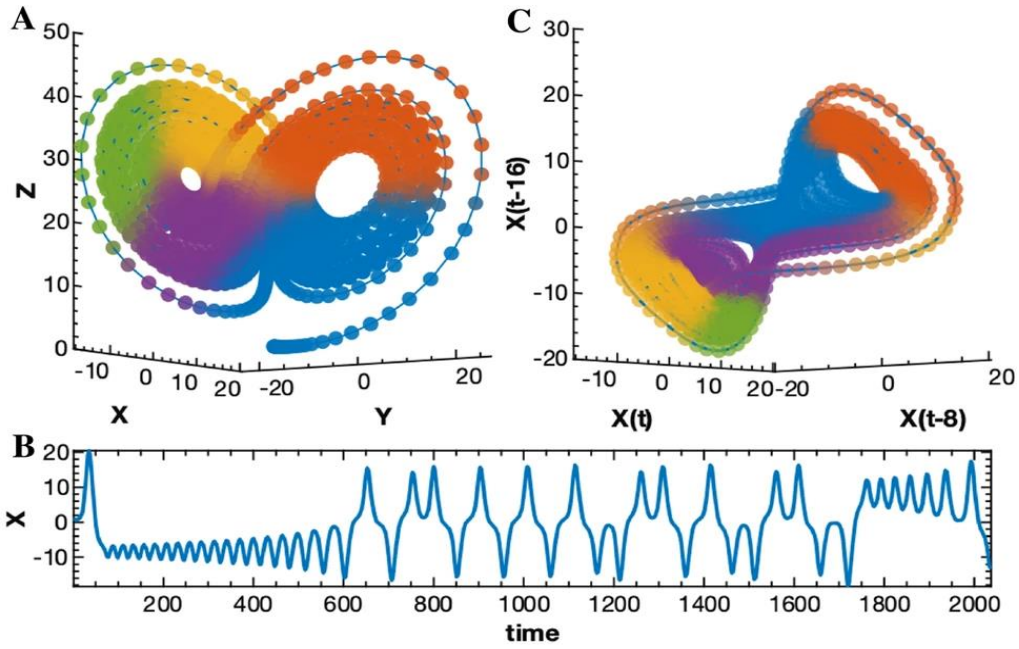

Figure 5.6: Illustration of Takens' theorem. **(A)** A Lorenz attractor with time points colored according to proximity. **(B)** Time series of the x coordinate. **(C)** Delay reconstruction from lagged x coordinates. The timepoints have the same colors as those in **A.** Notice how the delay reconstruction preserves the relative locations of the time points despite being transformed and warped. This demonstrates the homeomorphism between the two manifolds.

Methods

Convergent Cross Sorting

All SSR methods leverage Takens' theorem to reconstruct the higher dimensional attractor of the dynamical system which generated an observed time series. This attractor is the manifold of points, M, visited by the system as it evolves through state space. **(Fig 6A)** State space is a Euclidean space with axes corresponding to the state variables, $\{x, y, z \ldots\}$, of the system. Takens' theorem shows that one can produce a topology preserving embedding of M using delayed values of just one of its variables as surrogate coordinates. This means that there is a homeomorphism, or a smooth, invertible mapping, between the system's trajectory in the coordinates $\{x, y, z \ldots\}$ and $\{x(t),\ x(t+\tau),\ x(t+2\tau), \ldots\}$ **(Fig 6B-C)** (Takens, 1981). Furthermore, since homeomorphisms are transitive, the reconstructions created from each

variable will all be homeomorphic to one another. SSR methods rely on this transitivity by testing if there is a smooth mapping, $\sim$, between the manifolds, M_x and M_y, reconstructed from two different variables, x and y. If $M_x \sim M_y$, then x and y are likely components of the same dynamical system. In the case of unidirectional coupling, the driving variable is a component of the driven dynamical system but not vice versa. Therefore, there will only be a mapping from the driven variable to the undriven one (Sugihara et al, 2012, McCracken & Weigel, 2014).

The primary challenge in determining if there is a smooth mapping between reconstructed manifolds is that their topologies are unknown. SSRs represent geometric point clouds whose topologies must be inferred from the distances between their points. It follows that a test for a smooth mapping must measure the correspondence between the relative location of time points in each reconstruction. That is, if time points are relatively close (as compared to all other points) in one reconstruction then, if there is a smooth map, they should also be close in the other. Complicating this process is that many real-world variables that could benefit from SSRs tend to be noisy and sparsely sampled, which makes any resultant reconstruction only weakly representative of the true topology of the attractor.

CCM tests for this correspondence using the nearest neighbors (NN) of contemporary time points in each manifold **(Fig 7A)** (Sugihara et al, 2012; Ye et al, 2015). The NN implementation suffers from several practical problems. First, it requires a large number of points for the manifold to be densely sampled enough for the neighbors to be meaningful. Second, it fails to accurately estimate the interactions between strongly coupled or synchronous variables because their neighborhoods diverge at longer distances than those being considered (Mønster et al, 2017; Ye et al, 2015). This problem extends more generally to all oscillatory

signals whose nearest neighbors tend to be points close in time. Finally, its estimates are degraded by noise, and are unreliable for stochastic systems (Mønster et al, 2017).

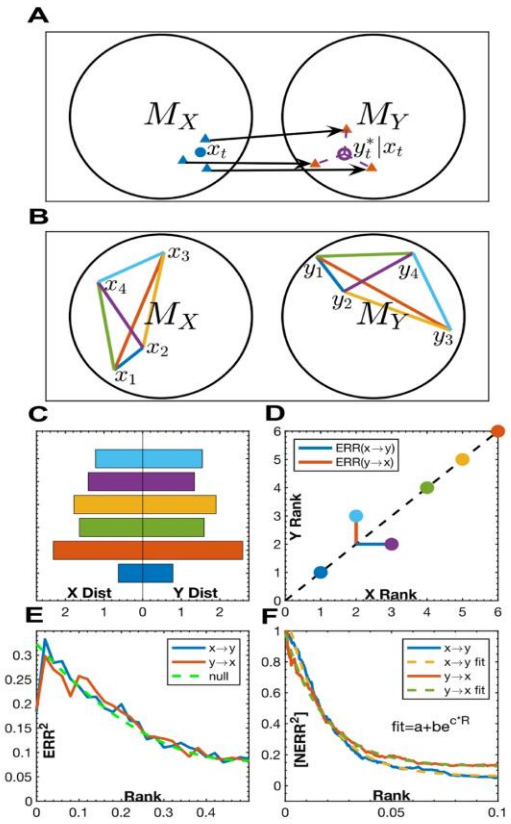

Figure 5.7: (A) An illustration of the CCM method. x_t is point in M_X. The blue triangular markers represent its $D + 1$ nearest neighbors where D is the embedding dimension. The arrows show the mapping of each neighbor in M_X to its location in M_Y. ${y_t}^*|x_t$ is the estimate of the point y_t from exponentially weighted average cross mapped neighbors from x_t. $CCM(y \to x) = corr({y_t}^*, y_t)$ **(B-F)** An illustration of the CCS method. **(B)** Pairwise distances between the same four timepoints in M_X and M_Y colored according to which time points they span. **(C)** The magnitude of the distances in both manifolds. **(D)** The rank of each distance in M_X, R_X, plotted against its rank in M_Y, R_Y. The black dashed line represents perfect correspondence. The blue and red lines show the error between ranks, $ERR = R_X$-R_Y, as a function of R_Y and R_X, respectively. $ERR(x \to y) = ERR(R_Y)$ and $ERR(y \to x) = ERR(R_X)$ because they measure how well ranks in the manifold of the driven variable predict ranks in the manifold of the driver. **(E)** ERR^2 as a function of rank for a bidirectionally coupled logistic map. The ranks have been normalized between 0 and 1. The dashed green line represents the null expected ERR^2 for uncorrelated ranks. **(F)** The cumulative average of the normalized error, $[NERR^2]$, as a function of rank, for the system shown in **E**. $NERR^2 = (null - ERR^2)/null$. $[NERR^2]$ is thresholded at a maximum rank and fit to an exponential curve. The CCS scores are given by the y-intercepts of the fitted curves. Extrapolating from the best fit curve improves the estimate of the local correspondence by leveraging information from larger scales to overcome the high variance in $NERR^2$ observed at very low ranks.

CCS overcomes these challenges by taking a more global perspective. Instead of just using local neighborhoods, it tests for a correspondence between the ranks of the pairwise distances between all the time points in each reconstruction. **(Fig 7B-F, SI Convergent Cross Sorting)** The primary advantage of this approach is that it creates a mechanism for only sampling the connections that are most informative of the topology of the space. By limiting the scope of the comparison to some lowest fraction of distances, CCS selectively considers the most densely covered portions of the manifold. This not only confers the direct benefit of eliminating the errors caused by outlying points but allows CCS to include far more pairwise distances than a KNN method because it doesn't risk including more erroneous points. This means CCS can integrate more information from sparsely sampled manifolds which improves its performance on short and noisy data. It also enables CCS to test for the long-range divergences that are necessary for differentiating between strongly driven systems and bidirectional causation. Additionally, using ranks, instead of raw distances, normalizes for geometric transformations that distort absolute distance but preserve relative order. This has been shown to be a more reliable indicator of manifold structure (Chicharro & Andrzejak, 2009).

Ethics Approval

All animal experiments and maintenance procedures were performed in accordance with NIH and IACUC regulations. Surgeries were performed in accordance with UCSD IACUC animal welfare standards. Additionally, the study was carried out in compliance with the ARRIVE guidelines.

Discussion

Non-linear dynamical systems analyses provide a vehicle for measuring coordinated activity across a variety of networks, whether they be social, behavioral, neural, or ecological.

Rooting the analyses of these systems in SSR methods expands the possibilities for uncovering dynamic relationships, revealing structure that goes beyond coupling strength to address directionality. This paper compares the performance of the new CCS algorithm with CCM on simulated data from multiple model systems (VDP, LM and AR) where coupling parameters are known. In addition to the simulation results, we provide an exemplar application of CCS to systems neuroscience using an animal model informed by brain connectomics.

On the simulated data, CCS had higher accuracy than CCM for almost all test conditions. CCS saw its largest advantages on VDPs and short time series Logistic Maps. These results mean that CCS is particularly relevant to systems in which network states change very quickly, requiring high temporal resolution, and those that have smooth oscillatory components. CCS also retained much better accuracy on the stochastic ARs for which CCM fell below chance. Additionally, CCS was better at capturing the relative strength of bidirectional coupling for all but the lowest noise LMs. This may allow it to better capture the state of many real-world complex systems in which all the variables are coupled to some degree.

As an exemplar application to complex data, CCS was used to estimate bidirectional coupling between neural populations in the olfactory bulb, hippocampus and amygdala during social and self-grooming behavior. This application reinforced previous findings from the neurophysiology literature and provided further insight into the temporal dynamics of coupling strength and direction between brain regions during social interaction

These regions switch rapidly from weak to strong oscillatory coupling. Whereas these oscillations typically maintain nested timescales, CCS was able to determine the strength and directionality of these interactions during social and self-grooming behavior. Grooming leads to a greater influence of autonomic input compared to social investigation, leading to stronger and

more balanced coupling. These findings suggest that grooming is not only tactile and motor behavior, but also engages olfactory and autonomic processing.

The observed coupling dynamics changed across time and differed according to behavioral circumstances, where social behavior increased coupling lead by structures involved in affective appraisal and social memory. The pheromonal and olfactory stimuli encountered during social sniffing behaviors is highly salient compared to the other conditions tested, so this likely engages interaction with amygdala. The hippocampus also had increased influence on the olfactory bulb during social behavior as well, and this is likely associated with processes that underlie social memory formation. The results showed that there was increased influence in a primary sensory region from the amygdala, this may be due to the amygdala having a key role in saliency detection. These findings further support the idea that amygdala, hippocampus and olfactory bulb are part of a memory network that elicits increased coupling in response to social stimuli (Bielsky & Young, 2004; Tendler & Wagner, 2015).

The experimental results demonstrate that CCS is a promising tool for uncovering dynamical relationships within systems that exhibit weak-to-strong coupling, rapidly changing network states, and/or oscillatory components. These systems include many types of physio-behavioral coupling both within and between individuals, and in larger groups or teams (Jakubik, 2020; Baxter & Murray, 2002; Strang et al, 2014).

CCS's improved performance on dynamical and measurement noise, as well as coupled stochastic autoregression, suggest that it is useful for examining systems that are largely deterministic but contain some stochastic elements, such as commodity futures yoked to climate fluctuations.

CCS's robust performance on a wide range of signals makes it a powerful tool for data analysis. It advances the state of the art by extending existing SSR methods to short, noisy, and oscillatory signals, greatly increasing the types of problems to which it applies. Furthermore, it is able to better distinguish relative coupling in bidirectionally coupled systems which improves its ability to reveal the coupling dynamics of real-world complex systems. We are releasing the method publicly such that other researchers can use CCS to investigate coupling within a diversity of nonlinear dynamical systems.

Acknowledgements

Chapter 5, in full, is a reprint of the material as it appears in material from a paper that has been published in the journal Scientific Reports, 2021, Breston, Leo, Leonardis, Eric J., Quinn, Laleh K., Tolston, Michael, Wiles, Janet, & Chiba, Andrea. A. The dissertation author designed the experiment, collected the data used in this paper, and was co-author of this paper.

CHAPTER 6:
DESIGNING AUTONOMOUS INTERACTIONS WITH THE PIRAT ROBOT

The content within the first section, titled “PiRat: An autonomous framework for studying social behavior in rats and robots.” reflects modified material from a paper that has been published in the conference proceedings of the IEEE/RSJ International Conference on Intelligent Robots and Systems. The full citation is as follows:

Heath, S., Ramirez, C., Arnold, J., Olsson, O., Taufatofua, J., Pounds, P., Wiles, J., Leonardis, E., Gygi, E., Leija, E., Quinn, L., Chiba, A. (2018) PiRat: An autonomous framework for studying social behavior in rats and robots. 2018 IEEE/RSJ International Conference on Intelligent Robots and Systems (IROS 2018), Madrid, Spain.

Introduction

Autonomy is a central question in robotics that relies on a robot's ability to successfully perform goal-directed actions successfully without human intervention (Beer, Fisk, & Rogers, 2014). Agency and autonomy have become a central focus of complex systems and cognitive science research within the past few decades. In machine learning, artificial intelligence, complex systems modeling, and agent-based modeling, the term agent has been expanded to a wide variety of computational mechanisms and devices, including reinforcement learning, biological cellular models, social networks, epidemiological models and much more (Sutton & Barto, 2018; Beer 2004). This chapter will use the insights from the previous chapters to design a new robot capable of autonomous adaptive behavior that mimics the familiarization process observed in the data.

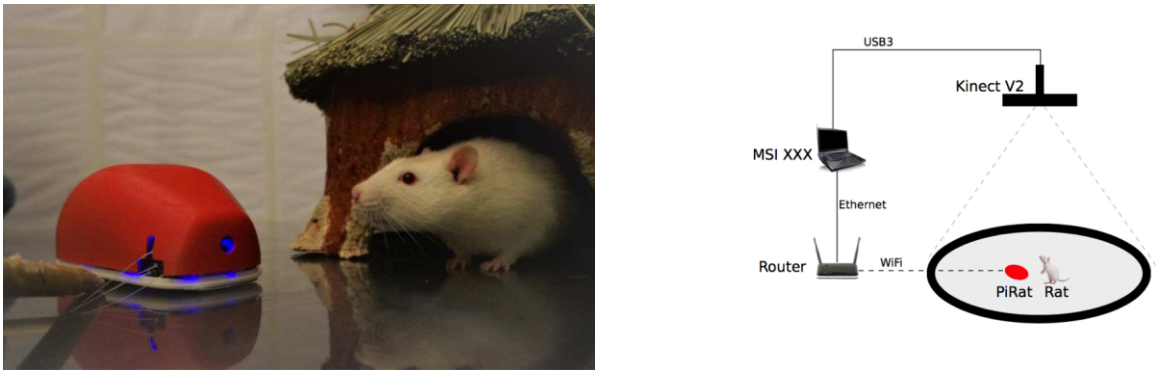

Figure 6.1: Live photo of the rat meeting PiRat and PiRat's overhead tracking system

The international iRat team collaborated to create a new robot specifically for the purpose of eliciting social interactions, using the Raspberry Pi microcontroller, known affectionately as the PiRat (Heath et al, 2018). The authors point out that there are several advantages to using embodied robots for interaction experiments, such as running online models of behavior and the

ability to manipulate a robot's sensorimotor properties in order to potentially identify critical features of sociality (**Figure 6.1**). They presented a low-latency platform for tracking both the rat and the robot in real-time, and preliminary results of the tracking system during habituation and an open field test (**Figure 6.3**). This system will allow for the robot to have autonomous behavior relative to the rat's position, and allows for the development of real-time computational models that govern the robot's behavior.

Wiles et al (2012) point out the design of an interactive social robot for neuroscience experiments with animals requires careful consideration. In social animals, contingencies in the form of mirroring and following exhibit fast timescale dynamics. Therefore, a socially capable robot must be able to respond quickly to an interlocutor's actions, which creates a series of computational constraints on the information processing from sensor to effector. In human-robot interaction experiments, often robots can take seconds to respond, while the design team chose 200ms as a maximum delay time to constrain contingent interactions. Strategic multithreading of the GUI and tracker was required to minimize computation time in the loop. The PiRat GUI allows for the simulation of virtual agents which are governed by the PiRat control system. The GUI allows for piloted, semi-autonomous (triggered), and autonomous behaviors. Ramp functions were created. Behaviors like approach, avoid, follow, and retreat have been defined as behavioral primitives. The PiRat utilizes lightweight low-friction gimbal motors to minimize any noise within distress call range. The design allows for the wheels and motors to be removed for easy cleaning and is attached to the chassis with magnets.

The results of this study also have implications for engineering design. From an engineering perspective, key considerations of social robots are safety, interactivity, and robustness. Safety is a critical aspect of autonomy, so significant measures must be taken to

avoid any harm to the rodents such as running over or pinching their tail or bumping into them. Multiple protocols were created to avoid collision with the rat, the walls of the field, or any objects in the environment. Safety must also be factored in when designing the shape of the chassis and cover. Care should be taken to ensure that all edges are rounded so that both rats and users would not be harmed or intimidated by the robot. The cover should also completely contain all mechanical and electrical components, preventing any damage to those interacting with the robot as well as protecting the robot itself.

Robustness is crucial and can be increased overall by increasing the durability and strength of individual components (Kragic, 2004). Falling under both safety and robustness constraints, covers should be designed so that they can be easily removed by users, but not by the animals, and made of a relatively non-porous material that can be easily cleaned in case of contamination by any substance. Robotic platforms made for interaction with non-human animals must be generally water-proof. This is because urination and urine marking are common occurrences based on our observations, thus the robot's shell or exterior coating must effectively seal the electrical components from an animal's urine. We observed multiple occasions where animal's urine marked the field, stationary objects and occasionally other conspecifics. Cloth, fibers, or other such materials should be avoided or carefully tucked away from the rats' access to prevent choking, shredding, or scent marking that would damage either the rat or the device. A robot's weight should also be considered and be carefully weighted for the agents it will be interacting with. If the robot is too light, it can be easily tipped over, dented or crushed in. If the robot is too heavy, it can impact the motors, adding strain, reducing speed or maneuverability, or cause damage to the environment or to the rodents.

Interactivity consists of multiple sensory stimuli implemented to engage with the rats, with highly stimulating robots contributing to a more engaging environment. However, these stimuli must not be overwhelming, irritating or frightening. Rats can hear frequencies around 250 Hz to 80 kHz, are able to hear ultrasound, as well as being highly sensitive to frequencies between 8 kHz and 38 kHz (Escabi et al., 2019). It is critical that interactive robots exhibit audio frequencies outside of the range of rodent distress calls, which induce panic, irritation, or stress responses. Ultrasonic motors or traditional servos generate too many high frequency sound emissions, as we discovered during the piloting and recording of ultrasonics. The solution for the PiRat was to use gimbal motors which were sufficiently quiet within the necessary frequency range (Heath et al, 2018). Olfactory tags were used in this experiment to engage the rodent's dominant sensory system. Each of the two iRats were tagged with either frankincense or myrrh essential oils, meant to comply with preference profiles indicative of a naturalistic, woody scent.

While it may seem making the robot more like a rat will elicit naturalistic social behaviors, that is complicated by the possibility of the "uncanny valley" effect for animals. While this is primarily an effect associated with humans (Mori, 1970; Saygin et al, 2012), previous studies like those with the Waseda rat showed that the rat-like robot resulted in an anxiety response (Ishii et al, 2006; Shi et al, 2013). This would mean that the closer the robot is to having that animal's appearance the more of a distressing stimulus it may be due to bearing high similarity to a rat but having some features that are a mismatch.

The iRats are visually unobtrusive, with a tapered, rounded 'nose', and a wider backside. They are approximately three to four inches tall and four to five inches in length. In addition to its rounded shell, the cover of iRat is smooth, hard plastic, durable enough to support the weight of a rat without damage to the robot and without pricking the paws of the rat. iRat maneuvers the

field with smooth, coordinated movements, pivoting around objects and rats at a sufficiently moderate speed so as not to provoke the rats, though the pace can be adjusted by the researchers so as to more accurately mimic the quick darting pace of a rat at play or the subdued crawl of a prowling robot. When associating the robot with a reward it is highly recommended that the robot and the reward site be separated from the agent. Gianelli et al. (2018) and Waseda Mouse No.8 had the robot itself act as the pellet dispenser. Ishi et al (2006) has shown separately that robots can easily teach rats to receive a reward at a nearby pellet dispenser. Interactive neurorobotics platforms would benefit from segregating the reward in order to avoid the confounding of extrinsic reward learning in the brain with the intrinsic reinforcement of the robotic stimulus.

The considerations must not only be viewed from the perspective of sound engineering design, but they must also be considered from the internal perspective of the animal meant to interact with the robot. For example, the observational data and quantitative analyses suggest that a key aspect of designing interactive robots is safety. In this case safety must be considered not only by making sure that the robot is designed with physical safety in mind but more importantly whether the animal interlocutor feels safe when interacting with the robot. Safety is a key first step towards the eventual goal of getting the animal to accept the robot as a potential social companion and, thus, a primary consideration in interactivity as well.

Safety and robustness must also be considered from the perspective of species specific behaviors. For rats, robot shells or covers should be designed so that it can be easily removed by users, but not by the animals, and made of a relatively non-porous material that can be easily cleaned in case of contamination by any substance. Robotic platforms made for interaction with non-human animals must be mostly water-proof. This is because urination and urine marking are

common occurrences based on our observations, as they are natural features of interactivity, and thus the robot's shell or exterior coating must effectively seal the electrical components from an animal's urine. We observed multiple occasions where animal's urine marked the field, stationary objects and occasionally other conspecifics. Urine marking is a communicative act, which can denote territoriality, dominance, and is full of rich social information (Leonardis et al, 2021). Marking may bias future interactions if the robot is contaminated with social odor from another conspecific.

Methods

PiRat - The Second Generation iRat

The PiRat system is designed to address the limitations of previous studies with regards to autonomy, and sensors, and to give more control of the study to the experimenters. The PiRat system is formed from several components including the robot platform, a Kinect v2 for tracking, a router for connecting components together and a laptop (see Figure 6.1). Multiple software components run on the laptop, including the tracking system, the behavior manager and MATLAB running a ROS server. Each of these components is outlined in the following sections. For a video overview of the framework and experimental set up, see https://www.youtube.com/watch?v=uzqJsvfEnr4.

PiRat is intended to be a smaller and faster version of our previous iRat [10]. Initial specifications were collected through extensive dialog between engineers and neuroscien- tists (see Table 6.1). PiRat consists of a shaped plastic shell that houses two gimbal motors — high-speed, brushless DC motors — and circuit boards that are required to drive the motors and communicate over WiFi. The shell is constructed from 2 pieces, both of which are 3D printed using a Form2 3D printer. The two pieces of the shell are held together using magnets, so that the

top half can be quickly removed (necessary for replacing PiRat's batteries and shell cleaning). The motors are mounted on a separate piece of plastic, which allows both motors to be easily removed and cleaned. PiRat electronics consist of three circuit boards stacked one on top of the other having an identical footprint to that of a Raspberry Pi Zero (Pi Zero), The top board in the stack is the Pi Zero (running Raspbian), allowing PiRat to connect to Wi-Fi networks through its inbuilt wireless card. The Pi Zero is connected to the distribution board through a novel USB connector that slots in at a right-angle to the other two boards. The second board (the distribution board) contains an STM32 F042 microcontroller that handles the USB connection to the Pi Zero, PWM connections to magnetic wheel encoders and a USART connection to the third circuit board. The third circuit board (the driver board) is a custom-made two gimbal motor driver based on Martinez Gimbal board1) that generates the control signals for PiRat's gimbal motors. Software on PiRat is minimal. The Pi Zero uses Robot Operating System (ROS) to communicate with a tracking system and behavior manager. Translational and angular velocities are forwarded from the Pi Zero to the gimbal motors. PiRat weighs 0.24 kg, has a top speed of 1.1m/s and a top angular velocity of 4.7m/s. The PiRat also includes Pi Zero camera and two new whisker sensors (that are still under development), neither of which are used in the current study.

Table 6.1: The technical specifications of the PiRat regarding size, speed, weight, auditory stimulus, autonomy and cleanliness.

Requirement	Value	Actual
Width	< 0.10 m	0.0875 m
Length	< 0.15 m	0.123 m
Height	< 0.08 m	0.055 m
Max. Speed	$1m/s$	$1.1m/s$
Max. Angular Velocity	$\pi rad/s$	$4.7rad/s$
Weight	0.25 kg	0.24 kg
Audio frequencies	$<$ 10 dB over 25 kHz	✓
GUI	Allow selecting behaviours Use XBOX controller	✓ ✓
Autonomy	Behaviours autonomous Needs to know where rat is	✓ ✓
Cleanliness	Shell and motors cleanable	✓

PiRat GUI and Online Tracker

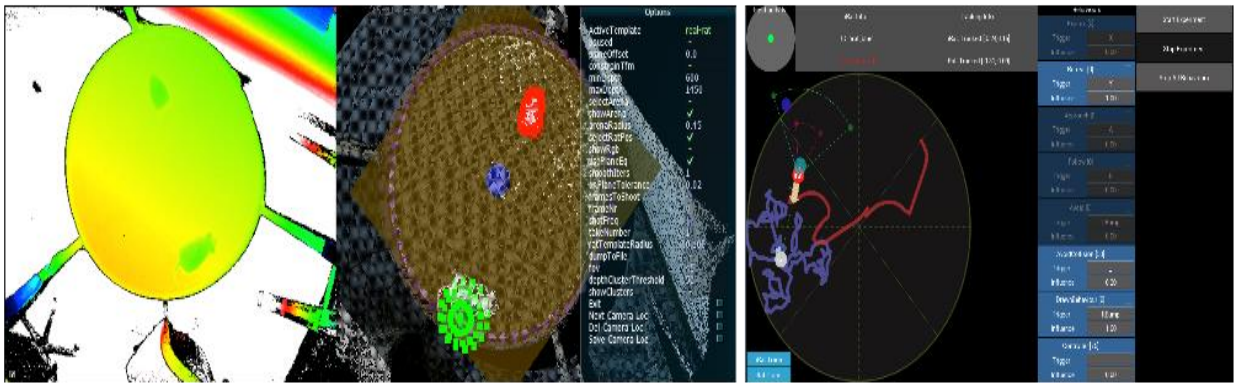

(a) (b)

Figure 6.2: PiRat GUIs a) the GUI used for tracking, b) the GUI used for managing PiRat behaviors.

The PiRat environment is a model of the circular arena and agents within it. The PiRat system contains a GUI and an online tracking system which provides an estimate of the absolute position, orientation, linear and angular velocity of rat and robot during interactions. The online tracker publishes the state variables to a ROS-based environment and the GUI serves to control

the robot and provide visualization capabilities to the experiment. The tracker allows for intervention from the experimenter in case there are any swaps or tracking errors.

Behavioral Design

The PiRat has been endowed with efficient deterministic behaviors such as approaching and retreating from the other agent in a continuous manner. There are also waypoint behaviors to allow for the reproduction of specific trajectories or going to a particular goal location such as a home base location. The GUI is designed so that the behaviors can either be triggered by the experimenter or autonomously selected. The behavior manager is a Python program that controls PiRat through a set of simple behaviors. Examples of behaviors are: approaching, following, retreating, exploring, avoiding, and collision-avoiding. The manager maintains a simple model of the environment (the tracked positions of PiRat and rat), which are the only inputs used by the behaviors (PiRat sensors are not used in this study). Only the approaching, avoiding, and collision-avoiding behaviors are used in this study.

Introduction: The PiRat follows a circular trajectory following the walls of the circular arena, due to the rats preference to stay by the wall, this behavior is meant to maximize their interaction while minimizing the perceived threat of occupying the center of the arena.

Approaching: PiRat calculates the distance between itself and the rat, and then moves towards the rat until the distance is half of the initial value.

Avoiding: PiRat calculates the direction of the rat from the center of the arena, then moves towards the diametrically opposite point on the boundary of the arena.

Collision-avoiding: When PiRat comes within close proximity of the rat or arena edge, forward velocity is slowed and angular velocity increased in proportion to the direction and distance away from the obstacles.

The manager additionally implements a random selection of the behaviors, such that behaviors can be run for a random amount of time, or until a natural completion condition before switching to another behavior. Multiple behaviors can simultaneously control the iRat's actuators through a time dependent influence that is used to mix the linear and angular velocities from each active behavior together.

Behavioral Experiment

The study consisted of rat-robot interaction trials with 8 rats (6 Sprague-Dawley and 2 Brown Norway rats) over 2 days. All studies were run with the room lights on. The procedure was as follows:

Day 1: Habituation

1) A rat is placed into the arena alone for 1 minute.

2) The rat is then removed from the arena.

3) The rat is placed into the arena with a stationary iRat for 1 minute.

Day 2: Trials

1) A rat is placed into the arena with the PiRat running circles of the arena (the Introduction) for 2 minutes.

2) The rat is removed from the arena.

3) The rat is placed in the arena with the PiRat running either the Avoid or Approach condition (counterbalanced across subjects) for 2 minutes.

4) The rat is removed from the arena.

5) The rat is placed in the arena with the PiRat running the second condition (Avoid or Approach) for 2 minutes.

Results

The RGB-D frames were post-processed using the tracking software offline. The positions of PiRat and rat were recorded for each frame. The positions taken from tracking the rat and PiRat show the different trajectories of the rat and PiRat in each condition (Figure 6.3). Distances between the rat and PiRat were calculated for each study. Metrics for the rats' responses to the robot yielded similar values across the approach and avoid behaviors, but were quite different for the Introduction when compared to the other behaviors (see Table 6.2). For the mean distance between rat and PiRat, the Introduction shows the lowest number across all the rats, while the approach behavior is lower than the avoid behavior for 7 of the 8 rats. This difference between avoid and approach could be explained by the behavior of PiRat alone. For the 1 rat where the metric is lower for the avoid behavior, the PiRat started an approach from very close to the rat and spent a significant period following the rat around before reaching half the distance.

The Introduction has the highest number of meetings for all rats, and lowest mean distance between for 7 of the 8 rats, but the component velocities in the direction of PiRat vary. This can be explained by the rat's behavior where in many of the Introduction trials, the rat would run ahead of PiRat, and then wait for PiRat to catch up (see component velocities in Figure 6.3).

One rat, S2, has the highest number of meetings, and shows differences from the other rats across all the phases. In particular, the velocity components in the direction of PiRat show that this rat was more active in creating meetings. In observations of the study, S2 often moved in front of PiRat in all the phases, temporarily blocking the robot from proceeding. Based on this

observation, further exploration of the way in which the dominant or subordinate behavioral phenotype of the rat impacts its interactions with robots should prove interesting.

Table 6.2: Individual rat-robot interactions. **μ** is the mean distance between rats. # is the number of meetings (distance drops below 0.2m), *d* is the sum of the positive components of the rat's velocity in the direction of the PiRat (m).

Rat ID	Study phases: Intro			Approach			Avoid		
	μ	#	d	μ	#	d	μ	#	d
BN2	0.58	8	48.22	0.51	5	21.02	1.07	0	62.16
BN3	0.57	8	19.58	0.87	0	20.64	1.09	0	19.20
EG5	0.58	10	36.76	0.77	0	42.97	1.02	1	38.01
EG6	0.49	12	28.53	0.82	0	33.90	1.10	0	37.78
EG8	0.53	12	31.61	0.84	0	31.27	1.09	0	18.46
R27	0.62	11	43.48	0.85	0	31.29	1.07	0	37.97
S1	0.62	11	44.39	0.85	0	13.63	1.09	0	14.80
S2	0.54	17	58.42	0.78	2	40.28	0.98	2	97.98

μ = the mean distance between rats (m)
= number of meetings (distance dropped below 0.2 m)
d = the sum of the positive components of rat velocity in direction of PiRat (m)

Trajectory Plots

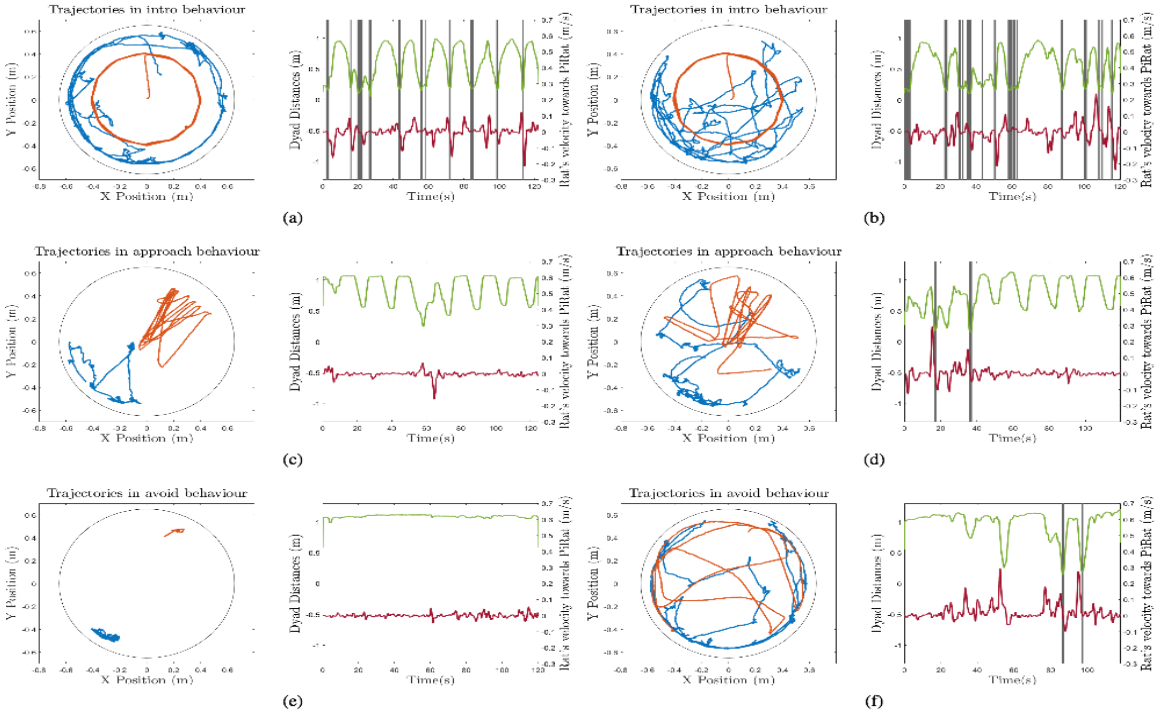

Figure 6.3: Trajectories of, and distances between, the rat and PiRat. The circular plots show the trajectories between rat (in blue) and PiRAt (in orange) and the component of the rat's velocity in relation to the PiRat. The black vertical bars in these plots show when an interaction encounter occurs (the distance between rat and PiRat drops below .2 meters). a),c),e) show the rat that had the least encounters (S1) across the introduction, approach and avoid behaviors respectively. b), d), f) show the rat that had the most encounters (S2) across the introduction, approach and retreat behaviors.

We divided our behaviors into two different conditions: approaching, and avoiding. The Introduction phase was added before initiating the other behaviors, to facilitate the rats' comfort around PiRat. We found that the difference between how rats responded to these two behaviors was minimal; however, differences in the Introduction phase were notable, with all the rats meeting the iRats more times in this phase than the other two phases. This may be because the Introduction featured a predictable motion in a space that the rat would usually occupy (PiRat always following the walls), whereas the other behaviors were dependent on the rat's motion. The introduction behavior shows an interactive strategy that is more successful at engaging than previous WoZ interactions like those in Chapter 2 which primarily occupy the center of the field. By periodically visiting the homebase and remaining closer to the wall that makes the robot more accessible to the rat. An interesting result is that in the avoid behavior (Figure 6.3 E), the rat learned the contingency that the robot responded to its movement so the rat stopped moving to ensure that the robot would not move either. The rat is capable of maintaining distance from the robot, often by running in the opposite direction of the robot's movement in an avoidant fashion.

Discussion

In this study, we aimed to create a rat animat and closed- loop control system that was capable of adapting its behavior to the state of a rat. Results showed that the rats took different trajectories in response to the different behaviors of the robot, showing a preference for the robot to behave in a predictable and repetitive manner. This result is an important benchmark in enabling a robot to autonomously interact with a rat, demonstrating the robot's relevance to the rat's behavior. Metrics for close interaction suggest that the rat attended to the robot in several of the cases, with the highest quality interactions occurring in the Introduction behavior. While the rats in this study had more meetings with PiRat in the habituation phase, we hypothesize that a

combination of further habituation, and changes that initially enable PiRat's behavior to approach less directly, will positively impact the number of encounters that the rat and robot have. These changes will allow rats sufficient time to accommodate to PiRat, reducing aspects of fear or perceived threat.

The framework presented in this paper was designed to facilitate rat-robot interaction studies through creation of an autonomous PiRat, by having the rat's position as a behavioral input to PiRat, by providing low-latency control of PiRat, and by making the system extensible to new behaviors. The first two metrics (mean, standard deviation, and number of meetings) are also influenced by the behavior of PiRat, while the third metric (average rat velocity in direction of PiRat) better captures the rat's behaviors, but can not capture sequences where the rat deliberately waits for the PiRat to approach. The framework was semi-autonomous, as a person was still required to correct tracking failures. However, the tracking for both rat and PiRat were robust, and the operation of the system required only occasional human intervention, in contrast with the constant human input required in previous iRat studies. The increased autonomy is what enables PiRat to ensure reproducible experimental conditions. The human intervention has only a minor effect on reproducibility, as the human is not controlling any of the behaviors, instead intervention is limited to correcting the world-view of the framework. Allowing the rat's position to be used as an input enables behaviors that are specific to each individual rat. While the rats in this study had more meetings with PiRat in the habituation phase, we hypothesize that a combination of further habituation, and changes that initially enable PiRat's behavior to approach less directly, will positively impact the number of encounters that the rat and robot have. These changes will allow the rats time to accommodate to PiRat, reducing aspects of fear or perceived threat.

For studies that use tracking as part of their behavior, the latency from sensors to robot behaviors is important. In contrast, for studies that use tracking for post-processing, the framerate of the sensor is the most important factor. It is important to note that for many sensors, latency can be much slower than framerate, e.g., the Kinect v2 has a latency of 100 ms from sensor to screen, but is able to provide a new image to a screen every 33.33 ms. Our framework has to consider latency so that the real-time response of PiRat happens as close as possible to any change in the rat's position, and these initial estimates suggest that the system maintains a fairly low total systems latency within the real-time loop.

Finally, the behaviors implemented on PiRat are still simple, but as the platform is extensible, we intend to extend the framework with further behaviors, model-driven approaches to social interaction, and the addition of PiRat's sensors as inputs to the framework. We intend for this new robot platform to allow us to continue exploring behavioral and neural responses of rats to a robot, allowing a systematic approach to the study of rat social behavior.

The Exploration-Regulation-Exploitation Dilemma

While the deterministic behaviors created in the previous section are highly efficient, they lack exploratory complexity and may be too simple to be interesting or engaging. By using adaptive learning methods, the robots may be able to generate behaviors that better engage the attention of living systems. By having a robot explore the environment as well as the agents it interacts with, like living creatures do, a rat may be more compelled to interact with it. By learning a behavioral policy a robot will learn how to act within each environmental state to best maximize some objective function. During the habituation process, an animal may begin to learn the policy of a robot just as they predict the actions of other social agents. By operationalizing our previous observations within a multi-agent reinforcement learning framework, we may be

able to develop autonomous robotic systems that are themselves curious, it may be able to better engage the curiosity of the rat.

A recurring theme in this dissertation is that there is a cost to exploration and that regulatory behaviors play an important function in the exploration process. A common paradigm for reinforcement learning is the exploration-exploitation dilemma. The exploration-exploitation dilemma is often depicted with the epsilon greedy reinforcement learning algorithm. Depending on the value of epsilon, the agent will either pick a greedy decision which maximizes reward based on past observations, or a random decision scaled by epsilon to stochastically explore the unknown state space. Based on previous observations, a modification to the classical paradigm is to include regulatory behaviors, resulting in our proposed framework known as the exploration-regulation-exploitation dilemma. This dilemma assumes that high exploration or high exploitation, purely in terms of maximizing information and reward, may lead to instability in the learning dynamics. This instability can be corrected by engaging in regulatory behaviors or including regulatory mechanisms within an artificial system.

Exploration is central to active perception and is important for the purposes of learning about other agents and the environment. Reinforcement learning models operationalize exploration in the form of epsilon greedy action selection and information maximization control. In previous chapters we use behavioral and local field potential data from the rat brain to examine exploratory behavior of novel stimuli and self-regulation of the autonomic nervous system. We seek to use those empirical observations to extract a framework for robots to include exploratory and regulatory behavioral events in their interactive algorithms. Robots that take their rodent interlocutors' exploration and regulation into account will be better at promoting engagement.

Regulatory behaviors provide an important link between autonomy, motivation and resource management (Aube and Senteni, 95; 96). Barandarian and Moreno (2008) argue that regulatory systems are a requirement for a system's adaptivity and argue that a basic metabolic organization may provide a conceptual framework for naturalizing the teleology of behavior. These regulatory subsystems involve an animal dynamically decoupling from the environment and coupling with its own body in the service of motivations. The role of motivation is often underappreciated and provides a promising framework for thinking about multi-agent systems.

Safety is a key issue in autonomous robotics and autonomous policies should not explore the state space so far that they can not recover. Adaptive stability is critical for the maintenance of a system's processes which go beyond the objective function, such as energy or hardware constraints. Reinforcement learning methods have demonstrated high instability and multiple methods for correction have been introduced to stabilize the learning dynamics of actor-critic models, such as the utilization of multiple critics and actors updating asynchronously to stabilize learning.

When collecting real data with rats, they often have to regulate their metabolism, hygiene, affect, and stress levels by engaging in regulatory behaviors like self-grooming. This paper seeks to use the regulatory behaviors observed in rodent exploratory data to develop principles to inform computational reinforcement learning paradigms. Regarding interactive robots, it is critical for the robot to take into account the rats' regulatory behaviors, such as the march back and forth to home base, and also its own way of regulating the learning process to increase stability. When potential danger or even conditions of high uncertainty are present, there is a cost to exploration. For example, exploring novel stimuli often comes at a metabolic and

regulatory cost, due to rats' natural propensity for neophobia (Mitchell, 1976; Modlinska, Stryjek, & Pisula, 2015).

While many algorithms are known to be greedy, i.e. choose the most optimal action relevant to the task at all times, Kirsh argues that there is often as much benefit to being immobile or going to a hiding place as actually engaging in a task. By not acting, animals can filter out hard initial states of the task and utilize a game theoretic notion known as the "just say no" strategy (Batali & Kitcher, 1996). Sometimes it may be useful to pump the brakes on greed and follow Herman Melville's immortal words "I would prefer not to." In addition to "just say no" strategies, there are two other less immediate strategies such as routine maintenance and undertaking exploratory actions (Kirsh, 1996). While Kirsh focused mainly on how the manipulates the external environment, this extends also to the maintenance of the body and internal milieu. Task-external conditions may require us to revise models of behavior to either include temporally and spatially distant actions as of the task in some way or that information-gathering actions that lie outside the boundary of the task are capable of changing the activity inside of it (Kirsh, 1996).

Interestingly, these reinforcement learning algorithms have been found to be related to human social dynamics. Movellan modeled the contingency of attentional dynamics of social interaction using a robotic arm with a sound detector that implemented Bellman's equation to select actions that maximize information return (Movellan, 2005). It was found that turn-taking behavior spontaneously emerged between the robot and human as a consequence of the information maximization algorithm. The use of adaptive reinforcement learning agents in game theoretic scenarios have also shown that when agents adapt to human input, humans perceive those artificial learning agents as more social than non-adaptive agents (Craig et al, 2013).

Proximal Policy Optimization (PPO) in Multi-Agent Scenarios

Actor-Critic methods are notoriously unstable and require regulatory mechanisms. Recent methods like TD3 and A3C are attempts to stabilize the high variance and dynamic updates of the actor and critic by training off-policy networks at every timestep but updating the on-policy network much less frequently. The regulatory mechanism in the PPO algorithm is the policy clip. PPO clips the probabilities of the policy update in order to stabilize learning dynamics to minimize rapid change of the policy and critic. Proximal Policy Optimization is a modification of Trust-Region Policy Optimization which also limits how much a policy can be updated from one timestep to the next by limiting KL Divergence between the old policy and new policies. PPO uses a generalized advantage estimation which measures how better off the agent is taking each particular action when in a certain state. Previous history of states and rewards informs the estimate of which action will lead to higher reward.

Multi-agent reinforcement learning is a challenging area with algorithms that are often highly unstable and not guaranteed to converge. By creating scenarios where agents can learn to cooperate, that can lead to more successful outcomes. A method known as Proximal Policy Optimization has been shown to perform surprisingly well in multi-agent scenarios when agents have cooperative or aligning reward functions (Yu et al, 2021). Proximal policy optimization (PPO) is a popular on-policy reinforcement learning algorithm. PPO is a stochastic policy gradient method that, while sample inefficient, tends to explore the state space sufficiently to eventually converge upon a near optimal solution. Policy gradient methods do not require a model of the environment but instead only models the value of particular states and operates on the policy directly. This method uses stochastic gradient descent across the policy gradient to maximize expected return.

Methods

PiRat Gym Environment

The GUI and tracker are limited to real-time operation so to enable faster than real-time simulation, the dynamic equations from the GUI were put inside an OpenAI Gym environment to allow for rapid training. Like the PiRat GUI, the PiRat Gym environment keeps track of agent position, velocity and orientation. The PiRat Gym environment simulates real-time operation of the GUI by updating 30 times within a simulated second, this process can be sped up significantly faster. The action space was discretized into four possible discrete actions: go, stop, turn left and turn right. See Figure 6.4 for a diagram of the multi-agent actor-critic scenario in the PiRat environment.

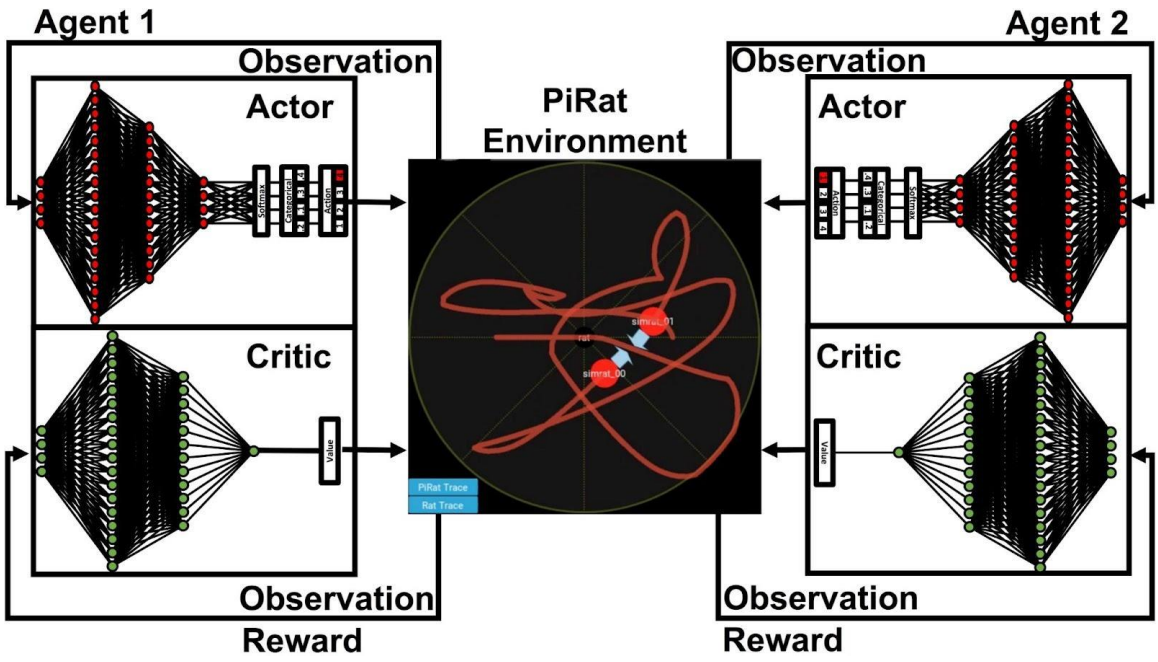

Figure 6.4: A diagram of a simulated multi-agent PPO scenario in the PiRat environment. Two actor critic agents receive observations and rewards from the environment. Value is estimated regarding the advantage of each action and the actor selects the next discrete action which runs through the environment.

Implementation Details

Deep reinforcement learning methods are sensitive to parameters and implementation details, so this implementation has integrated lessons from previous work for improving performance (Engstrom et al, 2020). PPO was implemented using PyTorch and was based on implementations by Phil Tabor . Adam optimizer was used to perform stochastic gradient ascent on parameters. Following recommendations, networks used fully connected linear layers and Tanh activation functions. The actor uses a softmax layer to select a discrete action, while the critic uses a linear layer which projects down to one value for the estimation of the value. To test the effectiveness of multi-agent PPO in the Pirat environment, a simple reward function was chosen to minimize inter-agent distance. Rewards were normalized to values between -.5 and 2. The observation is relative x and y which was normalized to -1 and 1, and relative orientation to the other agent was normalized between 0 and 2π. See Table 6.2 for the parameters used for the proof of concept multi-agent scenario.

Table 6.3. PPO parameters and their respective values for the proof of concept.

Parameters	**Value**
Batch Size	256
Learning Rate Alpha	.0001
Hidden Layer Size	256x256
Gamma	.9
GAE Lambda	.9
Policy Clip	.1

Proof of Concept - Multi-Agent PPO with PiRat

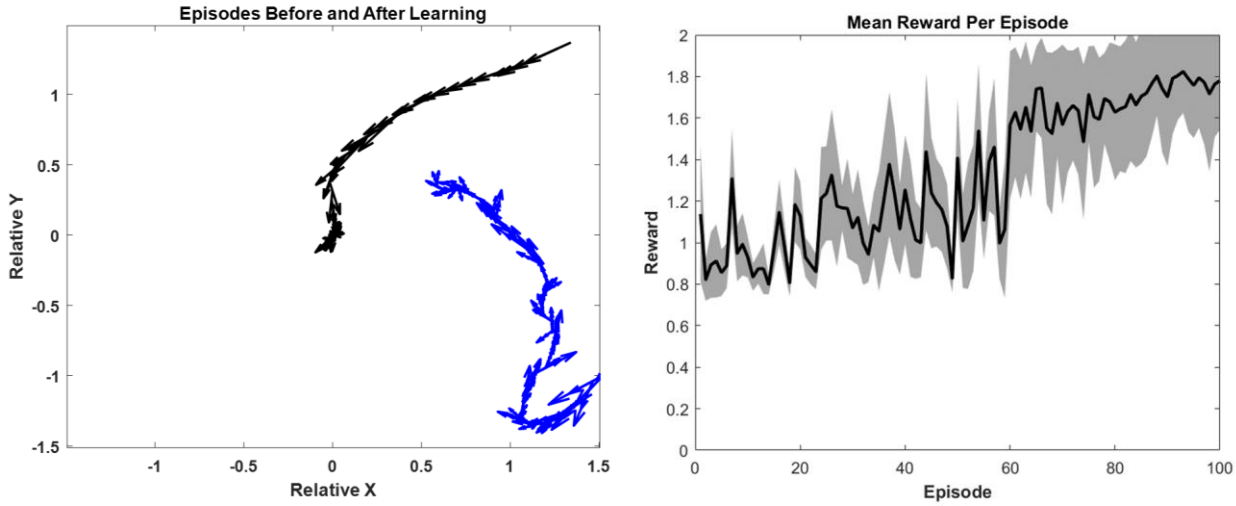

Figure 6.5: Sample relative trajectories for an episode before (blue arrows) and after (black arrows) learning. Mean reward per episode plotted in black with standard deviation in gray.

The sample trajectories in Figure 6.5 show both of the agents in an early learning episode exploring the state space and eventually tending towards each other in a very suboptimal fashion. After learning, in a later episode the two agents approach each other in a more optimal fashion.

Future Directions

Artificial curiosity is an area of reinforcement learning which seeks to model the intrinsic motivation an animal has to acquire information from the environment for learning (Gordon, 2018). Put more simply means that animals are internally rewarded for exploring new things. Embodied curiosity involves the use of curiosity-based computational models with an embodied, physical agent. Gordon (2019) suggests that social behavior is an emergent property of embodied curiosity. The goal of curious embodied agents is to learn as much as it can about itself and the environment, emphasizing the tight interactions between the model, body, sensors, motors, and situated embedded interactions (Gordon, 2018).

Presented in Figure 6.6 is a design for a policy selection mechanism for the PiRat based on Gordon's novelty management unit which will be utilized in future experiments. Novelty of the state space will decay upon each visit to those coordinates and orientation values, the novelty of the agent will decrease upon each subsequent approach within some distance threshold.

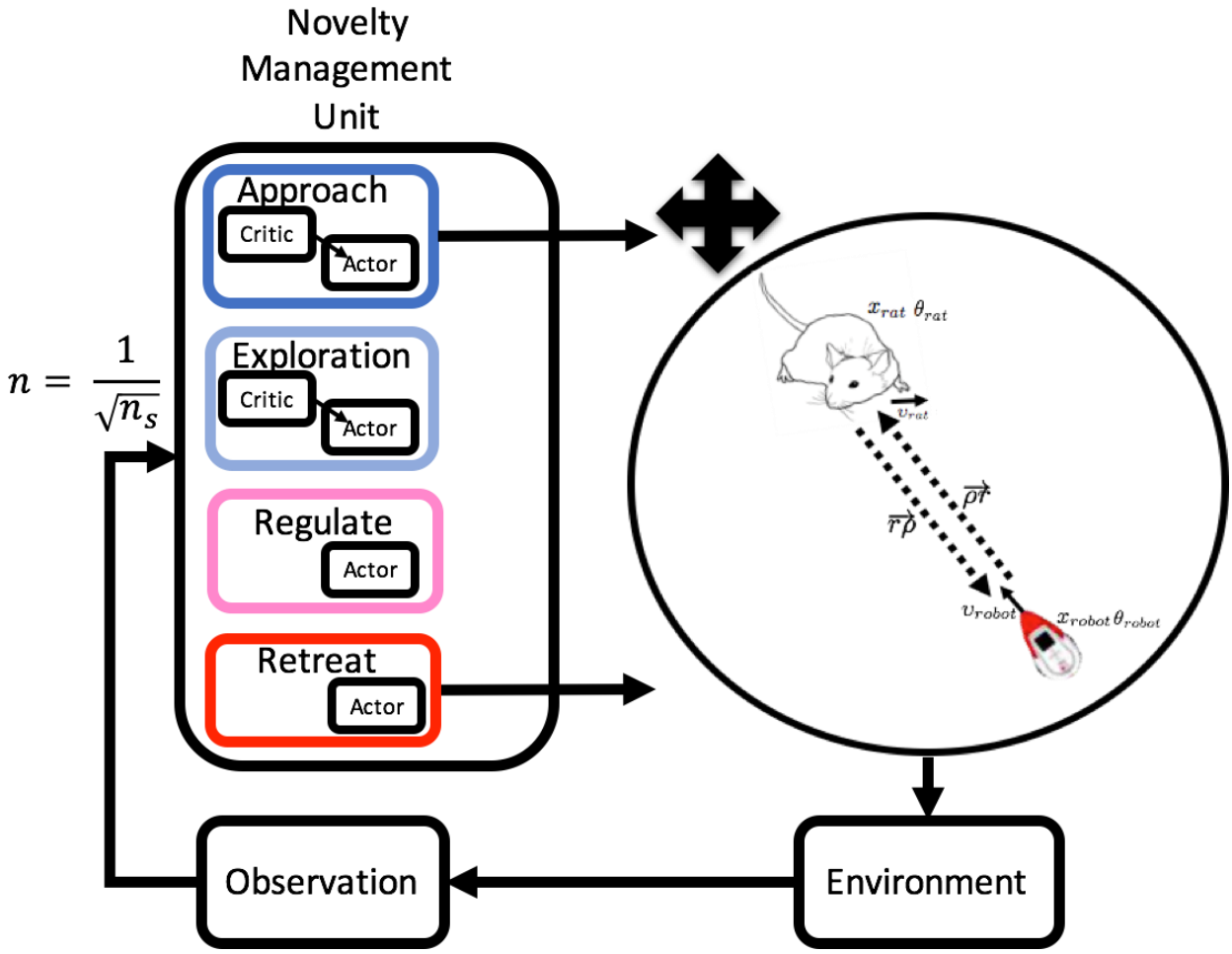

Figure 6.6: A diagram of a novelty management system for the PiRat which will use a policy selection mechanism based on the novelty of the current state.

Future directions for this system involve running optimal simulation parameters on the physical embodied PiRat system. Before embodying in the robot, a systematic search of the parameter space will be performed to identify optimal training parameters. The algorithm may be used twofold, one to control the robot that mimics naturalistic behavior and two to act as a model

of the rat so the robot can account for their exploration-regulation based interaction dynamics. It is important to note that the stability of the state space differs between rat and robot. Based on the rats behavioral response. A control barrier function, also known as safety certificates, have been shown to increase the stability of control algorithms in a variety of robotic applications and multi-agent systems (Marvi & Kiumarsi, 2021). This will enforce a safer environment for the rat because it will eliminate the algorithm from entering that state. The next step after verifying that the multi-agent scenario is feasible and safe using artificial agents, then a living agent can be introduced. We suggest that in this case the intrinsic reward function is not simply based on interagent distance, but instead maximizes how often the rat approaches the robot. Curiosity may also be a prerequisite for play (Gordon, 2019). Perhaps for robotic systems to be perceived as being truly cooperative and prosocial, they may require capabilities like curiosity to allow for play.

The general notion of maintenance involves keeping parts or systems in functional and operating order. Kirsh's notion of "routine maintenance" shapes the environment to help a creature circumvent performance-limiting situations and increase average yield on future actions (Kirsh, 1996). In this sense, self-grooming behaviors deform the topology of state space, possibly rendering more aversive behaviors. Rather than making progress on the task itself, it acts as a regulator of the affective variables that may increase the difficulty of the task. Situated cognition in cognitive science includes many actions as serving a type of "cognitive scaffolding" which was often left out of the story of optimal and sequential advancement to the goal. Kirsh argues that these actions which are less immediate to the goal that still serve to improve the animals performance on a task are "superoptimal."

While on-policy algorithms are useful for fully exploring the space, for future directions it may be more reasonable to use offline algorithms to ensure more stability for the learning process when interacting with a real rat. Methods like advantage weighted actor-critics and advantage weighted regression may allow for an algorithm to learn from previous empirical data in order to better account for the nonstationary nature of living systems. Future directions will explore other methods for ensuring the stability of the reinforcement learning process, such as the use of a KL constraint rather than the simple policy clipping method to create a "trust region" of the state space to explore. Lyapunov-based actor-critics are a method for guaranteeing stability for a critic which creates stability certification and returns to a safe part of the state space during exploration. Future models may also seek to incorporate a model of the rat into the actor-critic architecture to identify the rodent's home base and estimating the probability of future states.

Acknowledgements

Chapter 6, in part, is a reprint of the material as it appears in IEEE/RSJ International Conference on Intelligent Robots and Systems (IROS), Madrid, Spain, 2018, Heath, Scott, Ramirez-Brinez, Carlos, Arnold, J., Olsson, Ola, Taufatofua, Jon, Pounds, Pauline, Wiles, Janet, Leonardis, Eric, Gygi, Emmanuel, Leija, Estelita, Quinn, Laleh, Chiba, Anderea. The dissertation author collected the data used in this paper and was co-author of this paper.

CONCLUSION

This dissertation has been an attempt to ground the 4E approach to social cognition in the biophysics of brain and body coupling by introducing interactive neurorobotics. We have examined how the bodies of multiple artificial and biological agents coordinate with each other at the level of behavior, as well as how brain regions couple with each other at the level of neural population and autonomic nervous system dynamics. This dissertation has provided a novel methodology, Convergent Cross Sorting, for improving the reliability of coupling estimates expanding to a wider variety of applicable systems. Future directions will seek to use these validated methods to quantify interactions at multiple temporal and spatial scales in an effort to examine how social cognition emerges from brain-body-world coupling within and between agents.

This dissertation has shown that biological agents behave quite differently from their artificial counterparts in how they explore the world and regulate their bodily states. The brain data shows sophisticated frequency, amplitude and phase encoding mechanisms supporting the exploration of other agents and self-regulatory behaviors. A lesson from these data is that new technologies are stressful and often induce de-arousal behaviors. This should be a greater area of inquiry for human-computer interaction research. Much like math and coding anxiety, our data suggests that learning how to coexist with new technologies is not an implicitly pleasant experience but one that requires a significant amount of self-regulation. This dissertation has also demonstrated how taking a closer look at behavior and the brain can benefit the design motivation-based autonomous systems, and that robotic systems may benefit from their own forms of self-regulation of learning mechanisms. Future directions will seek to develop

regulatory self-grooming-like behaviors for artificial systems to serve the function of promoting stability in learning dynamics during exploration of a state space.

While animat approaches can provide information that may be relevant to animals, it is important not to confuse them with the animals themselves (Bullock, 2009). While animat literature often advocates for the anti-representational point of view Mandik (2002) points out that animats in synthetic neuroethology are strongly representational in nature. They are often written explicitly as programs or algorithms in the form of the symbolic representations that are explicitly written code that implement control systems. While focusing on situatedness and embeddedness may de-emphasize the role of symbolic representation, it is still an inevitability when creating machines that use digital processors and algorithms to implement control commands (Mandik, 2002). However, these often impoverished representational systems in animat systems fail to live up to the complexity of brain and body coupling demonstrated by the evidence provided in this dissertation. Representations are above all tools that scientists use to better understand and model target systems of interest. This is a key insight of the role of reflexivity in philosophy of science, which includes the role of the observer and the theorist themselves in the explanation of the target system. It is critical to note that while cognitive scientists often assume living creatures have internal symbolic representations like our animats, we must resist the temptation to assume the mind as a computer metaphor without justification. External representations can serve as valuable tools for scientific inquiry, but the existence of internal symbolic representations in animals and humans is still an open question which should be subject to rigorous debate. Some have argued that coupling between brain and body can serve as a deflationary account of representation performing similar explanatory work by implicitly tracking the state of the external world and its inhabitants (Orlandi, 2014).

This dissertation has provided a framework for extending Saygin's "Neural Turing Test" to rodent animal models allowing for increased temporal and spatial resolution of neural measurements. It appears, similarly to findings in human fMRI and EEG, that some social brain circuitry, this time at the level of the intracranial local field potential, is able to differentiate between other rats and robotic agents while other parts of these circuits do not (Urgen, Kutas, & Saygin, 2018). While this question is not definitively answered by this work, a significant amount of evidence has been provided in search of an answer. It is also important to note the limitations of imposing human points of view onto animals and that anthropocentrism is of key concern in animal model paradigms. The use of WoZ control in early chapters of the dissertation is easily subject to the critique from the point of anthropomorphism, but even autonomous systems are not free of the human point of view, after all humans are the ones constructing these systems in the first place. I have argued elsewhere that it is critical to question our human assumptions and attempt to dig deeper into the phenomenology of an animal's sensorimotor life to really begin to address concerns related to anthropomorphism (Leonardis, Semenuks, and Coulson, 2021).

Saygin's "Neural Turing Test" in humans has implications for ethical concerns about how humans interact with robotic technology, especially androids that have human-likeness. We have suggested that, as humanoid robots more closely resemble humans, they can lead to widespread unconscious processes such as priming, and through associative learning and neural plasticity, can lead to changes in our brains, and in turn, contribute to unintended sociocultural effects (Leonardis & Saygin, 2015**).** A majority of humanoid robots are highly gendered and modeled after young women and middle aged men with Caucasian and Asian appearance (Riek & Howard, 2014). "During an ethnographic study at a humanoid robotics lab, Saygin recorded a

video of a young male researcher, who during a lab tour, walked up to an android robot with gendered female appearance, slapped its face, and said ‘sometimes it is therapeutic to hit the android’” (Leonardis & Saygin, 2015, p. 1). Even with knowledge that no physical harm against a human has occurred, this video is visually and emotionally confusing (Leonardis and Saygin, 2015). Anecdotally, given the extremely humanlike qualities and physical presence of this robot, it becomes difficult to “unsee” this event as an act of violence. The possibility and ubiquity of this transference in the context of robotics still remains an open question, but it will likely have undesirable consequences, and the responsibility to speak out falls on the shoulders of the designers (Whitby, 2008)**.** This ethnography provided further evidence that humanoid robots are often constructed and controlled by the male gaze. By constructing humanoid robot bodies and introducing them into everyday human life, designers actively project their own vision of what bodies ‘should be like’ thus implicitly regulating and enforcing the designers' own cultural biases. Rather than being a revolutionary technology with endless possibilities, robotics often reinforces a very narrow and patriarchal view of gender and society.

It is important to promote the interdisciplinary ethical discourse that has recently emerged regarding the future of social robot construction (Riek and Howard, 2014). At The Emerging Policy and Ethics of Human-Robot Interaction (HRI) Workshop, groups of lawyers, policy makers, ethicists, scientists and engineers have gathered together to discuss and debate ethical problems and potential solutions in social, assistive and autonomous robotics. In recent years, conferences like NeurIPS are requiring that authors submit ethical considerations and list potential negative outcomes of their neural network algorithms. Accompanied by the We Robot Conference on Legal Policy Issues Relating To Robotics, the robotics community has begun to create ethical discourse that will be invaluable for the ethical regulation of a complicated and

nuanced technology. However, this must increasingly include scholars from Science and Technology Studies with experience in anthropology, philosophy and history to adequately assess the ethical nature of autonomous systems. Within the framework of research ethics, despite creating an "autonomous" robot the responsibility still falls on the shoulders of the experimenter. If the experimenter subjects an animal or humans to unnecessary harm using an autonomous system, that explicitly does not absolve them of the blame. Why should ethical responsibility of the deployment of autonomous systems out into the world be any different? The ethical status of interactive neurorobotics depends on institutional review boards, which may benefit from using the criteria outlined in Chapter 6 for building robots safe for interaction with animals.

This dissertation also outlines a methodology for using computational reinforcement learning for use in adaptive autonomous robots using an exploration-regulation strategy. Rather than purposefully developing "greedy" reinforcement learning algorithms we ought to imbue them with regulators which keep that greed in check in the interest of stability. Another alternative is to include safety and risk in the reward function itself to regulate the robot's decision making. Autonomy is a carefully negotiated category where institutions have sought to create a diffusion of responsibility. Suchman has pointed out that humans are still heavily involved in scaffolding situations where autonomous robots are deployed and can never truly be "out of the loop" (Suchman and Weber, 2016). While the authors of the articles making up this dissertation are seeking to design prosocial and cooperative robots, that is not always and perhaps not usually the case. There have also been recent efforts to use autonomous robot bees, fish, and plants for the purpose of promoting the survival of at-risk animal populations and sustainability in ecosystems (Schmickl et al, 2021). Pro-social and pro-environmental uses of

autonomous technologies are possible, but not without significant amounts of testing, deliberation, and regulation. The author emphasizes that human-robot interaction as a field is socially responsible for the agents they construct and their potential influence on society.

REFERENCES

Adams, E. (2003). The Construction of Ludic Space. *Proceedings of the 2003 DiGRA International Conference: Level Up. Vol. 2.*

Adhikari, A., Lerner, T. N., Finkelstein, J., Pak, S., Jennings, J. H., Davidson, T. J., ... & Deisseroth, K. (2015). Basomedial amygdala mediates top-down control of anxiety and fear. Nature, 527(7577), 179-185.

Aguilar-Rivera, M., Kim, S., Coleman, T. P., Maldonado, P. E., & Torrealba, F. (2020). Interoceptive insular cortex participates in sensory processing of gastrointestinal malaise and associated behaviors. *Scientific reports*, *10*(1), 1-12.

Ahuja, N., Lobellová, V., Stuchlík, A., & Kelemen, E. (2020). Navigation in a Space With Moving Objects: Rats Can Avoid Specific Locations Defined With Respect to a Moving Robot. Frontiers in behavioral neuroscience, 206.

Amir, A., Lee, S. C., Headley, D. B., Herzallah, M. M., & Pare, D. (2015). Amygdala signaling during foraging in a hazardous environment. Journal of Neuroscience, 35(38), 12994-13005.

Arnhold, J., Grassberger, P., Lehnertz, K. & Elger, C. E. (1999). A robust method for detecting interdependences: application to intracranially recorded EEG. *Physica D: Nonlinear Phenomena*, *134*(4), 419-430

Aubé, M., & Senteni, A. (1995). A foundation for commitments as resource management in multi-agents systems. In *Proceedings of the CIKM Workshop on Intelligent Information Agents. Baltimore, Maryland*.

Aubé, M., & Senteni, A. (1996). Emotions as commitments operators: A foundation for control structure in multi-agents systems. In *European Workshop on Modeling Autonomous Agents in a Multi-Agent World* (pp. 13-25). Springer, Berlin, Heidelberg.

Ball, D, Heath, S, Wyeth, G, & Wiles, J (2010) iRat: Intelligent Rat Animat Technology. In Wyeth, G & Upcroft, B (Eds.) Proceedings of the 2010 Australasian Conference on Robotics and Automation. Australian Robotics & Automation Association, Australia, pp. 1-9.

Barandiaran, X., & Moreno, A. (2008). Adaptivity: From metabolism to behavior. *Adaptive Behavior*, *16*(5), 325-344.

Bartal, I. B. A., Decety, J., & Mason, P. (2011). Empathy and pro-social behavior in rats. Science, 334(6061), 1427-1430.

Barry, C., Lever, C., Hayman, R., Hartley, T., Burton, S., O'Keefe, J., ... & Burgess, N. (2006). The boundary vector cell model of place cell firing and spatial memory. Reviews in the Neurosciences, 17(1-2), 71-98.

Bateson, P., & Laland, K. N. (2013). Tinbergen's four questions: an appreciation and an update. *Trends in ecology & evolution, 28*(12), 712-718.

Baxter, M. & Murray, E. (2002). The amygdala and reward. *Nature Reviews Neuroscience,* 3, 563–573

Beer, R. D. (2004). Autopoiesis and cognition in the game of life. *Artificial Life, 10*(3), 309-326.

Beer, J. M., Fisk, A. D., & Rogers, W. A. (2014). Toward a framework for levels of robot autonomy in human-robot interaction. Journal of human-robot interaction, 3(2), 74.

Bergan, J. F., Ben-Shaul, Y., & Dulac, C. (2014). Sex-specific processing of social cues in the medial amygdala. Elife, 3, e02743.

Bohacek, J. (2020). Deep learning-based behavioral analysis reaches human accuracy and is capable of outperforming commercial solutions. Neuropsychopharmacology, 45(11), 1942-1952.

Bielsky, I. F. & Young, L. J. (2004). Oxytocin, vasopressin, and social recognition in mammals. *Peptides*, *25*(9), 1565-1574.

Bullock, S. (2009). In Defense of the Abstracted Animat. *Adaptive Behavior*, *17*(4), 303-305.

Buzsáki, G. (2002). Theta oscillations in the hippocampus. Neuron, 33(3), 325-340.

Breston, L., Leonardis, E. J., Quinn, L. K., Tolston, M., Wiles, J., & Chiba, A. A. (2021). Convergent cross sorting for estimating dynamic coupling. Scientific reports, 11(1), 1-10.

Brodal, A. (1947). The hippocampus and the sense of smell; a review. Brain: A Journal of Neurology, 70, 179–222.

Chen, W. G., Schloesser, D., Arensdorf, A. M., Simmons, J. M., Cui, C., Valentino, R., ... & Langevin, H. M. (2021). The emerging science of interoception: sensing, integrating, interpreting, and regulating signals within the self. *Trends in neurosciences, 44*(1), 3-16.

Chicharro, D. & Andrzejak, R. G. (2009). Reliable detection of directional couplings using rank statistics. *Phys. Rev. E* 80, 026217

Chikama, M., McFarland, N. R., Amaral, D. G., & Haber, S. N. (1997). Insular cortical projections to functional regions of the striatum correlate with cortical cytoarchitectonic organization in the primate. *Journal of Neuroscience*, *17*(24), 9686-9705.

Choi, J. S., & Kim, J. J. (2010). Amygdala regulates risk of predation in rats foraging in a dynamic fear environment. Proceedings of the National Academy of Sciences, 107(50), 21773-21777.

Coates, A. & Ng, A. Y. (2012). Learning feature representations with k-means. In *Neural Networks: Tricks of the Trade* (pp. 561-580). Springer, Berlin, Heidelberg

Contestabile, A., Casarotto, G., Girard, B., Tzanoulinou, S., & Bellone, C. (2021). Deconstructing the contribution of sensory cues in social approach. European Journal of Neuroscience, 53(9), 3199-3211.

Cummins, B., Gedeon, T. & Spendlove, K. (2015). On the efficacy of state space reconstruction methods in determining causality. *SIAM Journal on Applied Dynamical Systems*, *14*(1), 335-381

Craig AD (2003). Interoception: the sense of the physiological condition of the body. Curr Opin Neurobiol 13, 500–505.

Dantzer, R., Tazi, A., & Bluthé, R. M. (1990). Cerebral lateralization of olfactory-mediated affective processes in rats. al brain research, 40(1), 53-60.

Datta, S. R., Anderson, D. J., Branson, K., Perona, P., & Leifer, A. (2019). Computational neuroethology: a call to action. *Neuron*, *104*(1), 11-24.

Datteri, E. (2020). The logic of interactive biorobotics. Frontiers in Bioengineering and Biotechnology, 8, 637.

De Jaegher, H., & Froese, T. (2009). On the role of social interaction in individual agency. Adaptive Behavior, 17(5), 444-460.

del Angel Ortiz, R., Contreras, C. M., Gutiérrez-Garcia, A. G., & González, M. F. M. (2016). Social interaction test between a rat and a robot: A pilot study. International Journal of Advanced Robotic Systems, 13(1), 4.

Eilam, D., & Golani, I. (1989). Home base behavior of rats (Rattus norvegicus) exploring a novel environment. Behavioural brain research, 34(3), 199-211.

Engel, A. K., Fries, P., & Singer, W. (2001). Dynamic predictions: oscillations and synchrony in top–down processing. *Nature Reviews Neuroscience*, *2*(10), 704-716.

Farovik, A., Place, R. J., Miller, D. R., & Eichenbaum, H. (2011). Amygdala lesions selectively impair familiarity in recognition memory. *Nature neuroscience*, *14*(11), 1416-1417.

Fernández-Teruel, A., & Estanislau, C. (2016). Meanings of self-grooming depend on an inverted U-shaped function with aversiveness. Nature Reviews Neuroscience, 17(9), 591-591.

Flash, T., & Hogan, N. (1985). The coordination of arm movements: an experimentally confirmed mathematical model. Journal of neuroscience, 5(7), 1688-1703.

Fotopoulou, A., & Tsakiris, M. (2017). Mentalizing homeostasis: The social origins of interoceptive inference. *Neuropsychoanalysis*, *19*(1), 3-28.

Fouse, A., Weibel, N., Hutchins, E., & Hollan, J. D. (2011). ChronoViz: a system for supporting navigation of time-coded data. In CHI'11 Extended Abstracts on Human Factors in Computing Systems (pp. 299-304).

Freeman, W. J., & Baird, B. (1987). Relation of olfactory EEG to behavior: Spatial analysis. *Behavioral Neuroscience, 101*(3), 393–408.

Fries, P. (2005). A mechanism for cognitive dynamics: neuronal communication through neuronal coherence. Trends in cognitive sciences, 9(10), 474-480.

Fries, P. (2015). Rhythms for cognition: communication through coherence. Neuron, 88(1), 220-235.

Gallagher, M., & Chiba, A. A. (1996). The amygdala and emotion. Current opinion in neurobiology, 6(2), 221-227.

Gazzola, V., Rizzolatti, G., Wicker, B., & Keysers, C. (2007). The anthropomorphic brain: the mirror neuron system responds to human and robotic actions. Neuroimage, 35(4), 1674-1684.

Gergely, A., Compton, A. B., Newberry, R. C., & Miklósi, Á. (2016). Social interaction with an "Unidentified Moving Object" elicits A-not-B error in domestic dogs. PloS one, 11(4), e0151600.

Gianelli, S., Harland, B., & Fellous, J. M. (2018). A new rat-compatible robotic framework for spatial navigation behavioral experiments. Journal of neuroscience methods, 294, 40-50.

Goosens, K. A., & Maren, S. (2001). Contextual and auditory fear conditioning are mediated by the lateral, basal, and central amygdaloid nuclei in rats. Learning & memory, 8(3), 148-155.

Gourévitch, B., Kay, L. M., & Martin, C. (2010). Directional coupling from the olfactory bulb to the hippocampus during a go/no-go odor discrimination task. Journal of neurophysiology, 103(5), 2633-2641.

Granger, C. W. (1969). Investigating causal relations by econometric models and cross-spectral methods. *Econometrica: Journal of the Econometric Society*, 424-438

Hlaváčková-Schindler, K., Paluš, M., Vejmelka, M. & Bhattacharya, J. (2007). Causality detection based on information-theoretic approaches in time series analysis. *Physics Reports*, 441, 1–46

Heath, S., Ramirez-Brinez, C. A., Arnold, J., Olsson, O., Taufatofua, J., Pounds, P., Wiles, J., Leonardis, E., Gygi, E., Leija, E., Quinn, L. K., & Chiba, A. A. (2018, October). PiRat: An autonomous framework for studying social behavior in rats and robots. In 2018 IEEE/RSJ International Conference on Intelligent Robots and Systems (IROS) (pp. 7601-7608). IEEE.

Heck, D. H., McAfee, S. S., Liu, Y., Babajani-Feremi, A., Rezaie, R., Freeman, W. J., ... & Kozma, R. (2017). Breathing as a fundamental rhythm of brain function. Frontiers in neural circuits, 10, 115.

Heider, F., & Simmel, M. (1944). An experimental study of apparent behavior. The American Journal of Psychology, 57, 243–259.

Hitti, F. L., & Siegelbaum, S. A. (2014). The hippocampal CA2 region is essential for social memory. Nature, 508(7494), 88-92.

Hoffman, G & Ju, W. (2014). Designing robots with movement in mind. J. Hum.-Robot Interact. 3, 1 (February 2014), 91–122.

Ishii, H., Ogura, M., Kurisu, S., Komura, A., Takanishi, A., Iida, N., & Kimura, H. (2006, September). Experimental study on task teaching to real rats through interaction with a robotic rat. International Conference on Simulation of Adaptive Behavior (pp. 643-654).

Jacinto, L. R., Cerqueira, J. J., & Sousa, N. (2016). Patterns of theta activity in limbic anxiety circuit preceding exploratory behavior in approach-avoidance conflict. Frontiers in behavioral neuroscience, 10, 171.

Jacobs, L. F. (2012). From chemotaxis to the cognitive map: the function of olfaction. Proceedings of the National Academy of Sciences, 109, 10693-10700.

Jacobs, L. F. (2022). How the evolution of air breathing shaped hippocampal function. Philosophical Transactions of the Royal Society B, 377(1844), 20200532.

Kalueff, A. V., Stewart, A. M., Song, C., Berridge, K. C., Graybiel, A. M., & Fentress, J. C. (2016). Neurobiology of rodent self-grooming and its value for translational neuroscience. Nature Reviews Neuroscience, 17(1), 45-59.

Karalis, N., & Sirota, A. (2022). Breathing coordinates cortico-hippocampal dynamics in mice during offline states. *Nature Communications*, *13*(1), 1-20.

Kay, L. M. (2005). Theta oscillations and sensorimotor performance. Proceedings of the National Academy of Sciences, 102(10), 3863-3868.

Kay, L. M. (2014). Circuit oscillations in odor perception and memory. Progress in brain research, 208, 223-251.

Kay, L. M., Beshel, J., Brea, J., Martin, C., Rojas-Líbano, D., & Kopell, N. (2009). Olfactory oscillations: the what, how and what for. Trends in neurosciences, 32(4), 207-214.

Kirsh, D. (1996). Adapting the environment instead of oneself. *Adaptive Behavior*, *4*(3-4), 415-452.

Kirsh, D. (2010). Thinking with external representations. *AI & society*, *25*(4), 441-454.

Kirsh, D., & Maglio, P. (1994). On distinguishing epistemic from pragmatic action. Cognitive science, 18(4), 513-549.

Lakatos, G., Gácsi, M., Konok, V., Bruder, I., Bereczky, B., Korondi, P., & Miklosi, A. (2014). Emotion attribution to a non-humanoid robot in different social situations. PloS one, 9(12), e114207.

Lebedev, M. A., Pimashkin, A., & Ossadtchi, A. (2018). Navigation patterns and scent marking: underappreciated contributors to hippocampal and entorhinal spatial representations? Frontiers in behavioral neuroscience, 12, 98.

Lever, C., Burton, S., & O'Keefe, J. (2006). Rearing on hind legs, environmental novelty, and the hippocampal formation. Reviews in the Neurosciences, 17(1-2), 111-134.

Lipkind, D., Sakov, A., Kafkafi, N., Elmer, G. I., Benjamini, Y., & Golani, I. (2004). New replicable anxiety-related measures of wall vs. center behavior of mice in the open field. Journal of applied physiology, 97(1), 347-359.

Livneh, Y., & Andermann, M. L. (2021). Cellular activity in insular cortex across seconds to hours: Sensations and predictions of bodily states. *Neuron*, *109*(22), 3576-3593.

Lockmann, A. L., Laplagne, D. A., Leão, R. N. & Tort, A. B. (2016). A respiration-coupled rhythm in the rat hippocampus independent of theta and slow oscillations. *Journal of Neuroscience*, *36*(19), 5338-5352

Luo, C., Zheng, X., & Zeng, D. (2014). Causal inference in social media using convergent cross mapping. In *Intelligence and Security Informatics Conference (JISIC), 2014 IEEE Joint* (pp. 260-263). IEEE

Ma, H., Aihara, K., & Chen, L., (2015). Detecting Causality from Nonlinear Dynamics with Short-term Time Series. *Scientific Reports* **4,** 7464

Mandik, P. (2002). Synthetic neuroethology. *Metaphilosophy*, *33*(1-2), 11-29.

Maris, E., Fries, P., & van Ede, F. (2016). Diverse phase relations among neuronal rhythms and their potential function. *Trends in neurosciences*, *39*(2), 86-99.

Marshall, A. C., Gentsch, A., Jelinčić, V., & Schütz-Bosbach, S. (2017). Exteroceptive expectations modulate interoceptive processing: repetition-suppression effects for visual and heartbeat evoked potentials. Scientific reports, 7(1), 1-15.

Martin, C., Beshel, J. & Kay L. M. An olfacto-hippocampal network is dynamically involved in odor-discrimination learning. Journal of neurophysiology, 98(4), 2196-2205 (2007).

Marvi, Z., & Kiumarsi, B. (2021). Safe reinforcement learning: A control barrier function optimization approach. *International Journal of Robust and Nonlinear Control*, *31*(6), 1923-1940.

McCracken, J. M. and Weigel, R. S. (2014). Convergent cross-mapping and pairwise asymmetric inference. Physical Review E, 90(6):062903

McGaugh, J. L., Cahill, L., & Roozendaal, B. (1996). Involvement of the amygdala in memory storage: interaction with other brain systems. *Proceedings of the National Academy of Sciences*, *93*(24), 13508-13514.

Mercer, A., Trigg, H. L., & Thomson, A. M. (2007). Characterization of neurons in the CA2 subfield of the adult rat hippocampus. Journal of Neuroscience, 27(27), 7329-7338.

Mitchell, D. (1976). Experiments on neophobia in wild and laboratory rats: a reevaluation. Journal of Comparative and Physiological Psychology, 90(2), 190.

Mobbs, D., & Kim, J. J. (2015). Neuroethological studies of fear, anxiety, and risky decision-making in rodents and humans. Current opinion in behavioral sciences, 5, 8-15.

Moberly, A. H., Schreck, M., Bhattarai, J. P., Zweifel, L. S., Luo, W., & Ma, M. (2018). Olfactory inputs modulate respiration-related rhythmic activity in the prefrontal cortex and freezing behavior. Nature communications, 9(1), 1-10.

Modlinska, K., Stryjek, R., & Pisula, W. (2015). Food neophobia in wild and laboratory rats (multi-strain comparison). behavioral Processes, 113, 41-50.

Mønster, D., Fusaroli, R., Tylén, K., Roepstorff, A. & Sherson, J. F. (2017). Causal inference from noisy time-series data—Testing the Convergent Cross-Mapping algorithm in the

presence of noise and external influence. *Future Generation Computer Systems*, *73*, 52-62

Mori, M. (1970). The Uncanny Valley. Energy, 7, 33-35.

Munia, T. T., & Aviyente, S. (2019). Time-frequency based phase-amplitude coupling measure for neuronal oscillations. *Scientific reports*, *9*(1), 1-15.

Nance P. W., Hoy C. S. (1996). Assessment of the autonomic nervous system. Phys. Med. Rehabil. 10, 15–35.

Narins, P. M., Hödl, W., & Grabul, D. S. (2003). Bimodal signal requisite for agonistic behavior in a dart-poison frog, Epipedobates femoralis. Proceedings of the National Academy of Sciences, 100(2), 577-580.

Narins, P. M., Grabul, D. S., Soma, K. K., Gaucher, P., & Hödl, W. (2005). Cross-modal integration in a dart-poison frog. Proceedings of the National Academy of Sciences, 102(7), 2425-2429.

Nitz, D., & McNaughton, B. (2004). Differential modulation of CA1 and dentate gyrus interneurons during exploration of novel environments. *Journal of neurophysiology*, *91*(2), 863-872.

Orlandi, N. (2014). *The innocent eye: Why vision is not a cognitive process*. Oxford University Press.

Paré, D., Collins, D. R., & Pelletier, J. G. (2002). Amygdala oscillations and the consolidation of emotional memories. Trends in cognitive sciences, 6(7), 306-314.

Pare, D., Dong, J., & Gaudreau, H. (1995). Amygdalo-entorhinal relations and their reflection in the hippocampal formation: generation of sharp sleep potentials. *Journal of Neuroscience*, *15*(3), 2482-2503.

Pereira, T. D., Shaevitz, J. W., & Murthy, M. (2020). Quantifying behavior to understand the brain. Nature neuroscience, 23(12), 1537-1549.

Pitkänen, A. (2000). "Connectivity of the rat amygdaloid complex" in J. P. Aggleton (Ed.), *The Amygdala: A functional analysis.* 2nd edition. Oxford University Press

Pitkänen, A., Pikkarainen, M., Nurminen, N., & Ylinen, A. (2000). Reciprocal connections between the amygdala and the hippocampal formation, perirhinal cortex, and postrhinal cortex in rats: a review. Annals of the New York Academy of Sciences, 911(1), 369-391.

Prut, L. and Belzung, C. (2003) The Open Field as a Paradigm to Measure the Effects of Drugs on Anxiety-Like Behaviors: A Review. European Journal of Pharmacology, 463, 3-33.

Quinn, L. K., Schuster, L. P., Aguilar-Rivera, M., Arnold, J., Ball, D., Gygi, E., Wiles, J., & Chiba, A. A. (2018). When rats rescue robots. Animal Behavior and Cognition, 5(4), 368-379.

Quyen, M. L. V., Martinerie, J., Adam, C., & Varela, F. J. (1999). Nonlinear analyses of interictal EEG map the brain interdependencies in human focal epilepsy. *Physica D* 127, 250–266

Rangel, L. M., Chiba, A. A., & Quinn, L. K. (2015). Theta and beta oscillatory dynamics in the dentate gyrus reveal a shift in network processing state during cue encounters. *Frontiers in systems neuroscience*, *9*, 96.

Riek, L., & Howard, D. (2014). A code of ethics for the human-robot interaction profession. *Proceedings of we robot*.

Rogers-Carter, M. M., Varela, J. A., Gribbons, K. B., Pierce, A. F., McGoey, M. T., Ritchey, M., & Christianson, J. P. (2018). Insular cortex mediates approach and avoidance responses to social affective stimuli. *Nature neuroscience*, *21*(3), 404-414.

Rojas-Líbano, D., Frederick, D. E., Egaña, J. I., & Kay, L. M. (2014). The olfactory bulb theta rhythm follows all frequencies of diaphragmatic respiration in the freely behaving rat. Frontiers in behavioral neuroscience, 8, 214.

Rojas-Líbano, D., & Parada, F. J. (2020). Body-world coupling, sensorimotor mechanisms, and the ontogeny of social cognition. *Frontiers in Psychology*, 3005.

Rosen, J. B., Asok, A., & Chakraborty, T. (2015). The smell of fear: innate threat of 2, 5-dihydro-2, 4, 5-trimethylthiazoline, a single molecule component of a predator odor. *Frontiers in neuroscience*, *9*, 292.

Ruggiero, D. A., Mraovitch, S., Granata, A. R., Anwar, M., & Reis, D. J. (1987). A role of insular cortex in cardiovascular function. *Journal of Comparative Neurology*, *257*(2), 189-207.

Rutte, C., & Taborsky, M. (2008). The influence of social experience on cooperative behavior of rats (Rattus norvegicus): direct vs generalized reciprocity. Behavioral Ecology and Sociobiology, 62(4), 499-505.

Saper CB (2002). The central autonomic nervous system: conscious visceral perception and autonomic pattern generation. Annu Rev Neurosci 25, 433–469.

Saygin, A. P., Wilson, S. M., Hagler, D. J., Jr, Bates, E., & Sereno, M. I. (2004). Point-light biological motion perception activates human premotor cortex. Journal of Neuroscience, 24(27), 6181–6188.

Saygin, A. P., Chaminade, T., Ishiguro, H., Driver, J., & Frith, C. (2012). The thing that should not be: predictive coding and the uncanny valley in perceiving human and humanoid robot actions. Social cognitive and affective neuroscience, 7(4), 413-422.

Schiff, S. J., So, Chang, P. T., Burke, R. E. & Sauer, T. (1996). Detecting dynamical interdependence and generalized synchrony through mutual prediction in a neural ensemble. Phys. Rev. E 54, 6708

Schmickl, T., Szopek, M., Mondada, F., Mills, R., Stefanec, M., Hofstadler, D. N., ... & Zahadat, P. (2021). Social integrating robots suggest mitigation strategies for ecosystem decay. *Frontiers in Bioengineering and Biotechnology*, *9*.

Shi, Q., Ishii, H., Kinoshita, S., Konno, S., Takanishi, A., Okabayashi, S., ... & Kimura, H. (2013). A rat-like robot for interacting with real rats. Robotica, 31(8), 1337-1350.

Sirota, A., Csicsvari, J., Buhl, D. & Buzsáki, G. Communication between neocortex and hippocampus during sleep in rodents. Proc Natl Acad Sci U S A 100:2065–2069 (2003).

Smith, A. S., Williams Avram, S. K., Cymerblit-Sabba, A., Song, J., & Young, W. S. (2016). Targeted activation of the hippocampal CA2 area strongly enhances social memory. Molecular psychiatry, 21(8), 1137-1144.

Sokolov, E. N. (1963). Higher nervous functions: The orienting reflex. *Annual review of physiology*, *25*(1), 545-580.

Song, C., Berridge, K. C., & Kalueff, A. V. (2016). 'Stressing' rodent self-grooming for neuroscience research. Nature Reviews Neuroscience, 17(9), 591-591.

Strang, A. J., Funke, G. J., Russell, S. M., Dukes, A. W. & Middendorf, M. S. (2014). Physio-behavioral coupling in a cooperative team task: Contributors and relations. *Journal of Experimental Psychology: Human Perception and Performance*, *40*(1), 145

Sturman, O., von Ziegler, L., Schläppi, C., Akyol, F., Privitera, M., Slominski, D., ... & Bohacek, J. (2020). Deep learning-based behavioral analysis reaches human accuracy and is capable of outperforming commercial solutions. Neuropsychopharmacology, 45(11), 1942-1952.

Suchman, L., & Weber, J. (2016). Human-machine autonomies. *Autonomous weapons systems: Law, ethics, policy*, 75-102.

Sugihara, G. May, R., Ye, H., Hsieh, C. H., Deyle, E., Fogarty, M., & Munch, S. Detecting causality in complex ecosystems. (2012). S*cience*, *338*(6106), 496-500

Sutton, R. S., & Barto, A. G. (2018). *Reinforcement learning: An introduction*. MIT press.

Swanson, L. W., & Petrovich, G. D. (1998). What is the amygdala?. Trends in neurosciences, 21(8), 323-331.

Takens, F. Detecting strange attractors in turbulence. (1981). In *Dynamical Systems and Turbulence, Warwick 1980* (pp. 366-381). Springer, Berlin, Heidelberg

Tang, W. Hippocampus and Rat Prefrontal Cortex. Scidraw.io: OpenSource scientific drawings (2019).

Tendler, A. & Wagner, S. Different types of theta rhythmicity are induced by social and fearful stimuli in a network associated with social memory. (2015). *Elife*, 4, e03614

Thompson, R. F. (2009). Habituation: a history. Neurobiology of learning and memory, 92(2), 127.

Todorov, E., & Jordan, M. I. (1998). Smoothness maximization along a predefined path accurately predicts the speed profiles of complex arm movements. Journal of Neurophysiology, 80(2), 696-714.

Tolston, M. T., Shockley, K., Riley, M. A. & Richardson, M. J. (2014). Movement constraints on interpersonal coordination and communication. *Journal of Experimental Psychology: Human Perception and Performance*, *40*(5), 1891.

Tolston, M. T., Funke, G. J. & Shockley, K. (2020). Comparison of Cross-Correlation and Joint-Recurrence Quantification Analysis Based Methods for Estimating Coupling Strength in Non-linear Systems. *Frontiers in Applied Mathematics and Statistics*, *29*(31), 32.

Tort, A. B., Brankačk, J., & Draguhn, A. (2018). Respiration-entrained brain rhythms are global but often overlooked. Trends in neurosciences, 41(4), 186-197.

Tort, A. B., Ponsel, S., Jessberger, J., Yanovsky, Y., Brankačk, J., & Draguhn, A. (2018). Parallel detection of theta and respiration-coupled oscillations throughout the mouse brain. Scientific reports, 8(1), 1-14.

Trimper, J. B., Galloway, C. R., Jones, A. C., Mandi, K., & Manns, J. R. (2017). Gamma oscillations in rat hippocampal subregions dentate gyrus, CA3, CA1, and subiculum underlie associative memory encoding. Cell reports, 21(9), 2419-2432.

Turing, A. (1950). Computing Machinery and Intelligence. *Mind*, 59 (236): 433–60.

Urgen, B. A., Kutas, M., & Saygin, A. P. (2018). Uncanny valley as a window into predictive processing in the social brain. *Neuropsychologia*, *114*, 181-185.

Van Strien, N. M., Cappaert, N. L. M., & Witter, M. P. (2009). The anatomy of memory: an interactive overview of the parahippocampal–hippocampal network. Nature reviews neuroscience, 10(4), 272-282.

Webb, B. (2000). What does robotics offer animal behavior? Animal behavior, 60(5), 545-558.

Wiles, J., Heath, S., Ball, D., Quinn, L., & Chiba, A. (2012, November). Rat meets iRat. In 2012 IEEE International Conference on Development and Learning and Epigenetic Robotics (ICDL) (pp. 1-2). IEEE.

Wilson, F.A., & Rolls, E.T. (2004). The effects of stimulus novelty and familiarity on neuronal activity in the amygdala of monkeys performing recognition memory tasks. Experimental Brain Research, 93, 367-382.

Wismüller, A., Wang, X., DSouza, A. M. & Nagarajan, M. (2014).. A Framework for Exploring Non-Linear Functional Connectivity and Causality in the Human Brain: Mutual Connectivity Analysis (MCA) of Resting-State Functional MRI with Convergent Cross-Mapping and Non-Metric Clustering. *arXiv preprint arXiv:1407.3809*

Ye, H., Deyle, E. R., Gilarranz, L. J. & Sugihara, G. (2015). Distinguishing time-delayed causal interactions using convergent cross mapping. *Scientific Reports*, *5*

Yu, C., Velu, A., Vinitsky, E., Wang, Y., Bayen, A., & Wu, Y. (2021). The Surprising Effectiveness of PPO in Cooperative, Multi-Agent Games. arXiv preprint arXiv:2103.01955.

Zhao, Q., Yu, C. D., Wang, R., Xu, Q. J., Dai Pra, R., Zhang, L., & Chang, R. B. (2022). A multidimensional coding architecture of the vagal interoceptive system. *Nature*, 1-7.